

NEW ASPECTS OF HEXAGONAL DUNGEONS

TRI LAI

INDIANA UNIVERSITY, BLOOMINGTON, IN 47405

ABSTRACT. In this paper we prove a multi-parameter generalization of Blum's (ex-)conjecture (Problem 25, J. Propp, *New Perspectives in Geometric Combinatorics*, Cambridge University Press, 1999) by using Kuo's Graphical Condensation Theorem (E. Kuo, *Applications of Graphical Condensation for Enumerating Matchings and Tilings*, Theoretical Computer Science, 2004). This implies a proof for a conjecture posed by Ciucu. We also investigate several new families of regions inspired by hexagonal dungeons and prove that their tilings are enumerated by perfect powers.

Keywords: perfect matchings, tilings, dual graphs, Aztec dungeons, graphical condensation.

Mathematics Subject Classifications: 05A15, 05E99

CONTENTS

1. Introduction	1
2. Preliminaries	2
3. Weighted Dungeon	6
4. Subgraphs of the square grid	23
5. Trimmed Aztec rectangle	43
6. More hexagonal dungeons	48
References	62

1. INTRODUCTION

In [2], Ciucu and author of the paper proved a long lasting conjecture of Blum on hexagonal dungeons (see Figure 1.1 for an example of a hexagonal dungeon). In particular, the result is given by the following theorem.

Theorem 1. *Assume that a and b are two positive integers so that $b \geq 2a$. Then the number of tilings of a hexagonal dungeon of sides $a, 2a, b, a, 2a, b$ (in cyclic order start from the northwestern side) is $13^{2a^2} 14^{\lfloor \frac{a^2}{2} \rfloor}$.*

We continue the line of work in [2] by investigating new aspects of similar regions whose tilings are enumerated by perfect powers.

Date: March 20, 2014.

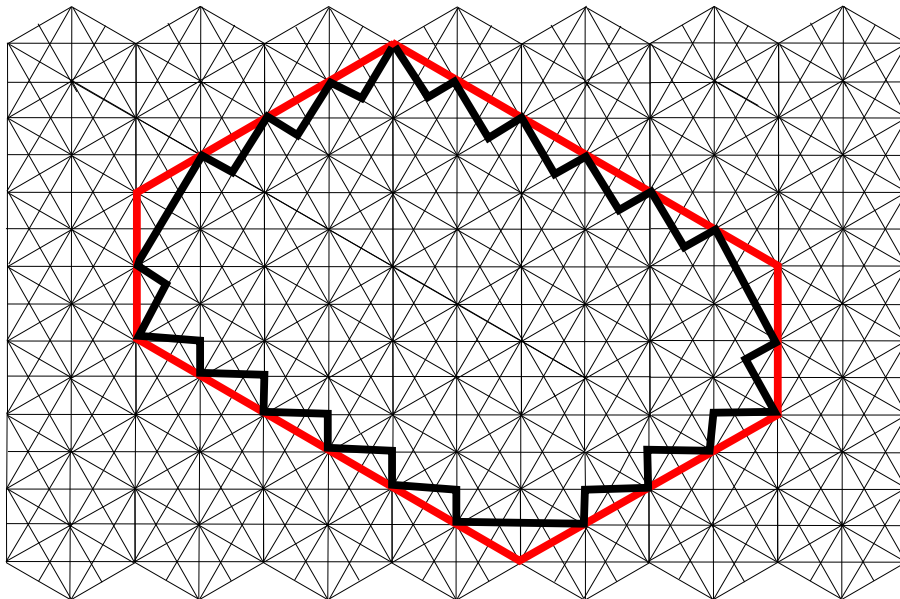


FIGURE 1.1. The hexagonal dungeon of sides 2, 4, 6, 2, 4, 6 (in cyclic order, starting from the western side). This Figure first appeared in [2].

In Section 3, we consider three subgraphs of the square grid obtained from the dual graph of a hexagonal dungeon by applying urban renewal in a certain way. We call those subgraphs *dungeon graphs*. By using the same method in [2], we prove that, with a certain periodic weight assignment on edges, the matching generating function of a dungeon graph is given by a simple product formula. This also implies the Blum's (ex-)conjecture as a special case.

Next, Section 4 investigate a variant of hexagonal dungeons on the lattice G_2 (i.e. the lattice obtained from the triangular lattice by drawing in all the altitudes in all the unit triangles; it is also the plane lattice corresponding to the affine Coxeter group G_2). We prove a conjecture posed by Ciucu that the number of tilings of the region is given by a product of perfect powers of prime numbers less than 13.

Section 5 discovers several new families of regions inspired by hexagonal dungeons. We show that their numbers of tilings are given by simply product formulas.

2. PRELIMINARIES

As a sequel of [2], this paper uses the same terminologies, definitions and preliminary results in the Preliminaries Section of [2].

Tilings and perfect matchings can carry weights. The weight of a tiling (resp., perfect matching) is the product of the weights of the constituent tiles (resp., edges). The *tiling generating function* (resp., *matching generating function*) is defined to be the sum of all the weights of the tilings (resp., perfect matching) of the region (resp.,

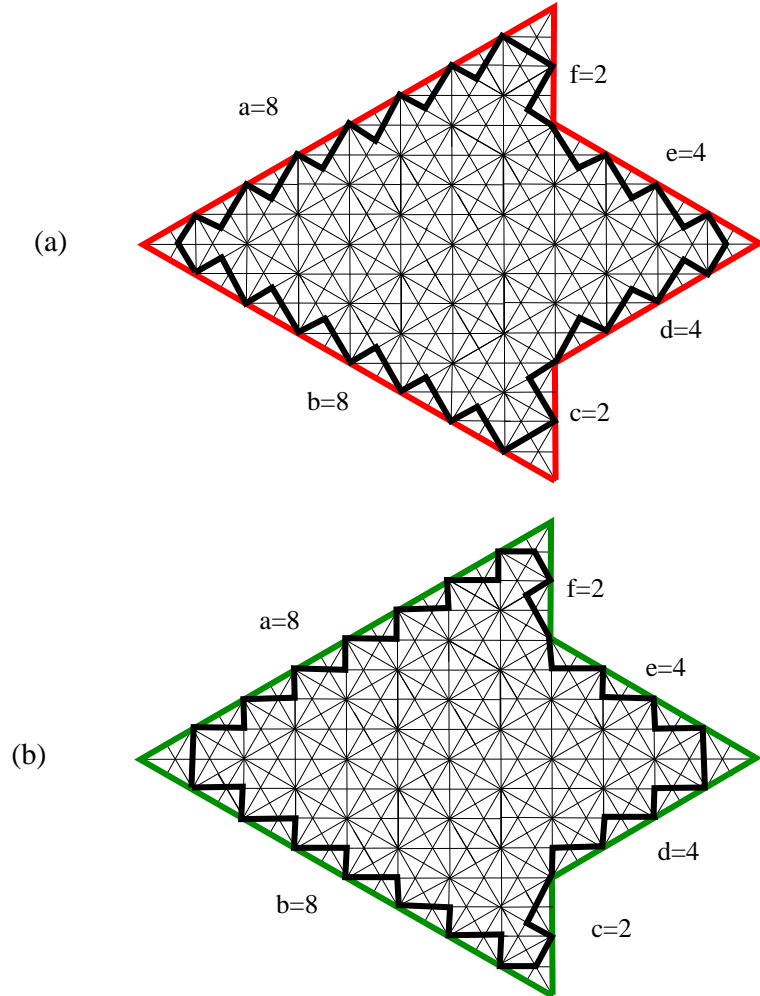


FIGURE 2.1. Example of the case $a > c + d$: the regions $D_{8,8,2}$ (a) and $E_{8,8,2}$ (b). This Figure first appeared in [2].

the graph). We still use the notation $M(\dots)$ for the tiling generating function and matching generating function.

Before going to the next section we recall briefly the definition of the regions $D_{a,b,c}$ and $E_{a,b,c}$ (one could see the detailed definition in [2]).

Let a, b, c, d, e, f be six nonnegative integers so that $b \geq 2$, $d = 2b - a - 2c$, $e = b + d - a$, and $f = |c + d - a|$. Starting from some lattice point, travel along lattice lines a units southwest (a unit being the side-length of the unit triangles), b units southeast, c units north, d units northeast, e units northwest, and f units north or south. In [2], we showed that the contour closed by the above constraints on its side-lengths.

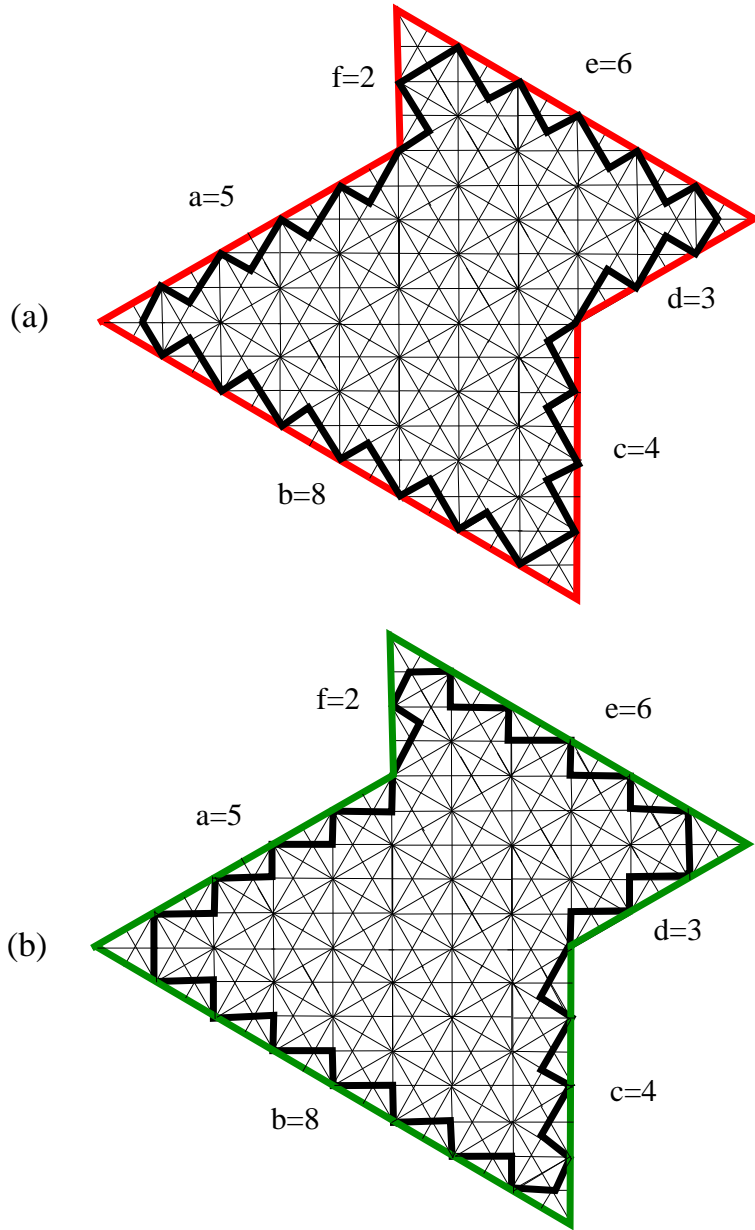


FIGURE 2.2. Example of the case $a \leq c + d$: the regions $D_{5,8,4}$ (a) and $E_{5,8,4}$ (b). This Figure first appeared in [2].

The contour is illustrated in Figure 2.1, for the case $a > c + d$; and in Figure 2.2, for the case $a \leq c + d$. If some sides have length 0, we assume that these sides shrink to a point. Denote by $\mathcal{C}(a, b, c)$ this contour.

Based on the contour $\mathcal{C}(a, b, c)$, we define two lattice regions $D_{a,b,c}$ and $E_{a,b,c}$ determined by the bold jagged contours as in Figure 2.1, for the case $a > c + d$, and by Figure 2.2, for the case $a \leq c + d$.

Let a, b, c be three integers. Define two functions ϕ and ψ by setting

$$(2.1) \quad \phi(a, b, c) := h(a, b, c) 13^{g(a, b, c)} 14^{q(a, b, c)}$$

and

$$(2.2) \quad \psi(a, b, c) := p(a, b, c) 13^{g(a, b, c)} 14^{q(a, b, c)},$$

where

$$(2.3) \quad g(a, b, c) = (b - a)(b - c) + \left\lfloor \frac{(a - c)^2}{3} \right\rfloor,$$

$$(2.4) \quad q(a, b, c) = \left\lfloor \frac{(a - b + c)^2}{4} \right\rfloor,$$

$$(2.5) \quad h(a, b, c) = \begin{cases} 2 & \text{if } 3b + a - c \equiv 4 \pmod{6}; \\ 3 & \text{if } 3b + a - c \equiv 1 \pmod{6}; \\ 5 & \text{if } 3b + a - c \equiv 5 \pmod{6}; \\ 1 & \text{otherwise,} \end{cases}$$

and

$$(2.6) \quad p(a, b, c) = \begin{cases} 2 & \text{if } 3b + a - c \equiv 2 \pmod{6}; \\ 3 & \text{if } 3b + a - c \equiv 5 \pmod{6}; \\ 5 & \text{if } 3b + a - c \equiv 1 \pmod{6}; \\ 1 & \text{otherwise.} \end{cases}$$

It was proved in [2] that

Theorem 2. *Assume that a , b , and c are three nonnegative integers satisfying $b \geq 2$, $2b - a - 2c \geq 0$ and $3b - 2a - 2c \geq 0$. Then*

$$(2.7) \quad M(D_{a, b, c}) = \phi(a, b, c) \text{ and } M(E_{a, b, c}) = \psi(a, b, c).$$

As mentioned in [2], the above theorem can be viewed as a common generalization of Blum's (ex-)conjecture and Aztec dungeon theorems (Theorem 3.10 in [1]). We prove this theorem by using Kuo's graphical condensation theorem to show that $M(D_{a, b, c})$ and $\phi(a, b, c)$, as well as $M(E_{a, b, c})$ and $\psi(a, b, c)$, satisfy the same recurrences.

Lemma 3 (Graph Splitting Lemma). *Let G be a bipartite graph, and let V_1 and V_2 be the two vertex classes.*

Assume that an induced subgraph H of G satisfies following two conditions:

- (i) (Separating Condition) *There are no edges of G connecting a vertex in $V(H) \cap V_1$ and a vertex in $V(G - H)$.*
- (ii) (Balancing Condition) $|V(H) \cap V_1| = |V(H) \cap V_2|$.

Then

$$(2.8) \quad M(G) = M(H) M(G - H).$$

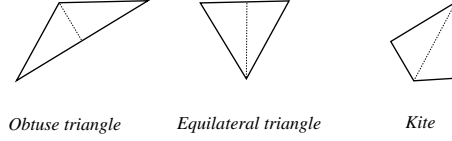


FIGURE 3.1. Three types of tiles of a hexagonal dungeon.

Finally, we include here the Kuo's graphical condensation Theorem.

Theorem 4 (Kuo [5]). *Let G be a planar bipartite graph, and let V_1 and V_2 be the two vertex classes. Assume that $|V_1| = |V_2|$. Let u, v, w and t be four vertices appear in a cyclic order on a face of G . Assume in addition that $u, v \in V_1$ and $w, t \in V_2$. Then*

$$(2.9) \quad \begin{aligned} M(G) M(G - \{u, v, w, t\}) &= M(G - \{u, v\}) M(G - \{w, t\}) \\ &\quad + M(G - \{t, u\}) M(G - \{v, w\}). \end{aligned}$$

3. WEIGHTED DUNGEON

There are three possible shapes of tiles of the lattice G_2 in the definition of hexagonal dungeons: an equilateral triangle, an obtuse triangle and a kite (see Figure 3.1). Assign three types of tiles weights y , x and 1, respectively. We will investigate the tilings generating functions of hexagonal dungeons and the regions $D_{a,b,c}$ and $E_{a,b,c}$ associating with the above weight assignment. For clarity, we denote by $D_{a,b,c}(x, y)$ and $E_{a,b,c}(x, y)$ the regions $D_{a,b,c}$ and $E_{a,b,c}$ with the weight assignment.

Define a new function by setting

$$(3.1) \quad \begin{aligned} \tau(a, b, c) &:= 2(b - c - 1)(c + d - 1) + c(c - 1) + f(f - 1) - 2g(a, b, c) - 2q(a, b, c) \\ &= 2(b - c - 1)(2b - a - c - 1) + c(c - 1) + |2a + c - 2b|(|2a + c - 2b| - 1) \\ &\quad - 2g(a, b, c) - 2q(a, b, c), \end{aligned}$$

where the functions $q(a, b, c)$ and $g(a, b, c)$ are defined as in Theorem 2. The tilings generating functions of $D_{a,b,c}(x, y)$ and $E_{a,b,c}(x, y)$ are given by the following theorem.

Theorem 5. *Assume that x, y are two positive integers, and the two functions $q(a, b, c)$ and $g(a, b, c)$ are defined as in Theorem 2. Assume in addition that $P_1 := P_1(x, y) = x^6 + 3x^4y^2 + 3x^2y^4 + y^6 + 2x^3 + 2xy^2 + 1$ and $P_2 := P_2(x, y) = (x^4 + 2x^2y^2 + y^4 + x^3 + xy^2 - y^2 + x + 1)(x^2 + y^2 - x + 1)$. Then*

$$(3.2) \quad M(D_{a,b,c}(x, y)) = \mu(a, b, c) x^{2g(a,b,c)+3q(a,b,c)} y^{q(a,b,c)} P_1^{g(a,b,c)} P_2^{q(a,b,c)},$$

and

$$(3.3) \quad M(E_{a,b,c}(x, y)) = \nu(a, b, c) x^{2g(a,b,c)+3q(a,b,c)} y^{q(a,b,c)} P_1^{g(a,b,c)} P_2^{q(a,b,c)},$$

where $q(a, b, c) = \tau(a, b, c) + (2b - a - 2c - 1) + (a - 1) + c + \min(2a + c - 2b, 0)$,

$$\mu(a, b, c) = \begin{cases} (x^4 + 2x^2y^2 + y^4 + x)x/y & \text{if } 3b + a - c \equiv 5 \pmod{6}; \\ (x^3 + xy^2 + 1)x/y & \text{if } 3b + a - c \equiv 1 \pmod{6}; \\ (x^2 + y^2) & \text{if } 3b + a - c \equiv 4 \pmod{6}; \\ y & \text{if } 3b + a - c \equiv 3 \pmod{6}; \\ 1 & \text{otherwise,} \end{cases}$$

$$\nu(a, b, c) = \begin{cases} (x^4 + 2x^2y^2 + y^4 + x)x/y & \text{if } 3b + a - c \equiv 1 \pmod{6}; \\ (x^3 + xy^2 + 1)x/y & \text{if } 3b + a - c \equiv 5 \pmod{6}; \\ (x^2 + y^2) & \text{if } 3b + a - c \equiv 2 \pmod{6}; \\ y & \text{if } 3b + a - c \equiv 3 \pmod{6}; \\ 1 & \text{otherwise.} \end{cases}$$

We notice that Theorem 5 implies Theorem 2 by specializing $x = y = 1$.

Denote by $HD_{a,2a,b}(x, y)$ the hexagonal dungeon of sides $a, 2a, ba, 2a, b$ with the above weight assignment. The following weighted version of Blum's (ex-)conjecture can be viewed as a corollary of Theorem 5.

Corollary 6. *Assume a, b are two positive integers so that $b \geq 2a$, then*

$$(3.4) \quad M(HD_{a,2a,b}(x, y)) = x^{3ab-2a^2+3\lfloor \frac{a^2}{2} \rfloor} y^{6ab-a^2+3a-b-2\lfloor \frac{a^2}{2} \rfloor + \gamma} P_1^{2a^2} P_2^{\lfloor \frac{a^2}{2} \rfloor},$$

where $\gamma = 1$ if b is even, and is y^2 if b is odd.

Proof. Apply Graph-splitting Lemma to the dual graph of $HD_{a,2a,b}(x, y)$ with two zigzag cuts as in the proof of Blum's conjecture.

$$(3.5) \quad M(HD_{a,2a,b}(x, y)) = M(G_1(x, y)) M(G_2(x, y)) M(G_3(x, y))$$

$$(3.6) \quad = M(D_{2a,3a,2a}(x, y))^2 x^{3a(b-2a)} y^{3a(b-2a+1)+(3a-1)(b-2a)},$$

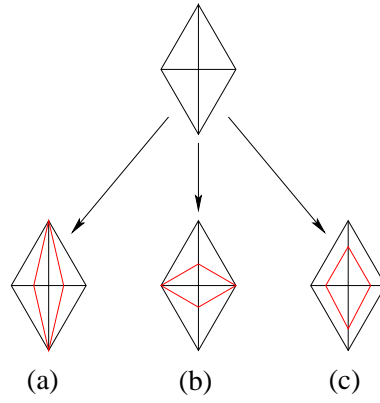
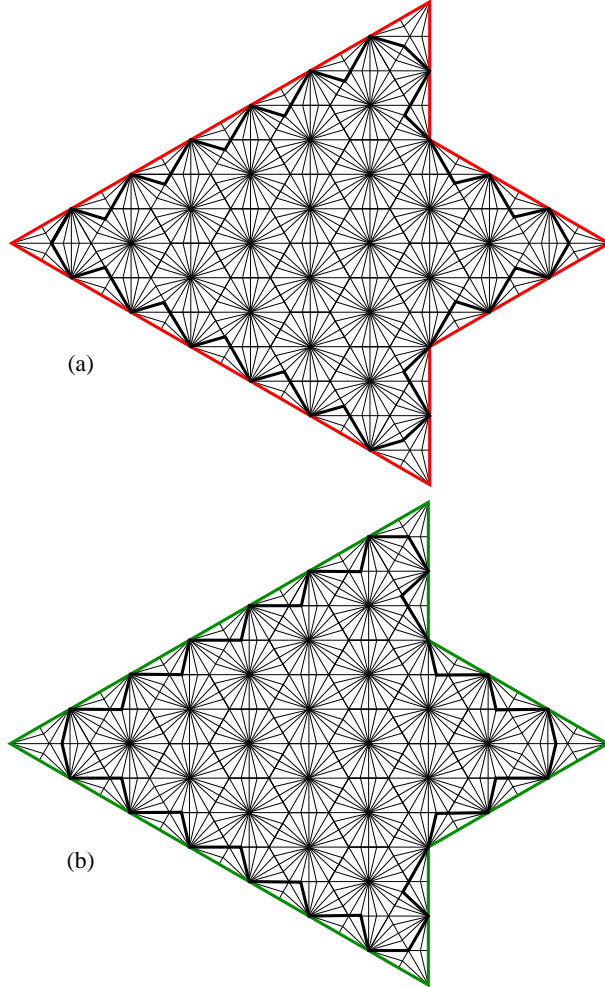
since the graph $G_2(x, y)$ has only one perfect matching with weight $x^{3a(b-2a)} y^{3a(b-2a+1)+(3a-1)(b-2a)}$.

By the definition of the functions $g(a, b, c)$, $q(a, b, c)$ and $\tau(a, b, c)$, we obtain $q(2a, 3a, 2b) = \lfloor \frac{a^2}{4} \rfloor$, $g(2a, 3a, 2a) = a^2$, and $\mu(2a, 3a, 2a) = \nu(2a, 3b, 2a) = 1$ if b is even, and is y^2 if b is odd. Thus, the corollary follows from Theorem 5. \square

Before presenting the proof of Theorem 5, which is similar to the proof of Theorem 2 in [2], we investigate several more applications of its.

The G_2 lattice can be partitioned into rhombi with two diagonals drawn in. We apply the following replacement rules to the rhombi as in Figure 3.2.

First, we apply the first replacement rule to all rhombi of G_2 lattice; we call the resulting lattice $G_2^{(1)}$ lattice. Draw the contour $\mathcal{C}(a, b, c)$ on the $G_2^{(1)}$ lattice, we consider a variant of regions $D_{a,b,c}$ and $E_{a,b,c}$ as in Figures 3.3 and 3.4. Denote by $D_{a,b,c}^{(1)}$ and $E_{a,b,c}^{(1)}$ the new regions. We have also a variant of hexagonal dungeon on this new lattice see Figure 3.5, denoted by $HD_{a,2a,b}^{(1)}$.

FIGURE 3.2. Three replacing rules for the rhombi of G_2 lattice.FIGURE 3.3. The region $D_{7,7,2}^{(1)}$ and $E_{7,2,2}^{(1)}$ on the $G_2^{(1)}$ lattice.

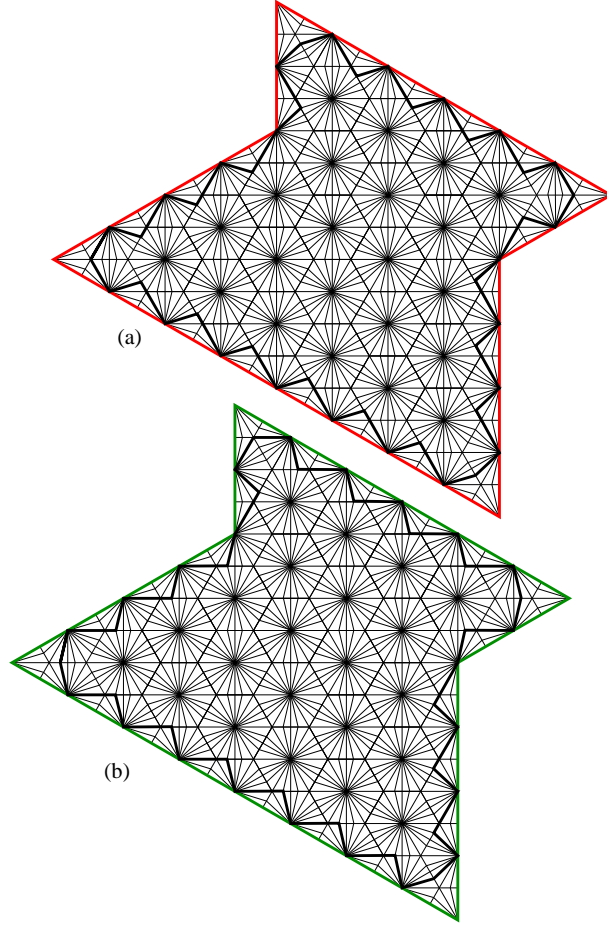


FIGURE 3.4. The region $D_{4,8,4}^{(1)}$ and $E_{4,8,4}^{(1)}$ on the $G_2^{(1)}$ lattice.

The numbers of tilings of the above new regions are given by the corollary stated below.

Corollary 7. (a) Assume that a , b , and c are three nonnegative integers satisfying $b \geq 2$, $2b - a - 2c \geq 0$ and $3b - 2a - 2c \geq 0$. Then

$$(3.7) \quad \begin{aligned} M\left(D_{a,b,c}^{(1)}\right) &= \mu^{(1)} 193^{g(a,b,c)} 5^q(a,b,c) 3^{2g(a,b,c)+5q(a,b,c)} \\ &\times 2^{(b-c)(c+d+1)+\frac{c(c+1)}{2}+\frac{f(f+1)}{2}-a+c+d-\min(a-c-d,0)-3g(a,b,c)-2f(a,b,c)}, \end{aligned}$$

$$(3.8) \quad \begin{aligned} M\left(E_{a,b,c}^{(1)}\right) &= \nu^{(1)} 193^{g(a,b,c)} 5^q(a,b,c) 3^{2g(a,b,c)+5q(a,b,c)} \\ &\times 2^{(b-c)(c+d+1)+\frac{c(c+1)}{2}+\frac{f(f+1)}{2}-a+c+d-\min(a-c-d,0)-3g(a,b,c)-2f(a,b,c)}, \end{aligned}$$

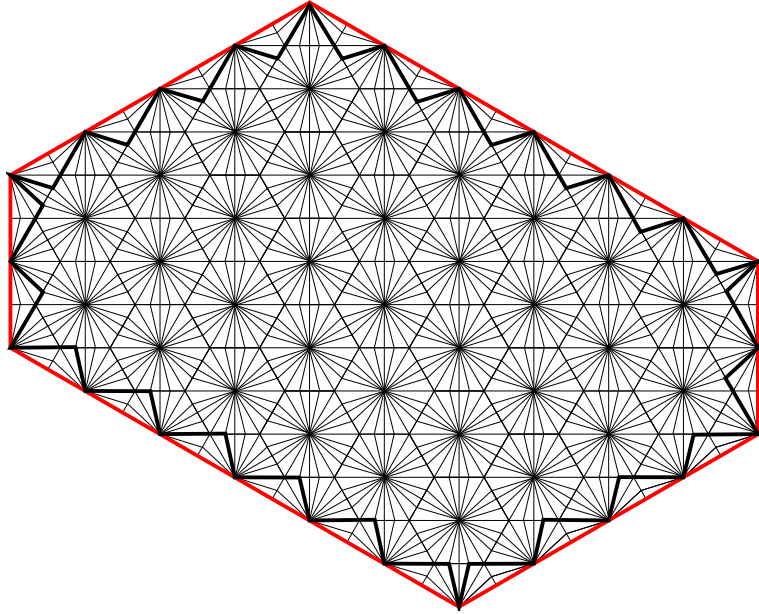


FIGURE 3.5. The variant $HD_{2,4,6}^{(1)}$ of the hexagonal dungeon $HD_{2,4,6}$ on the $G_2^{(1)}$ lattice.

where

$$\mu^{(1)} = \begin{cases} 93/4 & \text{if } 3b + a - c \equiv 5 \pmod{6}; \\ 93/8 & \text{if } 3b + a - c \equiv 1 \pmod{6}; \\ 5/2 & \text{if } 3b + a - c \equiv 4 \pmod{6}; \\ 1/2 & \text{if } 3b + a - c \equiv 3 \pmod{6}; \\ 1 & \text{otherwise,} \end{cases}$$

$$\nu^{(1)} = \begin{cases} 93/4 & \text{if } 3b + a - c \equiv 1 \pmod{6}; \\ 93/8 & \text{if } 3b + a - c \equiv 5 \pmod{6}; \\ 5/2 & \text{if } 3b + a - c \equiv 2 \pmod{6}; \\ 1/2 & \text{if } 3b + a - c \equiv 3 \pmod{6}; \\ 1 & \text{otherwise.} \end{cases}$$

(b) Assume that a and b are two positive integers, so that $b \geq 2a$. Then

$$(3.9) \quad M\left(HD_{a,b,c}^{(1)}\right) = 193^{2a^2} 5^{\lfloor \frac{a^2}{2} \rfloor} 3^{3ab-2a^2+5\lfloor \frac{a^2}{2} \rfloor} 2^{9a^2-6a-2\lfloor \frac{a^2}{2} \rfloor-\gamma},$$

where γ is defined as in Corollary 6

Proof. Consider the dual graph of $D_{a,b,c}^{(1)}$. One readily sees that it is obtained from the dual graph of $D_{a,b,c}$ by the local replacements as in Figures 3.6(a) and (a1), (b) and (b1), and (c) and (c1).

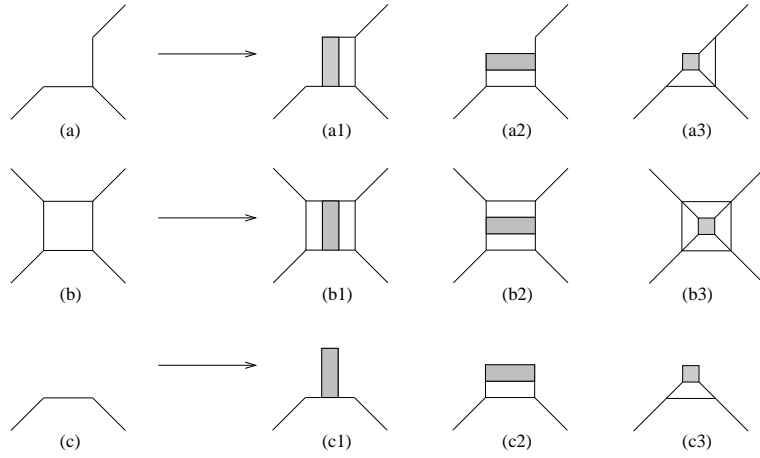


FIGURE 3.6. $D_{a,b,c}^{(i)}$, $E_{a,b,c}^{(i)}$ and $HD_{a,2a,b}^{(i)}$ are obtained from the dual graph of $D_{a,b,c}$, $E_{a,b,c}$ and $HD_{a,2a,b}$ by local repayments.

Apply the spider lemma at all shaded cells, we get the dual graphs of the region $D_{a,b,c}(x, y)$ with $x = 3/2$ and $y = 1/2$, and

$$(3.10) \quad M\left(D_{a,b,c}^{(1)}\right) = 2^{\#cells} M\left(D_{a,b,c}\left(\frac{3}{2}, \frac{1}{2}\right)\right),$$

and explicitly, the number of cells here is $(2(c+d)-1)(b-c) + (c+d)(b-c-1) + c(c-1) + c(c+1)/2 + f(f-1) + f(f+1)/2$. Then the first equality of the corollary follows from Theorem 5.

Similarly, we have the second and third equalities from Theorem 5 and Corollary 6, respectively. Notice that the number of cells in the dual graph of $E^{(1)}(a, b, c)$ is the same as that of the dual graph of $D_{a,b,c}^{(1)}$; and the number of cells in the dual graph of $HD_{a,2a,b}^{(1)}$ is $(6a-1)(b-2a) + 3a(b-2a+1) + 4a(2a-1) + 4a(4a-1)$. \square

Next, we apply the replacing rule (b) in Figure 3.2 to all rhombi of the G_2 lattice and denote by $G_2^{(2)}$ the resulting lattice. Consider the variant of the regions $D_{a,b,c}$ and $E_{a,b,c}$ on this lattice as in Figures 3.7 and 3.8. Similar to the lattice $G_2^{(1)}$, we have also a variant of the hexagonal dungeon $HD_{a,2a,b}$ on $G_2^{(2)}$ lattice (see Figure 3.9 for an example).

The numbers tilings of the new regions on $G_2^{(2)}$ lattice are given by the following corollary.

Corollary 8. (a) Assume that a, b , and c are three nonnegative integers satisfying $b \geq 2$, $2b - a - 2c \geq 0$ and $3b - 2a - 2c \geq 0$. Then

$$(3.11) \quad M(D_{a,b,c}^{(2)}) = \mu^{(2)} 17^{g(a,b,c)} 3^{2(b-c-1)(c+d-1)+c(c-1)+f(f-1)+2q(a,b,c)+(d-1)+(a-1)+c+\min(a-c-d,0)} \\ \times 2^{(b-c)(c+d+1)+c(c+1)/2+f(f+1)/2-a+c+d-\min(a-c-d,0)-3q(a,b,c)-3q(a,b,c)},$$

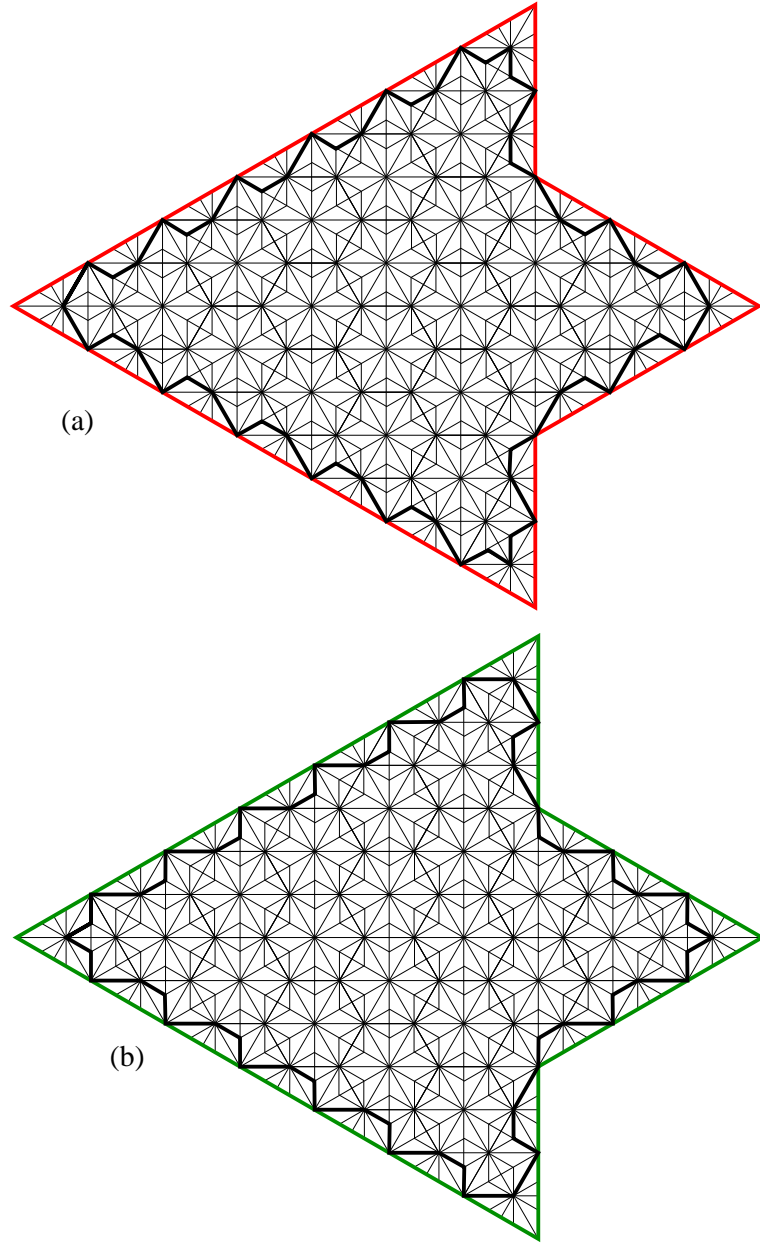
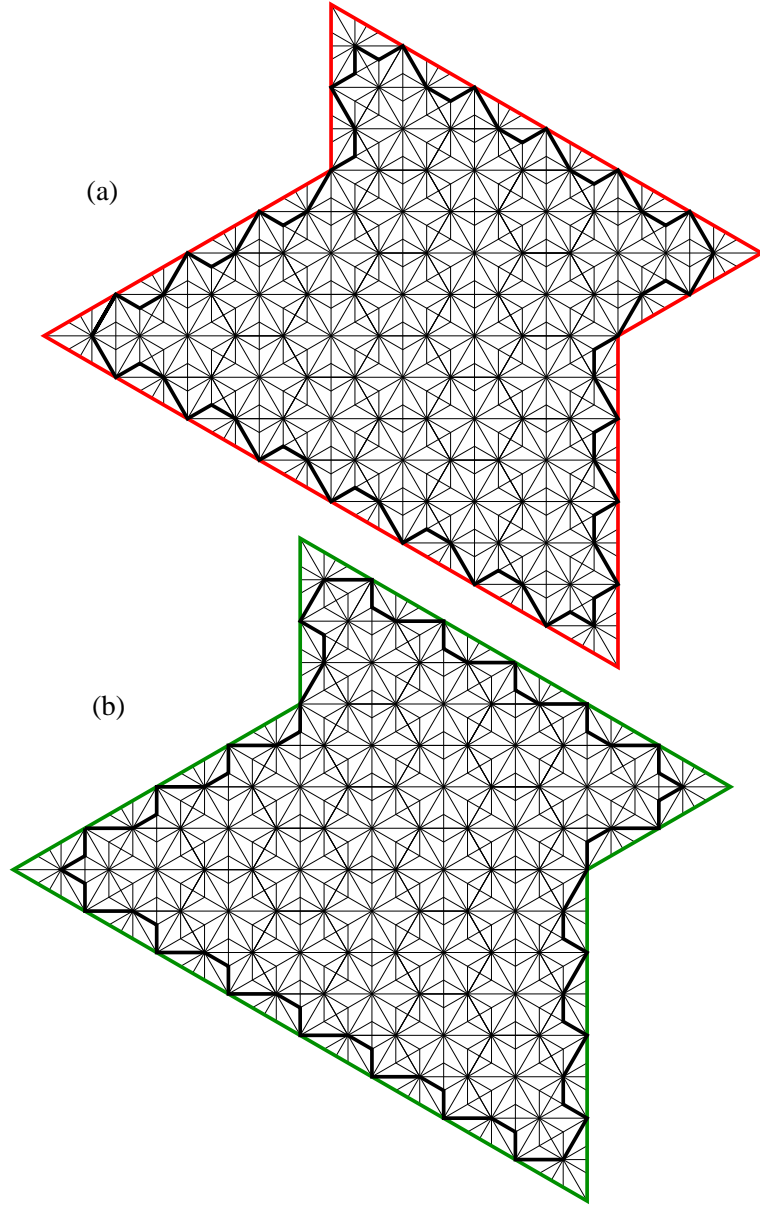


FIGURE 3.7. The region $D_{7,7,2}^{(2)}$ and $E_{7,2,2}^{(2)}$ on the $G_2^{(2)}$ lattice.

$$\begin{aligned}
 M(E_{a,b,c}^{(2)}) &= \nu^{(2)} 17^{g(a,b,c)} 3^{2(b-c-1)(c+d-1)+c(c-1)+f(f-1)+2q(a,b,c)+(d-1)+(a-1)+c+\min(a-c-d,0)} \\
 (3.12) \quad &\times 2^{(b-c)(c+d+1)+c(c+1)/2+f(f+1)/2-a+c+d-\min(a-c-d,0)-3q(a,b,c)-3q(a,b,c)},
 \end{aligned}$$

FIGURE 3.8. The region $D_{2,5,3}^{(2)}$ and $E_{2,7,3}^{(2)}$ on the $G_2^{(2)}$ lattice.

where

$$\mu^{(2)} = \begin{cases} 9/4 & \text{if } 3b + a - c \equiv 5 \pmod{6}; \\ 13/12 & \text{if } 3b + a - c \equiv 1 \pmod{6}; \\ 5/2 & \text{if } 3b + a - c \equiv 4 \pmod{6}; \\ 3/2 & \text{if } 3b + a - c \equiv 3 \pmod{6}; \\ 1 & \text{otherwise,} \end{cases}$$

$$\nu^{(2)} = \begin{cases} 9/4 & \text{if } 3b + a - c \equiv 1 \pmod{6}; \\ 13/12 & \text{if } 3b + a - c \equiv 5 \pmod{6}; \\ 5/2 & \text{if } 3b + a - c \equiv 2 \pmod{6}; \\ 3/2 & \text{if } 3b + a - c \equiv 3 \pmod{6}; \\ 1 & \text{otherwise.} \end{cases}$$

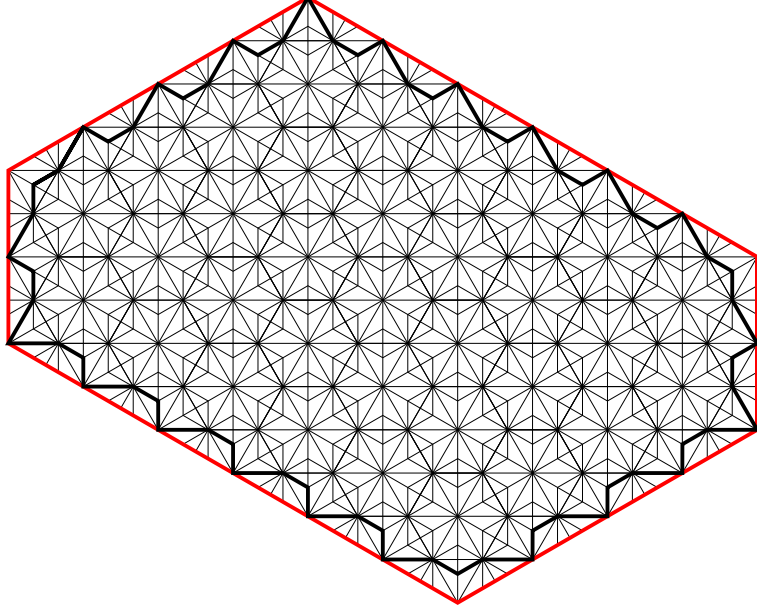


FIGURE 3.9. The variant $HD_{2,4,6}^{(2)}$ of the hexagonal dungeon $HD_{2,4,6}$ on the $G_2^{(2)}$ lattice.

(b) Assume that a and b are two positive integers, so that $b \geq 2a$. Then

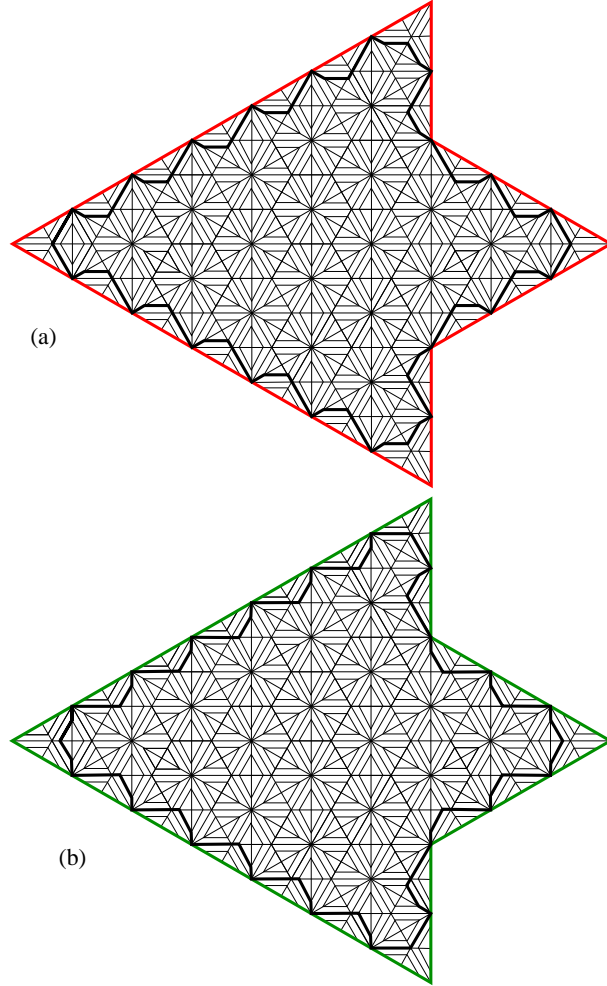
$$(3.13) \quad M\left(HD_{a,b,c}^{(2)}\right) = 17^{2a^2} 3^{3a^2 + 2\lfloor \frac{a^2}{2} \rfloor + 6ab + 3a - b + \gamma} 2^{9a^2 - 6a - 3\lfloor \frac{a^2}{2} \rfloor - \gamma},$$

where γ is defined as in Corollary 6.

Proof. Similar to Corollary 7, we consider the dual graphs of $D_{a,b,c}^{(2)}$, $E_{a,b,c}^{(2)}$, $HD_{a,b,c}^{(2)}$. They are obtained from the dual graphs of their corresponding counterpart in the lattice G_2 by applying the replacements in Figures 3.6(a) and (a2), (b) and (b2), and (c) and (c2).

Apply the spider lemma at all shaded cells, we get the dual graphs of the regions $D_{a,b,c}(x, y)$, $E_{a,b,c}(x, y)$, $HD_{a,b,c}(x, y)$ with $x = 1/2$ and $y = 3/2$, respectively. Then the corollary follows from Theorem 5 and Corollary 6. \square

Finally, we consider the application of replacing rule (c) in Figure 3.2 to all rhombi of the G_2 lattice, denoted by $G_2^{(3)}$ the resulting lattice. Denote also by $D_{a,b,c}^{(3)}$, $E_{a,b,c}^{(3)}$, and $HD_{a,2a,b}^{(3)}$ the variants of the regions $D_{a,b,c}$, $E_{a,b,c}$, and $HD_{a,2a,b}$, respectively, illustrated in Figures 3.10, 3.11, and 3.12. We can enumerate the tilings of the above new regions by the following corollary.

FIGURE 3.10. The region $D_{7,7,2}^{(3)}$ and $E_{7,2,2}^{(3)}$ on the $G_2^{(3)}$ lattice.

Corollary 9. (a) Assume that a , b , and c are three nonnegative integers satisfying $b \geq 2$, $2b - a - 2c \geq 0$ and $3b - 2a - 2c \geq 0$. Then

$$\begin{aligned}
 \text{M} \left(D_{a,b,c}^{(3)} \right) &= \mu^{(3)} 109^{q(a,b,c)} 13^{2g(a,b,c)+q(a,b,c)} 5^{g(a,b,c)} \\
 &\quad \times 3^{2(b-c-1)(c+d-1)+c(c-1)+f(f-1)+q(a,b,c)+(d-1)+(a-1)+c+\min(a-c-d,0)} \\
 (3.14) \quad &\quad \times 2^{(b-c)(c+d+1)+c(c+1)/2+f(f+1)/2-a+c+d-\min(a-c-d,0)-3g(a,b,c)-5q(a,b,c)},
 \end{aligned}$$

$$\begin{aligned}
 \text{M} \left(E_{a,b,c}^{(3)} \right) &= \nu^{(3)} 109^{q(a,b,c)} 13^{2g(a,b,c)+q(a,b,c)} 5^{g(a,b,c)} \\
 &\quad \times 3^{2(b-c-1)(c+d-1)+c(c-1)+f(f-1)+q(a,b,c)+(d-1)+(a-1)+c+\min(a-c-d,0)} \\
 (3.15) \quad &\quad \times 2^{(b-c)(c+d+1)+c(c+1)/2+f(f+1)/2-a+c+d-\min(a-c-d,0)-3g(a,b,c)-5q(a,b,c)},
 \end{aligned}$$

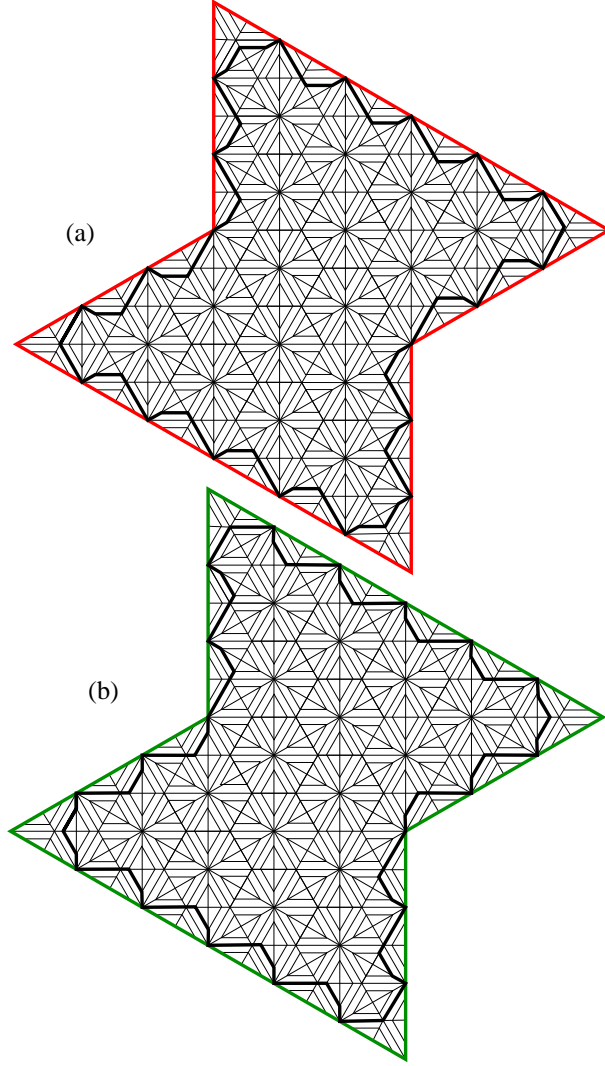


FIGURE 3.11. The region $D_{3,6,3}^{(3)}$ and $E_{3,6,3}^{(3)}$ on the $G_2^{(3)}$ lattice.

where

$$\mu^{(3)} = \begin{cases} 267/16 & \text{if } 3b + a - c \equiv 5 \pmod{6}; \\ 31/4 & \text{if } 3b + a - c \equiv 1 \pmod{6}; \\ 9/2 & \text{if } 3b + a - c \equiv 4 \pmod{6}; \\ 3/2 & \text{if } 3b + a - c \equiv 3 \pmod{6}; \\ 1 & \text{otherwise,} \end{cases}$$

$$\nu^{(3)} = \begin{cases} 267/16 & \text{if } 3b + a - c \equiv 1 \pmod{6}; \\ 31/4 & \text{if } 3b + a - c \equiv 5 \pmod{6}; \\ 9/2 & \text{if } 3b + a - c \equiv 2 \pmod{6}; \\ 3/2 & \text{if } 3b + a - c \equiv 3 \pmod{6}; \\ 1 & \text{otherwise.} \end{cases}$$

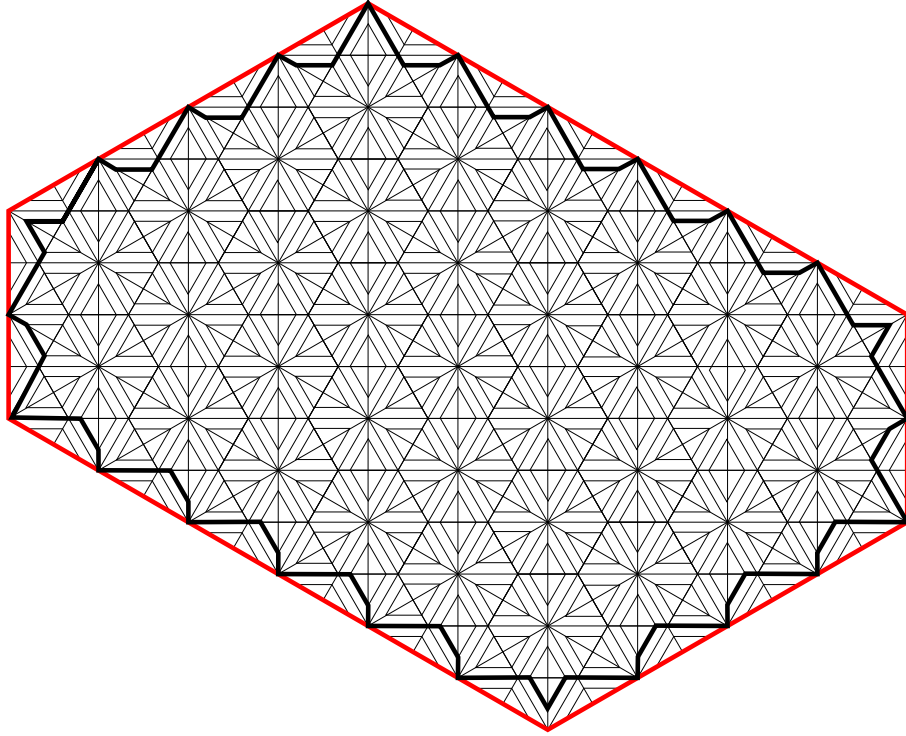


FIGURE 3.12. The variant $HD_{2,4,6}^{(3)}$ of the hexagonal dungeon $HD_{2,4,6}$ on the $G_2^{(3)}$ lattice.

(b) Assume that a and b are two positive integers, so that $b \geq 2a$. Then

$$(3.16) \quad M\left(HD_{a,b,c}^{(3)}\right) = 109^{\lfloor \frac{a^2}{2} \rfloor} 13^{4a^2 + \lfloor \frac{a^2}{2} \rfloor} 5^{2a^2} 3^{9ab - 3a^2 + \lfloor \frac{a^2}{2} \rfloor + 3a - b + \gamma} 2^{9a^2 - 6a - \lfloor \frac{a^2}{2} \rfloor - \gamma},$$

where γ is defined as in Corollary 6.

Proof. The dual graph of $D_{a,b,c}^{(3)}$, $E_{a,b,c}^{(3)}$ and $HD_{a,2a,b}^{(3)}$ are obtained from the dual graph of $D_{a,b,c}$, $E_{a,b,c}$ and $HD_{a,2a,b}$ by applying the replacements as in Figures 3.6(a) and (a3), (b) and (b3), and (c) and (c3). Similar to Corollaries 7 and 8, this corollary follows from Theorem 5 and Corollary 6 for $x = y = 3/2$. \square

Similar to the Lemmas 4.1–4.3 in [2], we have the following three lemmas by applying Kuo's graphical condensation theorem.

First, we present the weighted version of Lemma 4.1 in [2] as below.

Lemma 10. Let a , b and c be nonnegative integers so that $b \geq 5$, $c \geq 2$, $d := 2b - a - 2c \geq 0$, and $3b - 2a - 2c \geq 0$. Assume in addition that $a \geq c + d + 1$. Then

$$(3.17) \quad \begin{aligned} M(D_{a,b,c}(x, y)) M(D_{a-3,b-3,c-2}(x, y)) &= xy^2 M(D_{a-2,b-1,c}(x, y)) M(D_{a-1,b-2,c-2}(x, y)) \\ &\quad + x^2 y^4 M(D_{a-1,b-1,c-1}(x, y)) M(D_{a-2,b-2,c-1}(x, y)), \end{aligned}$$

and

(3.18)

$$\begin{aligned} M(E_{a,b,c}(x,y)) M(E_{a-3,b-3,c-2}(x,y)) &= xy^2 M(E_{a-2,b-1,c}(x,y)) M(E_{a-1,b-2,c-2}(x,y)) \\ &\quad + x^2 y^4 M(E_{a-1,b-1,c-1}(x,y)) M(E_{a-2,b-2,c-1}(x,y)). \end{aligned}$$

Proof. Apply the Kuo's Theorem 4 to the dual graph of the region $D_{a,b,c}(x,y)$ with the four vertices u, v, w, t chosen as in Figure 3.13(a). We notice that the positions of the four vertices u, v, w, t is exactly the same as that of the four vertices selected in the proof of Lemma 4.1 in [2].

By collecting the weights of forced edges (shown by circled edges in Figures 3.13(b)–(f)), we get

$$(3.19) \quad M(G - \{u, v\}) = x^{a+f-3} y^{2a+2f-7} M(D_{a-2,b-1,c}(x,y)),$$

$$(3.20) \quad M(G - \{v, w\}) = x^{c+f-2} y^{2c+2f-4} M(D_{a-1,b-1,c-1}(x,y)),$$

$$(3.21) \quad M(G - \{w, t\}) = x^{b+c-3} y^{2b+2c-7} M(D_{a-1,b-2,c-2}(x,y)),$$

$$(3.22) \quad M(G - \{t, u\}) = x^{a+b-3} y^{2a+2b-8} M(D_{a-2,b-2,c-1}(x,y)),$$

$$(3.23) \quad M(G - \{u, v, w, t\}) = x^{a+b+c+f-7} y^{2a+2b+2c+2f-16} M(D_{a-3,b-3,c-2}(x,y)).$$

Plug in the above equalities into the equation (2.9), we get (3.17).

Similarly, we obtain (3.18) by applying Theorem 4 to the dual graph of $E_{a,b,c}$ with the four vertices u, v, w, t chosen as in Figure 3.14. \square

By applying the Kuo's Theorem 4 to the dual graphs of $D_{a,b,c}(x,y)$ (similarly, the dual graph of $E_{a,b,c}(x,y)$) as in Figures 3.15 and 3.16, we get the following generalization of Lemma 4.2 in [2].

Lemma 11. *Let a, b and c be nonnegative integers satisfying $a \geq 2$, $b \geq 4$, $d := 2b - a - 2c \geq 2$, and $e := 3b - 2a - 2c \geq 2$.*

(a). *If $c \geq 1$, then*

$$(3.24) \quad \begin{aligned} M(D_{a,b,c}(x,y)) M(D_{a-2,b-2,c}(x,y)) &= x^2 y^4 M(D_{a-1,b-1,c}(x,y))^2 \\ &\quad + M(D_{a,b,c+1}(x,y)) M(D_{a-2,b-2,c-1}(x,y)) \end{aligned}$$

and

$$(3.25) \quad \begin{aligned} M(E_{a,b,c}(x,y)) M(E_{a-2,b-2,c}(x,y)) &= x^2 y^4 M(E_{a-1,b-1,c}(x,y))^2 \\ &\quad + M(E_{a,b,c+1}(x,y)) M(E_{a-2,b-2,c-1}(x,y)). \end{aligned}$$

(b). *If $c = 0$, then*

$$(3.26) \quad \begin{aligned} M(D_{a,b,0}(x,y)) M(D_{a-2,b-2,0}(x,y)) &= x^2 y^4 M(D_{a-1,b-1,0}(x,y))^2 \\ &\quad + M(D_{a,b,1}(x,y)) M(D_{e,d,1}(x,y)) \end{aligned}$$

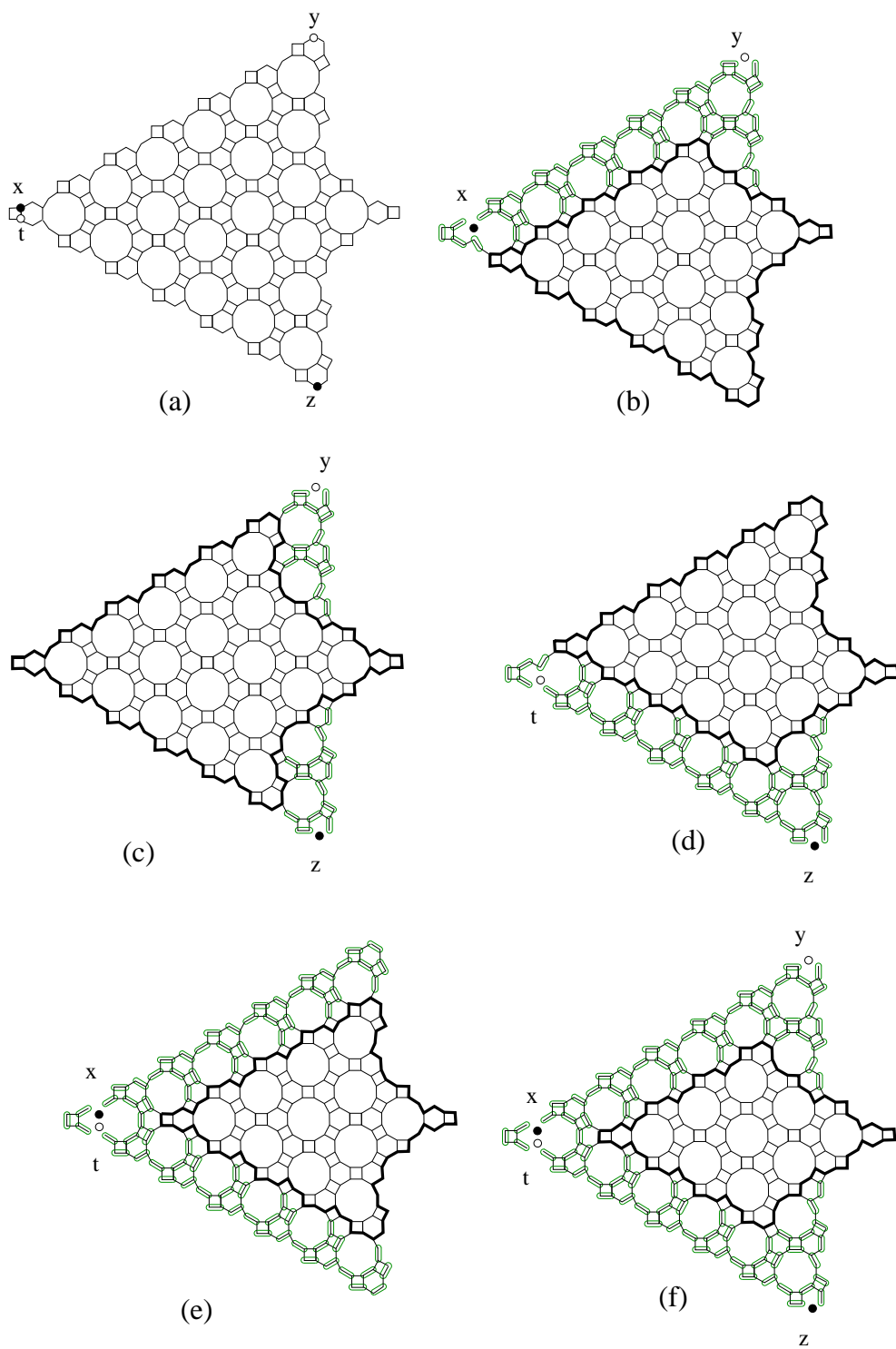


FIGURE 3.13. Illustrating the proof of equality (3.17) in Lemma 10. This Figure first appeared in [2].

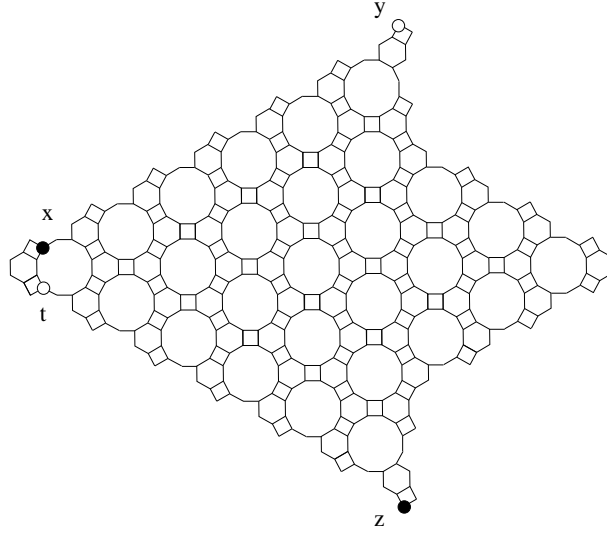


FIGURE 3.14. The dual graph of $E_{8,8,2}(x, y)$ and the four vertices u, v, w, t . This Figure was first appeared in [2]

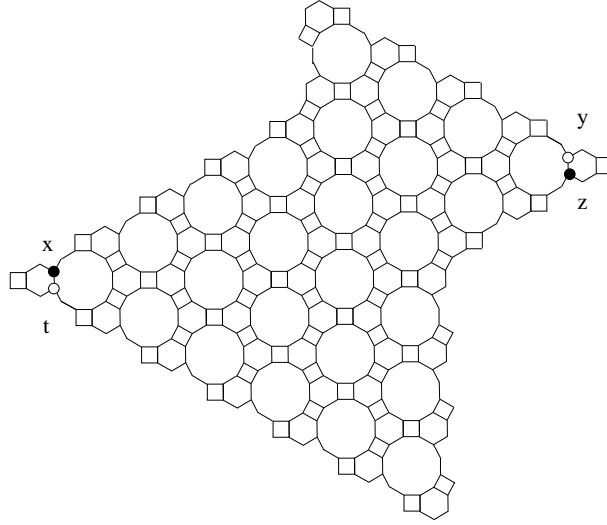


FIGURE 3.15. The dual graph of $D_{5,8,4}(x, y)$ and the four vertices u, v, w, t . This Figure first appeared in [2]

and

$$(3.27) \quad \begin{aligned} M(E_{a,b,0}(x, y)) M(E_{a-2,b-2,0}(x, y)) &= x^2 y^4 M(E_{a-1,b-1,0}(x, y))^2 \\ &\quad + M(E_{a,b,1}(x, y)) M(E_{e,d,1}(x, y)), \end{aligned}$$

where, as usual, $d = 2a - b - 2c$ and $e = 3a - 2b - 2c$.

Lemma 12. Assume that a, b, c are three nonnegative integers satisfying $a \geq 2$, $b \geq 5$, $c \geq 2$, $d := 2b - a - 2c \geq 0$, and $e := 3b - 2a - 2c \geq 0$. Assume in addition that $a \leq c + d$.

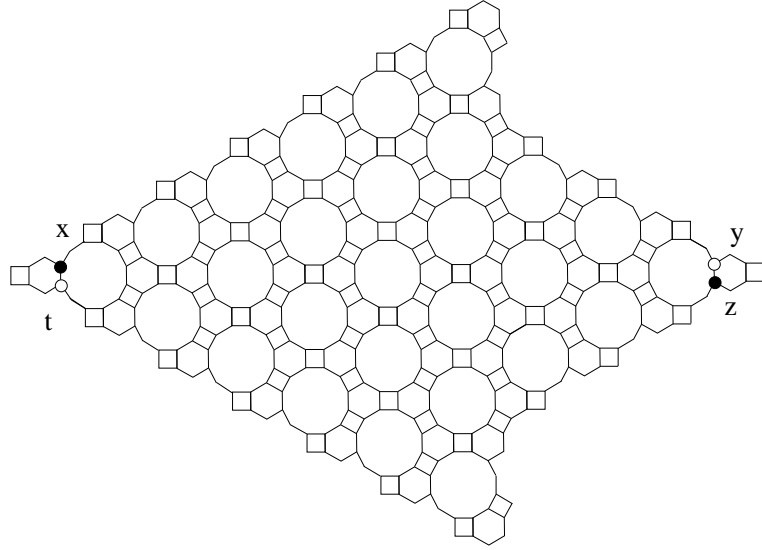


FIGURE 3.16. The dual graph of $D_{8,8,2}(x, y)$ and the four vertices u, v, w, t . This Figure first appeared in [2]

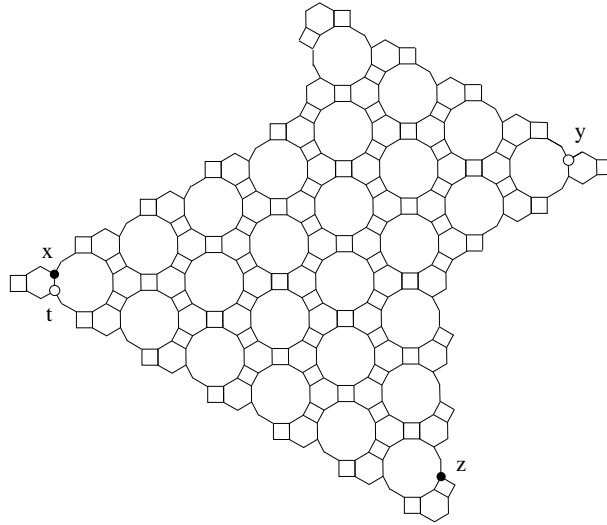


FIGURE 3.17. The dual graph of $D_{5,8,4}(x, y)$ and the vertices u, v, w, t . This Figure first appeared in [2]

(a). If $d \geq 1$, then

$$\begin{aligned}
 (3.28) \quad & M(D_{a,b,c}(x, y)) M(D_{a-2,b-3,c-2}(x, y)) = xy^2 M(D_{a-1,b-1,c}(x, y)) M(D_{a-1,b-2,c-2}(x, y)) \\
 & + xy^2 M(D_{a-2,b-2,c-1}(x, y)) M(D_{a,b-1,c-1}(x, y))
 \end{aligned}$$

and

(3.29)

$$\begin{aligned} M(E_{a,b,c}(x,y)) M(E_{a-2,b-3,c-2}(x,y)) &= xy^2 M(E_{a-1,b-1,c}(x,y)) M(E_{a-1,b-2,c-2}(x,y)) \\ &\quad + xy^2 M(E_{a-2,b-2,c-1}(x,y)) M(E_{a,b-1,c-1}(x,y)). \end{aligned}$$

(b). If $d = 0$, then

(3.30)

$$\begin{aligned} M(D_{a,b,c}(x,y)) M(D_{a-2,b-3,c-2}(x,y)) &= xy^2 M(E_{c,b-1,a-1}(x,y)) M(D_{a-1,b-2,c-2}(x,y)) \\ &\quad + xy^2 M(D_{a-2,b-2,c-1}(x,y)) M(D_{a,b-1,c-1}(x,y)) \end{aligned}$$

and

(3.31)

$$\begin{aligned} M(E_{a,b,c}(x,y)) M(E_{a-2,b-3,c-2}(x,y)) &= xy^2 M(D_{c,b-1,a-1}(x,y)) M(E_{a-1,b-2,c-2}(x,y)) \\ &\quad + xy^2 M(E_{a-2,b-2,c-1}(x,y)) M(E_{a,b-1,c-1}(x,y)). \end{aligned}$$

Outline of the proof of Theorem 5. We can prove the theorem by the same way as that of Theorem 2 in [2].

Denote by $\Phi(a, b, c; x, y)$ and $\Psi(a, b, c; x, y)$ the right hand sides of equalities in Theorem 5. One can verify that $\Phi(a, b, c; x, y)$ and $\Psi(a, b, c; x, y)$ satisfy the same recurrences in Lemma 10–12. The proof is completely similar to that of Lemmas 5.1–5.3 in [2]. This yields to an induction proof of the statement of the theorem.

For the base cases, we use **vaxmacs** and **Maple** to verify the statement of the theorem when at least one of the following condition hold:

$$(i) \mathcal{P}(a, b, c) \leq 14$$

$$(ii) b \leq 4$$

$$(iii) c + d \leq 2$$

For the induction step, we can repeat exactly the corresponding part in the proof of Theorem 2 in [2] \square

Remark 13. We notice that in the regions $D_{a,b,c}(x, y)$, $E_{a,b,c}(x, y)$ and $HD_{a,2a,b}(x, y)$ we assign each kite-shaped tile a weight 1. Of course we can weight these tiles by a weight $z > 0$ (each obtuse triangular tile is still weighted by x , and each equilateral triangular tile is still weighted by y). Denote by $D_{a,b,c}(x, y, z)$, $E_{a,b,c}(x, y, z)$ and $HD_{a,2a,b}(x, y, z)$ for the new weighted version of the regions $D_{a,b,c}$, $E_{a,b,c}$ and $HD_{a,2a,b}$, respectively. However, the tiling generating function of the new weighted regions can be obtained from the Theorem 5 and Corollary 6 as follows. We now divide the weights of each tiles in the region $D_{a,b,c}(x, y, z)$ by z . We get the weighted region $D_{a,b,c}\left(\frac{x}{z}, \frac{y}{z}\right)$ in Theorem 5 and obtain

$$(3.32) \quad M(D_{a,b,c}(x, y, z)) = 2^{C_1} M\left(D_{a,b,c}\left(\frac{x}{z}, \frac{y}{z}\right)\right),$$

where C_1 is the number of tiles in the region $D_{a,b,c}(x, y, z)$, and is also the number of tiles in $D_{a,b,c}$. The number of tiles C_1 is half of the number of fundamental regions in $D_{a,b,c}$. We count first the number of fundamental regions restricted in the contour $\mathcal{C}(a, b, c)$ is $12(b-c)(c+d) + 6c^2 + 6f^2$; and the number of fundamental regions inside the contour $\mathcal{C}(a, b, c)$ and outside the regions $D_{a,b,c}$ is $3P(a, b, c) - 4$. Thus,

$$C_1 = 6(b-c)(c+d) + 3c^2 + 3d^2 - \frac{3}{2}P(a, b, c) + 2.$$

Similarly, we get

$$(3.33) \quad M(E_{a,b,c}(x, y, z)) = 2^{C_1} M\left(E_{a,b,c}\left(\frac{x}{z}, \frac{y}{z}\right)\right),$$

and

$$(3.34) \quad M(HD_{a,2a,b}(x, y, z)) = 2^{C_2} M\left(HD_{a,2a,b}\left(\frac{x}{z}, \frac{y}{z}\right)\right),$$

where C_2 is the number of tiles in the region $HD_{a,2a,b}$, which is

$$6(3ab + 2a^2) - 3(3a + b).$$

4. SUBGRAPHS OF THE SQUARE GRID

In [4], [1] and [6], we investigate several families of (weighted) graphs on the square lattice whose perfect matchings are enumerated by perfect powers. However, (almost) all of those families consist of Aztec diamond graphs or its variants. In Section 4, we investigate new families of graphs in the square lattice inspired by hexagonal dungeons.

We first consider a well-known subgraph replacement trick called “urban renewal”. It was first discovered by Kuperberg.

Lemma 14. *Let G be a weighted graph. Assume that G has a subgraph K as one of the graphs on the left column in Figure 4.1, where only white vertices can be incident to vertices outside, and where all edges have weight 1. Let G' be the weighted graph obtained from G by replacing K by its corresponding graph K' on the right column of Figure 4.1, where all dotted edges have weight $\frac{1}{2}$, and where the shaded vertices are the new ones which were not in G . Then we always have $M(G) = 2M(G')$.*

We could classify the squares in the dual lattice of G_2 lattice into three types, based on their orientation: horizontal, southeast-to-northwest (SE-NW), and southwest-to-northeast (SW-NE) squares. Consider the appearances of SW-NE squares in the dual graph of the hexagonal dungeon $HD_{a,2a,b}$ (indicated by dotted triangles of the upper graph in Figure 4.2). Apply suitable replacement in Lemma 14, and deform the resulting graph into a weighted subgraph of the square grid (see the lower graph in Figure 4.2; the bold edges have weight $\frac{1}{2}$). By Theorem 1 and Lemma 14, the matching generating function of the new weighted graph is given by a product of some power of 2, 7 and 13. However, we are not interested in this immediate result;

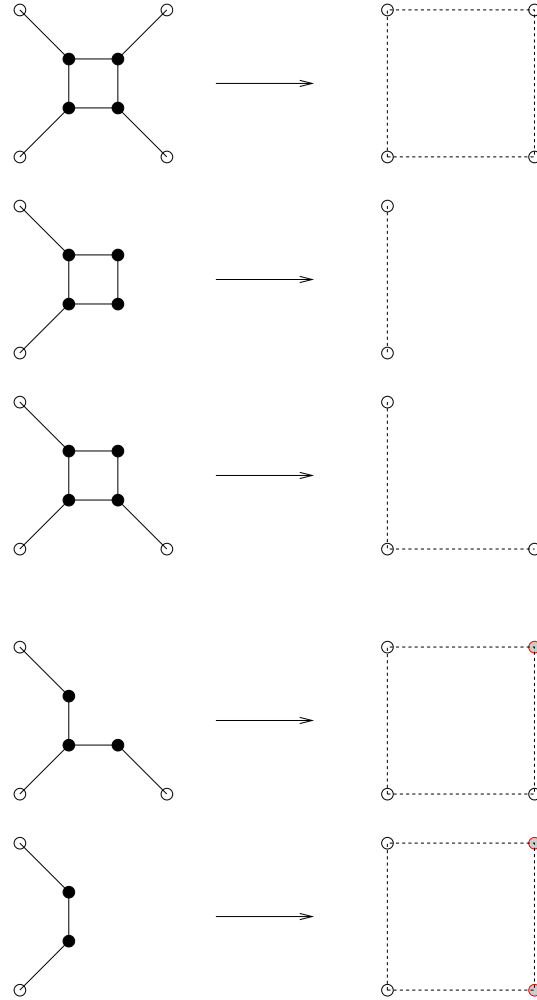


FIGURE 4.1. Urban renewal trick.

and we want to consider the new graph with different weight assignment. The most natural and simplest one is when all edges are weighted by 1. Denote by $G_{a,2a,b}$ the graph (i.e. all edges of $G_{a,2a,b}$ have weight 1).

Surprisingly, the number of perfect matching of $G_{a,2a,b}$ is given by perfect powers of 10 and 11.

Theorem 15. *Assume a and b are two positive integer so that $b \geq 2a$. Then number of perfect matchings of the graph $G_{a,2a,b}$ is*

$$10^{2a^2} 11^{\lfloor \frac{a^2}{2} \rfloor}.$$

In order to prove Theorem 15, we consider the following *six(!)* families of graphs.

First, we apply the suitable replacement rules in Lemma 14 at the position of each horizontal square (see the dotted rectangles in Figure 4.3(a)). We can deform the resulting graph into a weighted subgraph H of the square grid (see Figure 4.3(b);

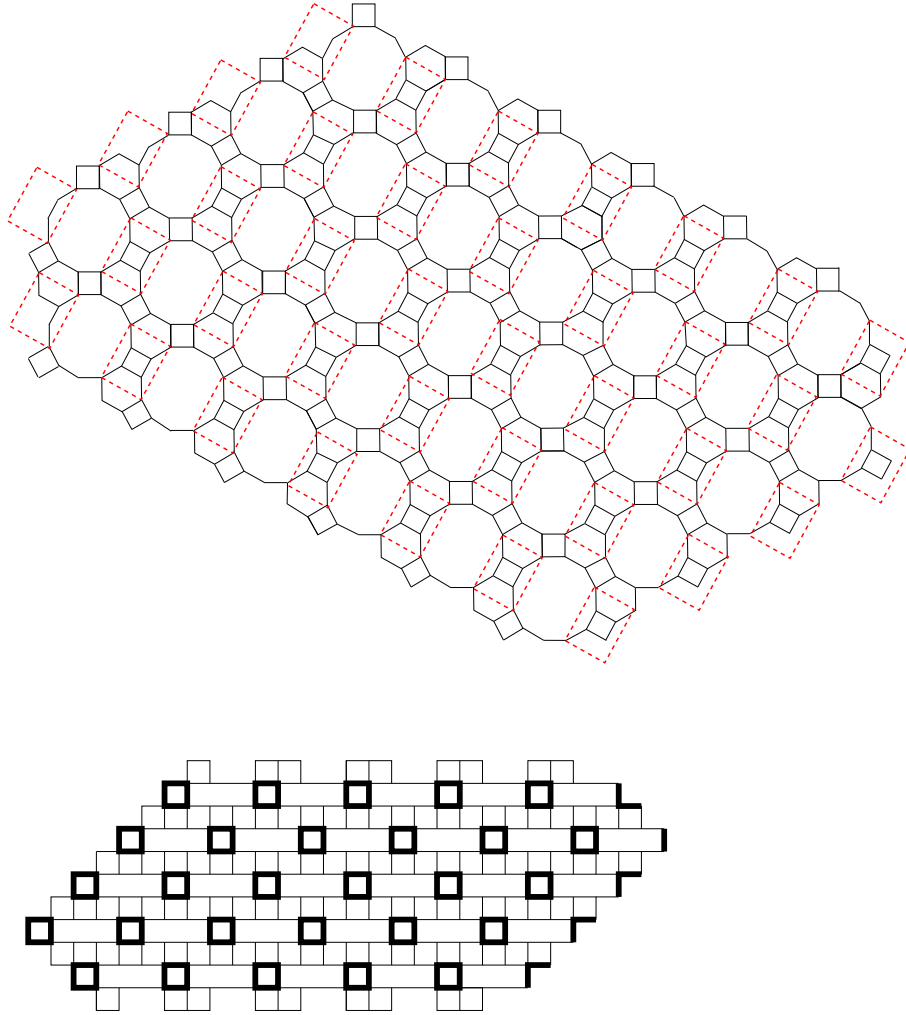


FIGURE 4.2. Deforming the dual graph of $HD_{2,4,6}$ into a weighted subgraph of the square grid.

the bold edges have weight $\frac{1}{2}$). We change the weights of edges of H to 1, and denote by $A_{a,b,c}^{(1)}$ the un-weighted version of H .

We do the same process with the other types of squares (see Figures 4.3(c)–(e)) and get two more weighted subgraphs of the square grid. Denote by $A_{a,b,c}^{(2)}$ and $A_{a,b,c}^{(3)}$ the un-weighted version of them, respectively. These three (un-weighted) graphs are illustrated in Figure 4.4 for the case $a > c+d$, and in Figure 4.6 for the case $a \leq c+d$. Denote by $F_{a,b,c}^{(1)}$, $F_{a,b,c}^{(2)}$ and $F_{a,b,c}^{(3)}$ the graphs obtained from the same process for the dual graph of the region $E_{a,b,c}$, respectively. These three graphs are illustrated in Figure 4.5 for the case $a > c+d$, and in Figure 4.7 for the case $a \leq c+d$.

We have the following theorem on the numbers of perfect matchings of the above six families of graphs.

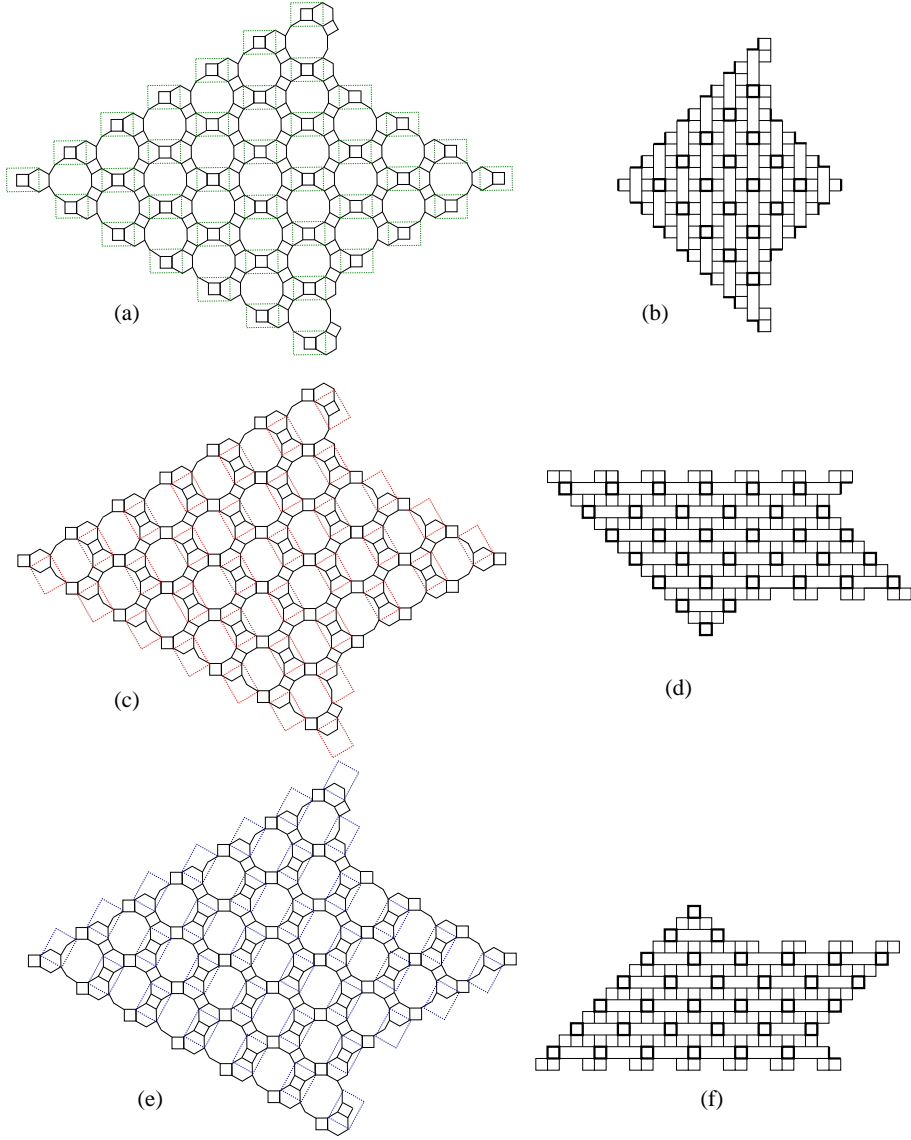


FIGURE 4.3. Deforming the dual graph of $D_{8,8,2}$ into weighted subgraphs of the square grid.

Theorem 16. Assume that a , b , and c are three nonnegative integers satisfying $b \geq 2$, $2b - a - 2c \geq 0$ and $3b - 2a - 2c \geq 0$. Then the numbers of perfect matchings of the six graphs above can be obtained by the following formulas

$$(4.1) \quad M\left(A_{a,b,c}^{(1)}\right) = \alpha(a, b, c) 2^{g(a,b,c+1)} 5^{g(a,b,c)} 11^{q(a,b,c)},$$

$$(4.2) \quad M\left(A_{a,b,c}^{(2)}\right) = \alpha(a, b, c) 2^{g(a,b,c-1) - \lfloor (a-c+1)/3 \rfloor + (a-b)} 5^{g(a,b,c)} 11^{q(a,b,c)},$$

$$(4.3) \quad M\left(A_{a,b,c}^{(3)}\right) = \alpha(a, b, c) 2^{g(a,b,c-1) - \lfloor (a-c+1)/3 \rfloor} 5^{g(a,b,c)} 11^{q(a,b,c)},$$

$$(4.4) \quad M\left(F_{a,b,c}^{(1)}\right) = \beta(a, b, c) 2^{g(a,b,c-1)} 5^{g(a,b,c)} 11^{q(a,b,c)},$$

$$(4.5) \quad M\left(F_{a,b,c}^{(2)}\right) = \beta(a, b, c) 2^{g(a,b,c+1)+\lfloor (a-c+1)/3 \rfloor - (a-b)} 5^{g(a,b,c)} 11^{q(a,b,c)},$$

$$(4.6) \quad M\left(F_{a,b,c}^{(3)}\right) = \beta(a, b, c) 2^{g(a,b,c+1)+\lfloor (a-c+1)/3 \rfloor} 5^{g(a,b,c)} 11^{q(a,b,c)},$$

where $q(a, b, c)$ and $g(a, b, c)$ are defined as in Theorem 2, and where

$$(4.7) \quad \alpha(a, b, c) := \begin{cases} 2 & \text{if } 3b + a - c \equiv 1 \pmod{6}; \\ 3 & \text{if } 3b + a - c \equiv 5 \pmod{6}; \\ 1 & \text{otherwise,} \end{cases}$$

$$(4.8) \quad \beta(a, b, c) := \begin{cases} 3 & \text{if } 3b + a - c \equiv 1 \pmod{6}; \\ 2 & \text{if } 3b + a - c \equiv 2 \pmod{6}; \\ 1 & \text{otherwise.} \end{cases}$$

Similar to Lemma 4.1–4.3 in [2], we have the following recurrences from Kuo's graphical condensation.

Lemma 17. *Let a, b and c be nonnegative integers so that $b \geq 5$, $c \geq 2$, $d := 2b - a - 2c \geq 0$, and $3b - 2a - 2c \geq 0$. Assume in addition that $a \geq c + d + 1$. Then for $i = 1, 2, 3$*

$$(4.9) \quad M\left(A_{a,b,c}^{(i)}\right) M\left(A_{a-3,b-3,c-2}^{(i)}\right) = M\left(A_{a-2,b-1,c}^{(i)}\right) M\left(A_{a-1,b-2,c-2}^{(i)}\right) \\ + M\left(A_{a-1,b-1,c-1}^{(i)}\right) M\left(A_{a-2,b-2,c-1}^{(i)}\right)$$

and

$$(4.10) \quad M\left(F_{a,b,c}^{(i)}\right) M\left(F_{a-3,b-3,c-2}^{(i)}\right) = M\left(F_{a-2,b-1,c}^{(i)}\right) M\left(F_{a-1,b-2,c-2}^{(i)}\right) \\ + M\left(F_{a-1,b-1,c-1}^{(i)}\right) M\left(F_{a-2,b-2,c-1}^{(i)}\right).$$

Proof. This lemma can be proved similarly to Theorem 10. Apply Kuo's theorem to the graphs $A_{a,b,c}^{(i)}$ with four vertices x, y, z, t chosen as in Figure 4.4, we get (4.9). Apply the same process to the graphs $F_{a,b,c}^{(i)}$ with four vertices x, y, z, t chosen as in Figure 4.5, we get (4.10). \square

Lemma 18. *Let a, b and c be nonnegative integers satisfying $a \geq 2$, $b \geq 4$, $d := 2b - a - 2c \geq 2$, and $e := 3b - 2a - 2c \geq 2$.*

(a) *If $c \geq 1$, then for $i = 1, 2, 3$*

$$(4.11) \quad M\left(A_{a,b,c}^{(i)}\right) M\left(A_{a-2,b-2,c}^{(i)}\right) = M\left(A_{a-1,b-1,c}^{(i)}\right) M\left(A_{a-1,b-1,c}^{(i)}\right) \\ + M\left(A_{a,b,c+1}^{(i)}\right) M\left(A_{a-2,b-2,c-1}^{(i)}\right)$$

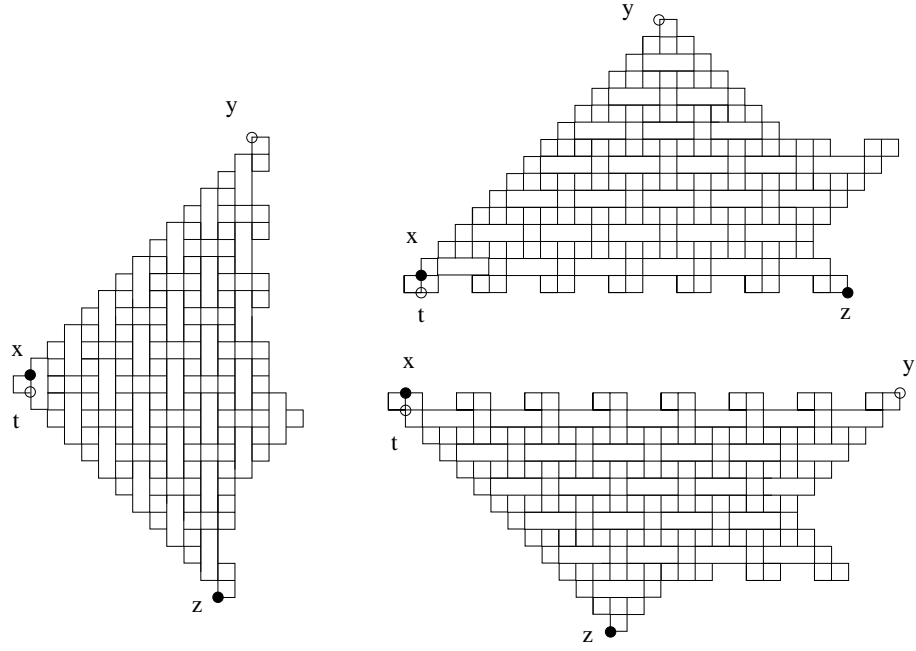


FIGURE 4.4. The graphs $A_{9,8,2}^{(1)}$, left, $A_{9,8,2}^{(2)}$, upper-right, and $A_{9,8,2}^{(3)}$, lower-right

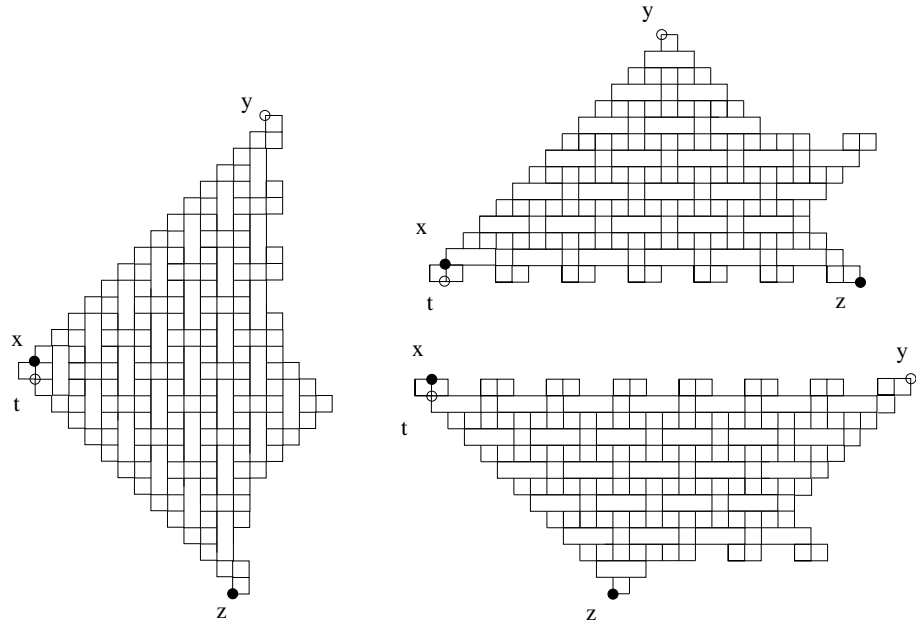


FIGURE 4.5. The graphs $F_{9,8,2}^{(1)}$, left, $F_{9,8,2}^{(2)}$, upper-right, and $F_{9,8,2}^{(3)}$, lower-right

and

$$(4.12) \quad \begin{aligned} M(F_{a,b,c}^{(i)}) M(F_{a-2,b-2,c}^{(i)}) &= M(F_{a-1,b-1,c}^{(i)}) M(F_{a-1,b-1,c}^{(i)}) \\ &\quad + M(F_{a,b,c+1}^{(i)}) M(F_{a-2,b-2,c-1}^{(i)}). \end{aligned}$$

(b) If $c = 0$, then

$$(4.13) \quad \begin{aligned} M(A_{a,b,0}^{(1)}) M(A_{a-2,b-2,0}^{(1)}) &= M(A_{a-1,b-1,0}^{(1)}) M(A_{a-1,b-1,0}^{(1)}) \\ &\quad + M(A_{a,b,1}^{(1)}) M(A_{e,d,1}^{(1)}) \end{aligned}$$

$$(4.14) \quad \begin{aligned} M(A_{a,b,0}^{(2)}) M(A_{a-2,b-2,0}^{(2)}) &= M(A_{a-1,b-1,0}^{(2)}) M(A_{a-1,b-1,0}^{(2)}) \\ &\quad + M(A_{a,b,1}^{(2)}) M(A_{e,d,1}^{(3)}) \end{aligned}$$

$$(4.15) \quad \begin{aligned} M(A_{a,b,0}^{(3)}) M(A_{a-2,b-2,0}^{(3)}) &= M(A_{a-1,b-1,0}^{(3)}) M(A_{a-1,b-1,0}^{(3)}) \\ &\quad + M(A_{a,b,1}^{(3)}) M(A_{e,d,1}^{(2)}), \end{aligned}$$

$$(4.16) \quad \begin{aligned} M(F_{a,b,0}^{(1)}) M(F_{a-2,b-2,0}^{(1)}) &= M(F_{a-1,b-1,0}^{(1)}) M(F_{a-1,b-1,0}^{(1)}) \\ &\quad + M(F_{a,b,1}^{(1)}) M(F_{e,d,1}^{(1)}), \end{aligned}$$

$$(4.17) \quad \begin{aligned} M(F_{a,b,0}^{(2)}) M(F_{a-2,b-2,0}^{(2)}) &= M(F_{a-1,b-1,0}^{(2)}) M(F_{a-1,b-1,0}^{(2)}) \\ &\quad + M(F_{a,b,1}^{(2)}) M(F_{e,d,1}^{(3)}), \end{aligned}$$

$$(4.18) \quad \begin{aligned} M(F_{a,b,0}^{(3)}) M(F_{a-2,b-2,0}^{(3)}) &= M(F_{a-1,b-1,0}^{(3)}) M(F_{a-1,b-1,0}^{(3)}) \\ &\quad + M(F_{a,b,1}^{(3)}) M(F_{e,d,1}^{(2)}). \end{aligned}$$

Proof. (a) This part is completely analogous to Theorem 11(a). Apply Kuo's theorem 4 to the graphs $A_{a,b,c}^{(i)}$ with four vertices x, y, z, t located as in Figure 4.6, we get (4.11). The recurrence (4.12) is obtained from applying Theorem 4 to the graphs $F_{a,b,c}^{(i)}$ with four vertices x, y, z, t as in Figure 4.7, for $a = 3$, $b = 8$ and $c = 3$.

(b) Apply Kuo's theorem to the graph $A_{a,b,c}^{(1)}$ (resp., $A_{a,b,c}^{(2)}$, $A_{a,b,c}^{(3)}$) with four vertices x, y, z, t as in Figure 4.8, for $a = 4$, $b = 5$ and $c = 0$. Note that the graph after removing x and t , and then removing forced edges (the one restricted by the bold contour) is isomorphic to $A_{(e,d,1)}^{(1)}$ (resp., $A_{e,d,1}^{(3)}$, $A_{e,d,1}^{(2)}$). Therefore we get (4.13) (resp., (4.14), (4.15)).

The recurrences (4.15), (4.16), (4.17) are obtained similarly, based on Figure 4.9, for $a = 4$, $b = 5$ and $c = 0$. \square

Lemma 19. Assume that a, b, c are three nonnegative integers satisfying $a \geq 2$, $b \geq 5$, $c \geq 2$, $d := 2b - a - 2c \geq 0$, and $e := 3b - 2a - 2c \geq 0$. Assume in addition that $a \leq c + d$.

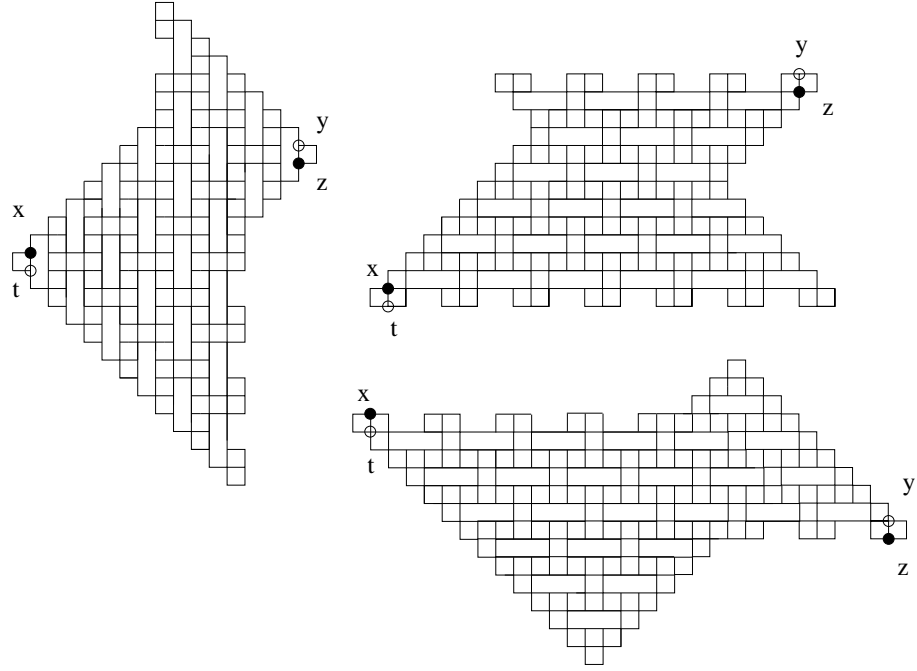


FIGURE 4.6. The graphs $A_{5,8,4}^{(1)}$, left, $A_{5,8,4}^{(2)}$, upper-right, and $A_{5,8,4}^{(3)}$, lower-right

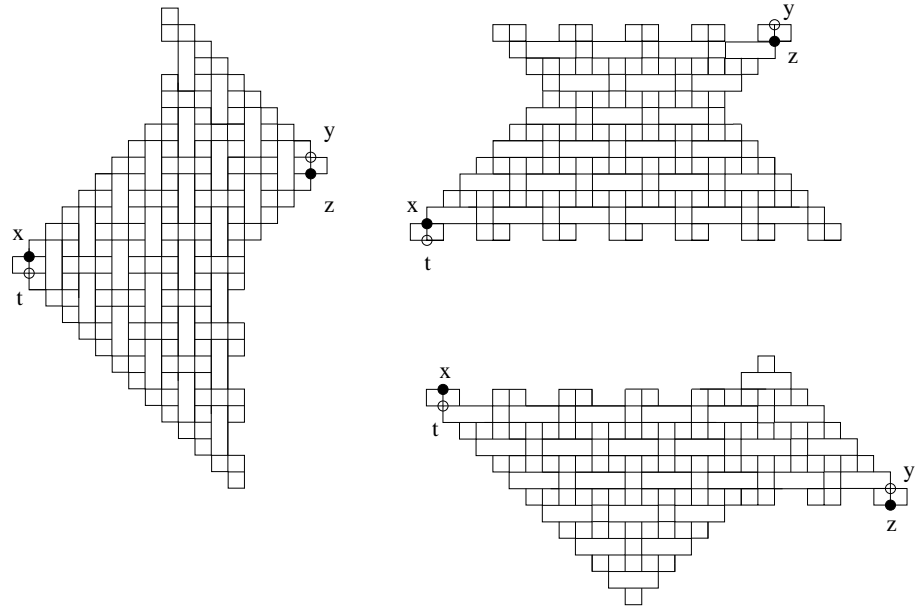


FIGURE 4.7. The graphs $F_{5,8,4}^{(1)}$, left, $F_{5,8,4}^{(2)}$, upper-right, and $F_{5,8,4}^{(3)}$, lower-right

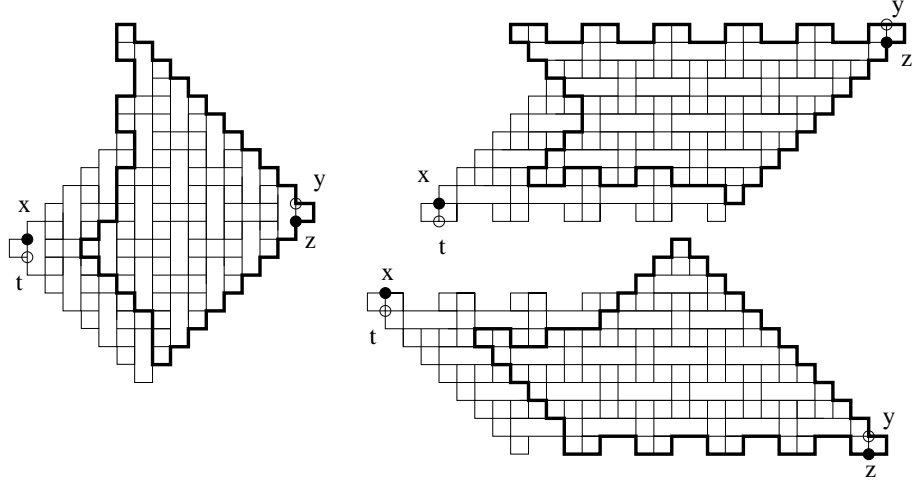


FIGURE 4.8. The graphs $A_{4,5,0}^{(1)}$, left, $A_{4,5,0}^{(2)}$, upper-right, and $A_{4,5,0}^{(3)}$, lower-right

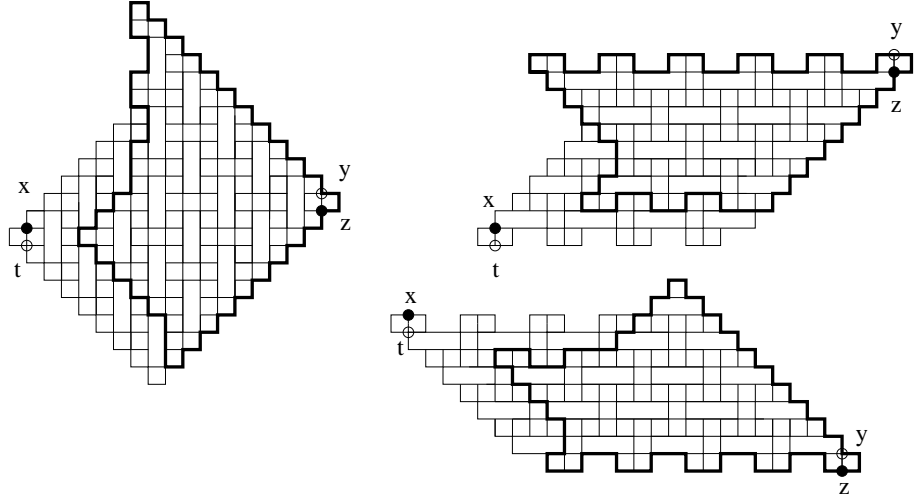


FIGURE 4.9. The graphs $F_{4,5,0}^{(1)}$, left, $F_{4,5,0}^{(2)}$, upper-right, and $F_{4,5,0}^{(3)}$, lower-right

(a) If $d \geq 1$, then for $i = 1, 2, 3$

$$(4.19) \quad \begin{aligned} M(A_{a,b,c}^{(i)}) M(A_{a-2,b-3,c-2}^{(i)}) &= M(A_{a-1,b-1,c}^{(i)}) M(A_{a-1,b-2,c-2}^{(i)}) \\ &\quad + M(A_{a-2,b-2,c-1}^{(i)}) M(A_{a,b-1,c-1}^{(i)}) \end{aligned}$$

and

$$(4.20) \quad \begin{aligned} M(F_{a,b,c}^{(i)}) M(F_{a-2,b-3,c-2}^{(i)}) &= M(F_{a-1,b-1,c}^{(i)}) M(F_{a-1,b-2,c-2}^{(i)}) \\ &\quad + M(F_{a-2,b-2,c-1}^{(i)}) M(F_{a,b-1,c-1}^{(i)}) . \end{aligned}$$

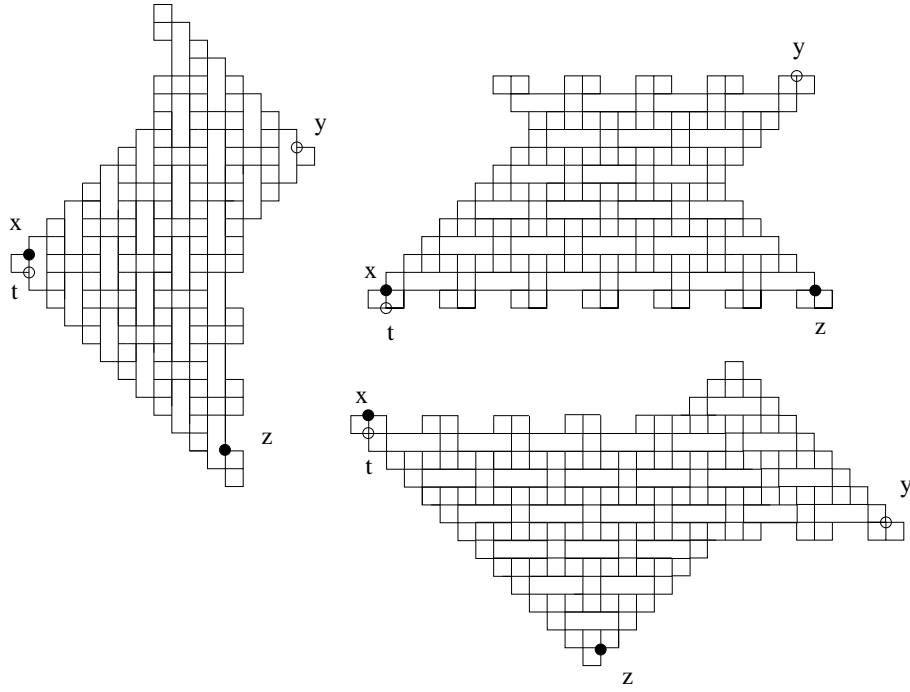


FIGURE 4.10. The graphs $A_{5,8,4}^{(1)}$, left, $A_{5,8,4}^{(2)}$, upper-right, and $A_{5,8,4}^{(3)}$, lower-right, with the selection of vertices x, y, z, t in Lemma 19

(b) If $d = 0$, then for $i = 1, 2, 3$

$$(4.21) \quad \begin{aligned} M\left(A_{a,b,c}^{(i)}\right) M\left(A_{a-2,b-3,c-2}^{(i)}\right) &= M\left(F_{c,b-1,a-1}^{(4-i)}\right) M\left(A_{a-1,b-2,c-2}^{(i)}\right) \\ &\quad + M\left(A_{a-2,b-2,c-1}^{(i)}\right) M\left(A_{a,b-1,c-1}^{(i)}\right) \end{aligned}$$

and

$$(4.22) \quad \begin{aligned} M\left(F_{a,b,c}^{(i)}\right) M\left(F_{a-2,b-3,c-2}^{(i)}\right) &= M\left(A_{c,b-1,a-1}^{(4-i)}\right) M\left(F_{a-1,b-2,c-2}^{(i)}\right) \\ &\quad + M\left(F_{a-2,b-2,c-1}^{(i)}\right) M\left(F_{a,b-1,c-1}^{(i)}\right). \end{aligned}$$

Proof. (a) Apply Kuo's theorem to the graph $A_{a,b,c}^{(i)}$ with four vertices x, y, z, t chosen as in Figure 4.10, for $a = 3$, $b = 8$ and $c = 3$, we get (4.19). Apply similar process to the graph $F_{a,b,c}^{(i)}$ with four vertices x, y, z, t as in Figure 4.11, for $a = 3$, $b = 8$ and $c = 3$, we get (4.20).

(b) Apply Kuo's theorem to the graphs $A_{a,b,c}^{(i)}$ (resp., $F_{a,b,c}^{(i)}$) with four vertices x, y, z, t as in Figure 4.12 (resp., Figure 4.13), for $a = 4$, $b = 8$ and $c = 6$. Note that the graph after removing two vertices x and y , and then removing forced edges (the graph restricted by the bold contour) is isomorphic to $F_{a,b,c}^{(4-i)}$ (resp., $A_{a,b,c}^{(4-i)}$). We get (4.21) (resp., (4.22)). \square

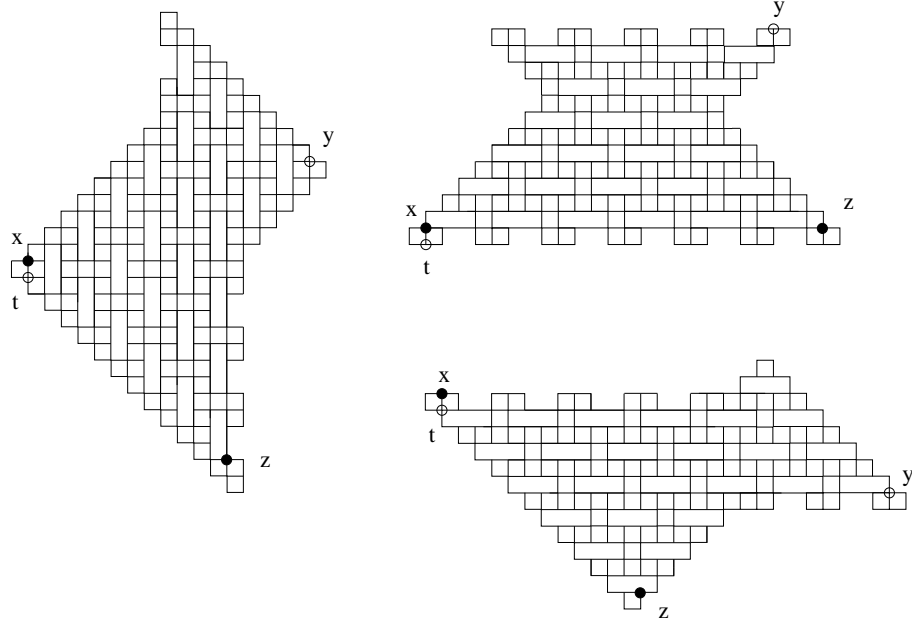


FIGURE 4.11. The graphs $F_{5,8,4}^{(1)}$, left, $F_{5,8,4}^{(2)}$, upper-right, and $F_{5,8,4}^{(3)}$, lower-right, with the selection of vertices x, y, z, t in Lemma 19

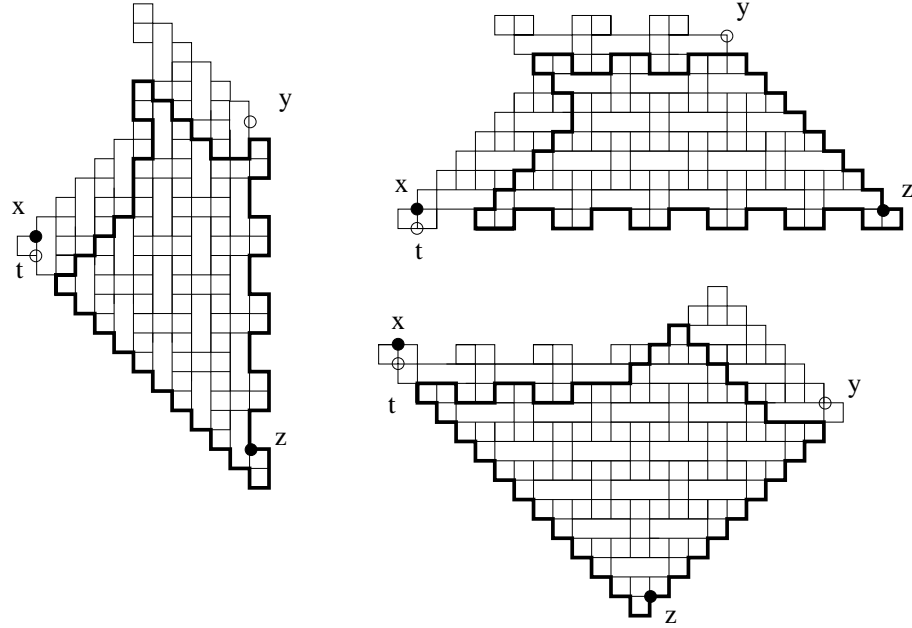


FIGURE 4.12. The graphs $A_{4,8,6}^{(1)}$, left, $A_{4,8,6}^{(2)}$, upper-right, and $A_{4,8,6}^{(3)}$, lower-right

Denote by $\Psi_i(a, b, c)$, for $i = 1, 2, \dots, 6$, the right hand sides of equations in Theorem 16, respectively. Denote $k_i(a, b, c)$ by the exponent of 2 in $\Psi_i(a, b, c)$, for $i = 1, 2, \dots, 6$. In particular, $k_1(a, b, c) = g(a, b, c + 1)$, $k_2(a, b, c) = g(a, b, c - 1) -$

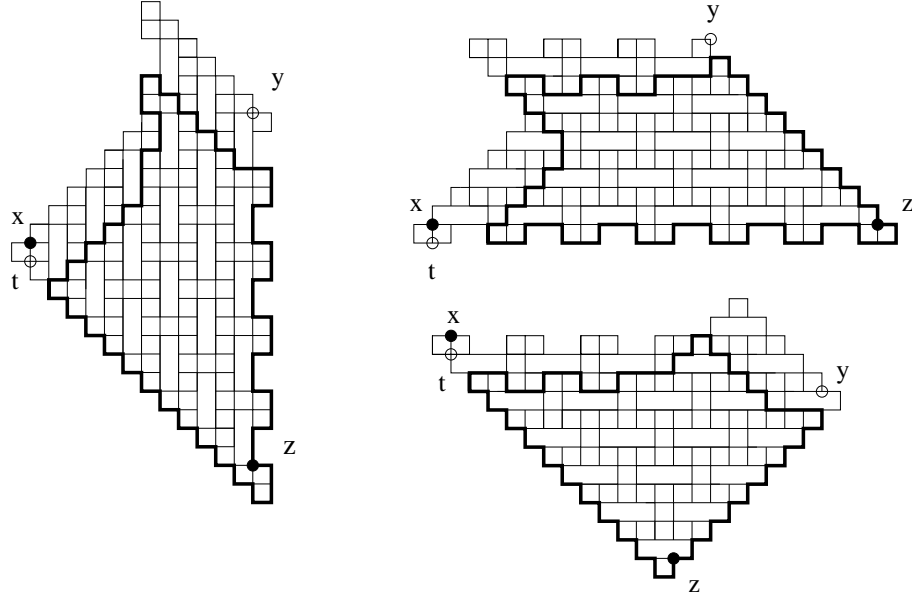


FIGURE 4.13. The graphs $F_{4,8,6}^{(1)}$, left, $F_{4,8,6}^{(2)}$, upper-right, and $F_{4,8,6}^{(3)}$, lower-right

$\lfloor (a - c + 1)/3 \rfloor + (a - b)$, $k_3(a, b, c) = g(a, b, c - 1) - \lfloor (a - c + 1)/3 \rfloor$, $k_4(a, b, c) = g(a, b, c - 1)$, $k_5(a, b, c) = g(a, b, c + 1) + \lfloor (a - c + 1)/3 \rfloor - (a - b)$ and $k_6(a, b, c) = g(a, b, c + 1) + \lfloor (a - c + 1)/3 \rfloor$. Similar to the proof of Theorem 2 (shown in [2]), we next show that the functions $\Psi_i(a, b, c)$, for $i = 1, 2, 3, 4, 5, 6$, satisfy the same recurrences in the Lemmas 17–19.

Lemma 20. *For any integers a, b, c , and for $i = 1, 2, 3, 4, 5, 6$*

$$(4.23) \quad \begin{aligned} \Psi_i(a, b, c)\Psi_i(a - 3, b - 3, c - 2) &= \Psi_i(a - 2, b - 1, c)\Psi_i(a - 1, b - 2, c - 2) \\ &\quad + \Psi_i(a - 1, b - 1, c - 1)\Psi_i(a - 2, b - 2, c - 1). \end{aligned}$$

Proof. We quote the fact (i)–(iv) in Lemma 5.1 in [2]. Besides the above four facts, we have the following facts on the exponents of 2:

$$(4.24) \quad \begin{aligned} \text{(v) If } a - c \equiv 1 \text{ or } 2 \pmod{3}, \text{ then for } i = 1, 2, \dots, 6 \\ k_i(a, b, c) + k_i(a - 3, b - 3, c - 2) &= k_i(a - 2, b - 1, c) + k_i(a - 1, b - 2, c - 2) \\ &= k_i(a - 1, b - 1, c - 1) + k_i(a - 2, b - 2, c - 1)' \end{aligned}$$

$$(4.25) \quad \begin{aligned} \text{(vi) otherwise} \\ k_i(a, b, c) + k_i(a - 3, b - 3, c - 2) + 1 &= k_i(a - 2, b - 1, c) + k_i(a - 1, b - 2, c - 2) \\ &= k_i(a - 1, b - 1, c - 1) + k_i(a - 2, b - 2, c - 1) + 1 \end{aligned}$$

Arguing the same as the proof of Lemma 5.1 in [2], we only need to consider the case of even b , and the case of odd b follows. We consider the value of $a - c \pmod{6}$.

If $a - c \equiv 0 \pmod{6}$, from the facts (i), (iii) and (vi) above we can cancel out the exponents of 2, 5 and 11 from both sides of (4.23). This equation becomes

$$(4.26) \quad \begin{aligned} 11\alpha(a, b, c)\alpha(a - 3, b - 3, c - 2) &= 2\alpha(a - 2, b - 1, c)\alpha(a - 1, b - 2, c - 2) \\ &+ \alpha(a - 1, b - 1, c - 1)\alpha(a - 2, b - 2, c - 1), \end{aligned}$$

for $i = 1, 2, 3$; and check that

$$(4.27) \quad \begin{aligned} 11\beta(a, b, c)\beta(a - 3, b - 3, c - 2) &= \beta(a - 2, b - 1, c)\beta(a - 1, b - 2, c - 2) \\ &+ \beta(a - 1, b - 1, c - 1)\beta(a - 2, b - 2, c - 1), \end{aligned}$$

for $i = 4, 5, 6$. That hold by the definitions of $\alpha(a, b, c)$ and $\beta(a, b, c)$.

We can check the 5 remaining cases by the 6 facts above together with the definition of $\alpha(a, b, c)$ and $\beta(a, b, c)$. \square

Lemma 21. (a) For any integers a, b, c , and for $i = 1, 2, \dots, 6$

$$(4.28) \quad \begin{aligned} \Psi_i(a, b, c)\Psi_i(a - 2, b - 2, c) &= \Psi_i^2(a - 1, b - 1, c) \\ &+ \Psi_i(a, b, c + 1)\Psi_i(a - 2, b - 2, c - 1) \end{aligned}$$

(b) For $i = 1, 4$

$$(4.29) \quad \begin{aligned} \Psi_i(a, b, 0)\Psi_i(a - 2, b - 2, 0) &= \Psi_i^2(a - 1, b - 1, 0) \\ &+ \Psi_i(a, b, 1)\Psi_i(3b - 2a, 2b - a, 1) \end{aligned}$$

For $i = 2, 5$

$$(4.30) \quad \begin{aligned} \Psi_i(a, b, 0)\Psi_i(a - 2, b - 2, 0) &= \Psi_i^2(a - 1, b - 1, 0) \\ &+ \Psi_i(a, b, 1)\Psi_{i+1}(3b - 2a, 2b - a, 1) \end{aligned}$$

For $i = 3, 6$

$$(4.31) \quad \begin{aligned} \Psi_i(a, b, 0)\Psi_i(a - 2, b - 2, 0) &= \Psi_i^2(a - 1, b - 1, 0) \\ &+ \Psi_i(a, b, 1)\Psi_{i-1}(3b - 2a, 2b - a, 1) \end{aligned}$$

Proof. (a) Besides four facts (i)–(iv) in the proof of Lemma 5.2 in [2], we have the following facts of the exponents of 2.

(v) If $a - c \equiv 2 \pmod{3}$, then for $i = 1, 2, 3$

$$(4.32) \quad \begin{aligned} k_i(a, b, c) + k_i(a - 2, b - 2, c) &= 2k_i(a - 1, b - 1, c) \\ &= k_i(a, b, c + 1) + k_i(a - 2, b - 2, c - 1) \end{aligned}$$

otherwise

$$(4.33) \quad \begin{aligned} k_i(a, b, c) + k_i(a - 2, b - 2, c) &= 2k_i(a - 1, b - 1, c) + 1 \\ &= k_i(a, b, c + 1) + k_i(a - 2, b - 2, c - 1) + 1 \end{aligned}$$

(iv) If $b - c \equiv 0 \pmod{3}$, then for $i = 4, 5, 6$

$$(4.34) \quad \begin{aligned} k_i(a, b, c) + k_i(a - 2, b - 2, c) &= 2k_i(a - 1, b - 1, c) \\ &= k_i(a, b, c + 1) + k_i(a - 2, b - 2, c - 1) \end{aligned}$$

otherwise

$$(4.35) \quad \begin{aligned} k_i(a, b, c) + k_i(a - 2, b - 2, c) &= 2k_i(a - 1, b - 1, c) + 1 \\ &= k_i(a, b, c + 1) + k_i(a - 2, b - 2, c - 1) + 1 \end{aligned}$$

Arguing the same as the proof of Lemma 5.1 in [2], we only need to consider for the case of even b , and the case of odd b follows.

If $a - c \equiv 0 \pmod{6}$, from 6 facts above (4.28) is simplified to

$$(4.36) \quad \begin{aligned} 10\alpha(a, b, c)\alpha(a - 2, b - 2, c) &= \alpha^2(a - 1, b - 1, c) \\ &+ \alpha(a, b, c + 1)\alpha(a - 2, b - 2, c - 1), \end{aligned}$$

for $i = 1, 2, 3$; and to

$$(4.37) \quad \begin{aligned} 5\beta(a, b, c)\beta(a - 2, b - 2, c) &= \beta^2(a - 1, b - 1, c) \\ &+ \beta(a, b, c + 1)\beta(a - 2, b - 2, c - 1), \end{aligned}$$

for $i = 4, 5, 6$. Both equations are correct from the definition of $\alpha(a, b, c)$ and $\beta(a, b, c)$.

Five remain cases can be verified similarly. We leave this work for readers.

(b) From the proof of Lemma 5.2 in [2], we have

$$(4.38) \quad q(a - 2, b - 2, -1) = q(3b - 2a, 2b - a, 1).$$

Similarly

$$(4.39) \quad \alpha(a - 2, b - 2, -1) = \alpha(3b - 2a, 2b - a, 1)$$

and

$$(4.40) \quad \beta(a - 2, b - 2, -1) = \beta(3b - 2a, 2b - a, 1).$$

By the definition of the function $g(a, b, c)$, we have for any t

$$(4.41) \quad g(a - 2, b - 2, t) = g(3b - 2a, 2b - a, t + 2)$$

Let $t = 0$ and -2 in the fact (4.41) we get for $i = 1$ and 4

$$(4.42) \quad k_i(a - 2, b - 2, -1) = k_i(3b - 2a, 2b - a, 1).$$

Thus, (4.38), (4.39) and (4.40) imply

$$(4.43) \quad \Psi_i(a - 2, b - 2, -1) = \Psi_i(3b - 2a, 2b - a, 1),$$

then from part (a), for the case $c = 0$, we get (4.29).

Similarly, from (4.38), (4.39), (4.40) and (4.41), we have for $i = 2, 5$

$$(4.44) \quad \Psi_i(a - 2, b - 2, -1) = \Psi_{i+1}(3b - 2a, 2b - a, 1),$$

and for $i = 3, 6$

$$(4.45) \quad \Psi_i(a - 2, b - 2, -1) = \Psi_{i-1}(3b - 2a, 2b - a, 1).$$

Again, from part (a), for the case $c = 0$, implies (4.30) and (4.31). \square

Similarly, Lemma 12 we have the following recurrences

Lemma 22. (a) For any integers a, b, c , and for $i = 1, 2, 3, 4, 5, 6$

$$(4.46) \quad \begin{aligned} \Psi_i(a, b, c)\Psi_i(a-2, b-3, c-2) &= \Psi_i(a-1, b-1, c)\Psi_i(a-1, b-2, c-2) \\ &\quad + \Psi_i(a-2, b-2, c-1)\Psi_i(a, b-1, c-1) \end{aligned}$$

(b) Assume that $d = 2b - a - 2c = 0$. Then for $i = 1, 2, 3, 4, 5, 6$

$$(4.47) \quad \begin{aligned} \Psi_i(a, b, c)\Psi_i(a-2, b-3, c-2) &= \Psi_{7-i}(c, b-1, a-1)\Psi_i(a-1, b-2, c-2) \\ &\quad + \Psi_i(a-2, b-2, c-1)\Psi_i(a, b-1, c-1) \end{aligned}$$

Proof. (a) This can be treated similarly to Lemma 20

(b) From part (a), for $d = 0$, we only need to prove that

$$(4.48) \quad \Psi_i(a-1, b-1, c) = \Psi_{7-i}(c, b-1, a-1),$$

where $2b - a - 2c = 0$.

One readily verify the following equation from definition

$$(4.49) \quad k_i(a-1, b-1, c) = k_{7-i}(c, b-1, a-1).$$

From the proof of Lemma 5.2 in [2], we have for $2b - a - 2c = 0$

$$(4.50) \quad q(a-1, b-1, c) = g(c, b-1, a-1),$$

$$(4.51) \quad g(a-1, b-1, c) = g(c, b-1, a-1).$$

Similarly to the equality of the function $h(a, b, c)$ in this proof

$$(4.52) \quad \alpha(a-1, b-1, c) = \alpha(c, b-1, a-1)$$

and

$$(4.53) \quad \beta(a-1, b-1, c) = \beta(c, b-1, a-1).$$

From (4.49), (4.50), (4.51), (4.52), and (4.53), we get (4.48). \square

Proof of Theorem 16. From the Lemmas 17–19 and the Lemmas 20–22, the number of perfect matchings of $A_{a,b,c}^{(i)}$ and $\Psi_i(a, b, c)$, for $i = 1, 2, 3$; and the number of perfect matchings of $F_{a,b,c}^{(i)}$ and $\Psi_{i+3}(a, b, c)$ satisfy the same recurrences. Similar to the proof of Blum's conjecture in [2], we can prove by induction on the perimeter of the regions $D_{a,b,c}$ and $E_{a,b,c}$ that

$$(4.54) \quad M(A_{a,b,c}^{(i)}) = \Psi_i(a, b, c) \text{ and } M(F_{a,b,c}^{(i)}) = \Psi_{3+i}(a, b, c),$$

for $i = 1, 2, 3$.

The base cases corresponding to the same triples (a, b, c) for the Blum's conjecture, and can be verified by using `vaxmacs`. The induction step here is almost the same as that of the Blum's conjecture in [2]. The differences are only the reflections used in Case I.2 and Case II.2 of the proof. We consider the reflection in Case I.2 first. Recall that we are assuming that $a \leq c + d$. After reflecting $A_{a,b,c}^{(1)}$ over a horizontal

line, we get the graph $F_{f,e,d}^{(3)}$; and we get $F_{f,e,d}^{(4-i)}$ from reflecting the graph $A_{a,b,c}^{(i)}$ over a vertical line, for $i = 2, 3$. Moreover, we can verify from the definition of the functions $\Psi_i(a, b, c)$ that

$$\Psi_i(a, b, c) = \Psi_{7-i}(f, e, d)$$

for $i = 1, 2, \dots, 6$. Thus, we can apply the reflecting process similarly to Case I.2.

For the reflection in Case II.2, we are assuming that $a > c + d$. We also reflect the graphs $A_{a,b,c}^{(1)}$ and $F_{a,b,c}^{(1)}$ over a horizontal line; and reflect the graphs $A_{a,b,c}^{(i)}$ and $F_{a,b,c}^{(i)}$, for $i = 2, 3$, over a vertical line. We have the diagram of the reflection as follows.

$$\begin{aligned} A_{a,b,c}^{(1)} &\Leftrightarrow A_{b,a,f}^{(1)} \\ A_{a,b,c}^{(2)} &\Leftrightarrow A_{b,a,f}^{(3)} \\ A_{a,b,c}^{(3)} &\Leftrightarrow A_{b,a,f}^{(2)} \\ F_{a,b,c}^{(1)} &\Leftrightarrow F_{b,a,f}^{(1)} \\ F_{a,b,c}^{(2)} &\Leftrightarrow F_{b,a,f}^{(3)} \\ A_{a,b,c}^{(3)} &\Leftrightarrow A_{b,a,f}^{(2)} \end{aligned}$$

Moreover, one readily gets from the definition of the functions $\Psi_i(a, b, c)$ that

$$\begin{aligned} \Psi_1(a, b, c) &= \Psi_1(b, a, f) \\ \Psi_2(a, b, c) &= \Psi_3(b, a, f) \\ \Psi_3(a, b, c) &= \Psi_2(b, a, f) \\ \Psi_4(a, b, c) &= \Psi_4(b, a, f) \\ \Psi_5(a, b, c) &= \Psi_6(b, a, f) \\ \Psi_6(a, b, c) &= \Psi_5(b, a, f) \end{aligned}$$

Again, we can apply the process in Case II.2 here. □

Proof of Theorem 15. We can split the graph $G_{a,2a,b}$ into three subgraphs G_1 , G_2 and G_3 by two dotted zigzag cuts as in Figure 4.14, for $a = 2$ and $b = 6$. Arguing similarly to the case of original hexagonal dungeon, we have

$$(4.55) \quad M(G_{a,2a,b}) = M(G_1) M(G_2) M(G_3)$$

It is easy to see that G_2 have a unique perfect matching, G_1 is isomorphic to $A_{2a,3a,2a}^{(3)}$, and G_3 is isomorphic to $F_{2a,3a,2a}^{(1)}$. Thus,

$$\begin{aligned} M(G_{a,2a,b}) &= M(A_{2a,3a,2a}^{(3)}) M(F_{2a,3a,2a}^{(1)}) \\ &= 2^{g(2a,3a,2a-1)+g(2a,3a,2a+1)} 5^{2g(2a,3a,2a)} 11^{2q(2a,3a,2a)} \\ &= 2^{a(a+1)+a(a-1)} 5^{2a^2} 11^{2\lfloor \frac{a^2}{4} \rfloor} \\ (4.56) \quad &= 10^{2a^2} 11^{\lfloor \frac{a^2}{2} \rfloor}. \end{aligned}$$

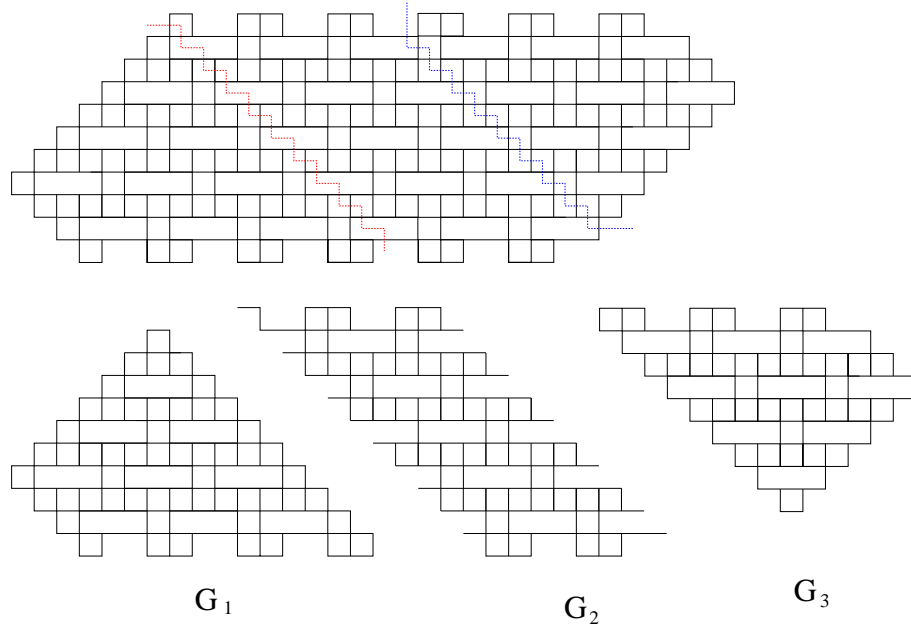


FIGURE 4.14. The graphs $F_{4,8,6}^{(1)}$, left, $F_{4,8,6}^{(2)}$, upper-right, and $F_{4,8,6}^{(3)}$, lower-right

□

Remark 23. The six families of graphs $A_{a,b,c}^{(i)}$ and $F_{a,b,c}^{(i)}$, for $i = 1, 2, 3$, were inspired by the dual graphs of the regions $D_{a,b,c}$ and $E_{a,b,c}$. We did not mention them as the dual graphs of some regions. However, there are actually families of regions whose dual graphs are isomorphic to $A_{a,b,c}^{(i)}$ or $F_{a,b,c}^{(i)}$. The Figure 4.15 shows examples of two of such regions.

We conclude this section by stating a generalization of Theorem 16 as follows. We consider a brick lattice B , where the even rows consist of 1×1 bricks, the $4k + 1$ rows consists of 1×3 bricks and 1×1 bricks alternatively, and the $4k + 3$ row is obtained from the $4k + 1$ row by shifting to right 2 units (see Figure 4.16). One readily sees that all graphs $A_{a,b,c}^{(i)}$ and $F_{a,b,c}^{(i)}$ are all subgraphs of the lattice B .

The lattice B can be partitioned into edge-disjoint “cross” consisting of a 1×3 brick and two 1×1 bricks (the portion of the B lattice restricted in the dotted diamonds in Figure 4.16).

We now assign weights to edges of B so that each cross are weighted as in Figure 4.17. Denote by $A_{a,b,c}^{(i)}(x, y, z)$ and $F_{a,b,c}^{(i)}(x, y, z)$ the corresponding weighted version of the graphs $A_{a,b,c}^{(i)}$ and $F_{a,b,c}^{(i)}$, respectively.

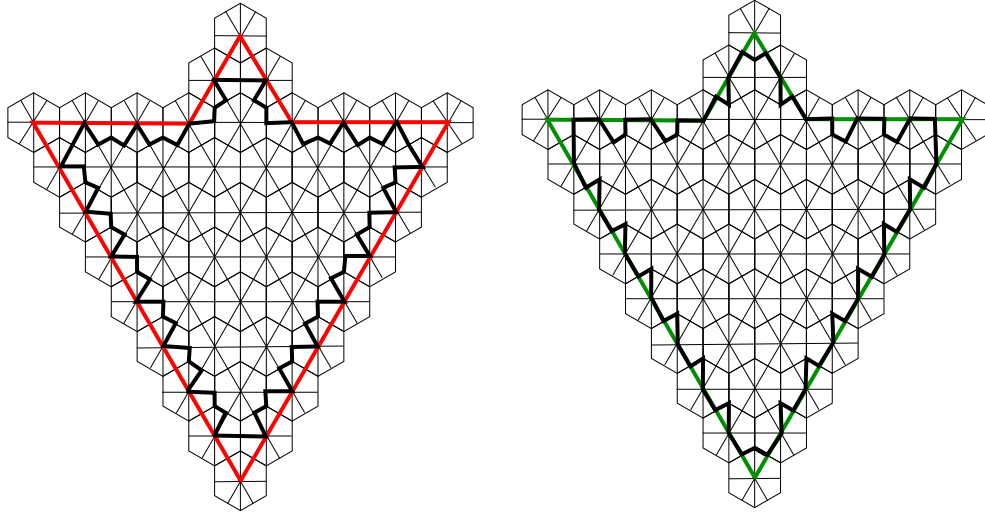


FIGURE 4.15. The regions whose dual graphs are isomorphic to $A_{8,8,3}^{(1)}$ (left) and $F_{8,8,3}^{(1)}$ (right).

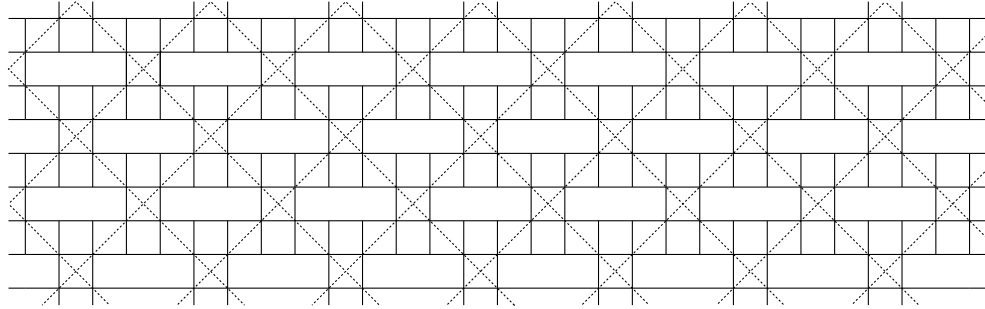


FIGURE 4.16. The B lattice (solid lines), and its partition into crosses.

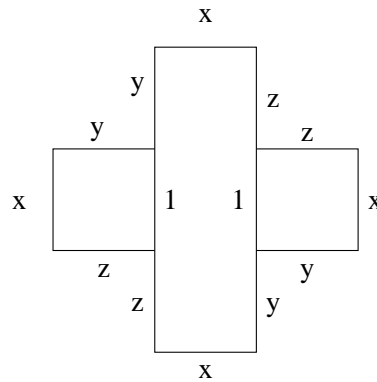


FIGURE 4.17. The weight assignment for each cross in Theorem 24.

By the same fashion in the proof of Theorem 16, one can get the following formula for the matching generating functions of the weighted graphs $A_{a,b,c}^{(i)}(x, y, z)$ and $F_{a,b,c}^{(i)}(x, y, z)$, for $i = 1, 2, 3$, that are weighted by the above weight pattern.

First, we redefine two functions $\alpha(a, b, c)$ and $\beta(a, b, c)$

$$(4.57) \quad \alpha(a, b, c) = \begin{cases} \frac{(x+2yz)yz}{x^2} & \text{if } 3b + a - c \equiv 5 \pmod{6}; \\ \frac{yz}{x} & \text{if } 3b + a - c \equiv 3 \pmod{6}; \\ \frac{x+yz}{x} & \text{if } 3b + a - c \equiv 1 \pmod{6}; \\ 1 & \text{otherwise} \end{cases}$$

$$(4.58) \quad \beta(a, b, c) = \begin{cases} \frac{(x+2yz)}{yz} & \text{if } 3b + a - c \equiv 1 \pmod{6}; \\ \frac{x}{yz} & \text{if } 3b + a - c \equiv 3 \pmod{6}; \\ \frac{(x+yz)x}{y^2z^2} & \text{if } 3b + a - c \equiv 5 \pmod{6}; \\ 1 & \text{otherwise} \end{cases}$$

Then the matching generating functions of the 6 families of graphs are obtained as follows.

Theorem 24. *Assume that a , b , and c are three nonnegative integers satisfying $b \geq 2$, $2b - a - 2c \geq 0$ and $3b - 2a - 2c \geq 0$. Assume in addition that x, y, z are three positive numbers. Then*

$$(4.59) \quad \begin{aligned} M\left(A_{a,b,c}^{(1)}(x, y, z)\right) &= \alpha(a, b, c) 2^{g(a,b,c+1)} \\ (4.60) \quad &\times (x^2 + 2xyz + 2y^2z^2)^{g(a,b,c)} (2x^2 + 5xyz + 4y^2z^2)^{q(a,b,c)} \\ &\times x^{\kappa_1} y^{2g(a,b,c+1)+3q(a,b,c)} z^{2g(a,b,c+1)+3q(a,b,c)}, \end{aligned}$$

where

$$(4.61) \quad \kappa_1 = \tau(a, b, c) + (d-1) + (a-1) + c - \min(a-c-d, 0) - 2g(a, b, c+1) - 3q(a, b, c).$$

$$(4.62) \quad \begin{aligned} M\left(A_{a,b,c}^{(2)}(x, y, z)\right) &= \alpha(a, b, c) 2^{g(a,b,c-1) - \lfloor (a-c+1)/3 \rfloor + (a-b)} \\ (4.63) \quad &\times (x^2 + 2xyz + 2y^2z^2)^{g(a,b,c)} (2x^2 + 5xyz + 4y^2z^2)^{q(a,b,c)} \\ &\times x^{\kappa_2} y^{2g(a,b,c+1)+3q(a,b,c)+b+e-c-\min(a-c-d,0)} z^{2g(a,b,c+1)+3q(a,b,c)}, \end{aligned}$$

where

$$(4.64) \quad \kappa_2 = \tau(a, b, c) + (a-1) + c + d + (f-1) - 2g(a, b, c+1) - 3q(a, b, c).$$

$$(4.65) \quad \begin{aligned} M\left(A_{a,b,c}^{(3)}(x, y, z)\right) &= \alpha(a, b, c) 2^{g(a,b,c-1) - \lfloor (a-c+1)/3 \rfloor} \\ &\times (x^2 + 2xyz + 2y^2z^2)^{g(a,b,c)} (2x^2 + 5xyz + 4y^2z^2)^{q(a,b,c)} \\ &\times x^{\kappa_3} y^{2g(a,b,c+1)+3q(a,b,c)} z^{2g(a,b,c+1)+3q(a,b,c)+a+d-\max(a-c-d,0)}, \end{aligned}$$

where

$$(4.66) \quad \kappa_3 = \tau(a, b, c) + b + c + e + f - 2 - 2g(a, b, c + 1) - 3q(a, b, c).$$

$$(4.67) \quad \begin{aligned} M\left(F_{a,b,c}^{(1)}(x, y, z)\right) &= \beta(a, b, c) 2^{g(a,b,c+1)} \\ &\quad \times (x^2 + 2xyz + 2y^2z^2)^{g(a,b,c)} (2x^2 + 5xyz + 4y^2z^2)^{q(a,b,c)} \\ &\quad \times x^{\varepsilon_1} y^{\omega_1} z^{\theta_1}, \end{aligned}$$

where

$$(4.68) \quad \theta_1 + \varepsilon_1 = \tau(a, b, c) + a - 1 + b - 1 + d + e + \max(a - c - d, 0),$$

$$(4.69) \quad \theta_1 = 2g(a, b, c + 1) + 3q(a, b, c) + 4b - 2a - 3c - \min(a - c - d, 0),$$

$$(4.70) \quad \omega_1 = \theta_1 + 2(b - a).$$

$$(4.71) \quad M\left(F_{a,b,c}^{(2)}\right) = \beta(a, b, c) 2^{g(a,b,c+1) + \lfloor (a-c+1)/3 \rfloor - (a-b)}$$

$$(4.72) \quad \begin{aligned} &\times (x^2 + 2xyz + 2y^2z^2)^{g(a,b,c)} (2x^2 + 5xyz + 4y^2z^2)^{q(a,b,c)} \\ &\times x^{\varepsilon_2} y^{\omega_2} z^{\theta_2}, \end{aligned}$$

where

$$(4.73) \quad \omega_2 = \theta_1,$$

$$(4.74) \quad \varepsilon_2 + \theta_2 = \tau(a, b, c) + (b - 1) + c + e + (f - 1),$$

$$(4.75) \quad \theta_2 - \omega_2 = b + e - a - d + \max(a - c - d, 0).$$

$$(4.76) \quad \begin{aligned} M\left(F_{a,b,c}^{(3)}\right) &= \beta(a, b, c) 2^{g(a,b,c+1) + \lfloor (a-c+1)/3 \rfloor} \\ &\quad \times (x^2 + 2xyz + 2y^2z^2)^{g(a,b,c)} (2x^2 + 5xyz + 4y^2z^2)^{q(a,b,c)} \\ &\quad \times x^{\varepsilon_3} y^{\omega_3} z^{\theta_3}, \end{aligned}$$

where

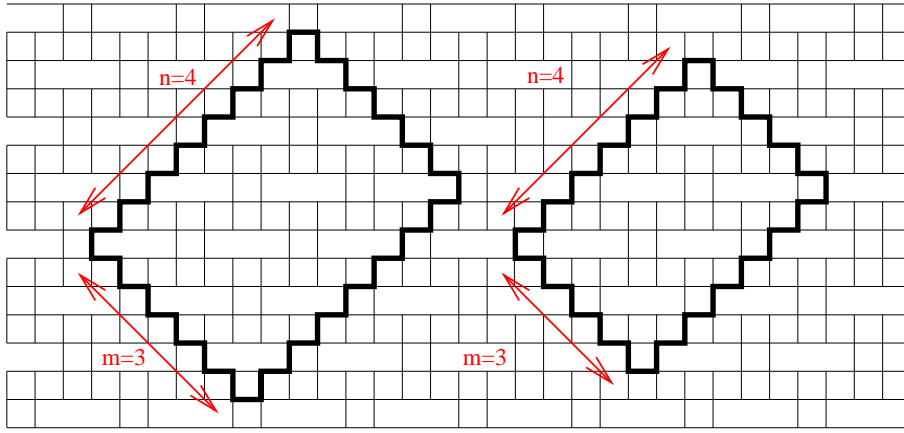
$$(4.77) \quad \omega_3 = \theta_1,$$

$$(4.78) \quad \varepsilon_3 + \theta_3 = \tau(a, b, c) + b - 1 + e + \max(a - c - d, 0) - 1,$$

$$(4.79) \quad \theta_3 - \omega_3 = -\max(a - c - d, 0).$$

The proof of the theorem is essentially the same as that of Theorem 16 and is omitted.

Finally, we notice that, by Graph-splitting Lemma, one can get the formula for the matching generating function of the corresponding weighted version of the graph $G_{a,2a,b}$.

FIGURE 5.1. Two types of Aztec rectangle graphs on the lattice B .

5. TRIMMED AZTEC RECTANGLE

One can consider a honeycomb graph as a subgraph of an Augmented Aztec rectangle trimmed by two horizontal lines, see Figure 5.2 for an example.

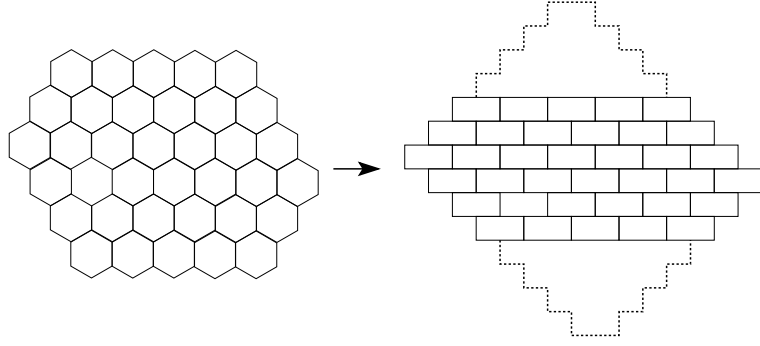
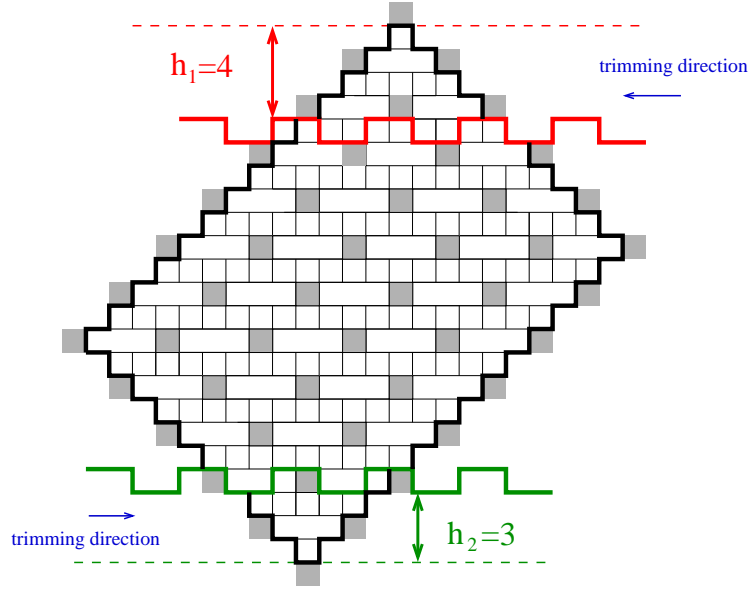
We now consider a similar situation for a certain Aztec rectangle graphs on the B lattice defined in Section 4 as follows.

Consider an Aztec rectangle contour of size $2m \times 2n$ on the lattice B , so that a 1×3 face on the right of the western most edge of the contour (see the graph on the left in Figure 5.1). Denote by $AR_{2m,2n}^{(1)}$ the induced subgraph of B whose vertices are inside or on the contour. We consider next an Aztec rectangle contour of size $(2m-1) \times (2n-1)$ on the lattice B , so that a 1×3 face on the right of the western most edge of the contour (illustrated by the graph on the right in Figure 5.1). Denote by $AR_{2m-1,2n-1}^{(2)}$ the induced subgraph of B corresponding to the vertices inside or on the contour.

We trim the Aztec rectangle graph $AR_{2m,2n}^{(1)}$ by two zigzag paths with the direction as in Figure 5.3, for $m = 7$ and $n = 5$. Assume that the distance from the top of the Aztec rectangle to the upper trimming path and the distance from the bottom of Aztec rectangle to the lower trimming path are h_1 and h_2 , respectively. Denote by $TA_{m,n,h_1,h_2}^{(1)}$ the “trimmed Aztec rectangle” above. Ciucu conjectured that the number of perfect matching of the trimmed Aztec rectangle $TA_{m,n,h_1,h_2}^{(1)}$ has all of its prime factors less than or equal to 13. Moreover, if the edges of shaded squares are weighted $\frac{1}{2}$, then the matching generating function of the resulting weighted graph has the same property.

Similarly, one can trim the Aztec rectangle $AR_{2m-1,2n-1}^{(2)}$, and denote by $TA_{m,n,h_1,h_2}^{(2)}$ the resulting graph (see Figure 5.4)

The following theorem proves the Ciucu’s conjecture.

FIGURE 5.2. Honeycomb $H_{3,4,5}$ and trimmed Aztec rectangleFIGURE 5.3. The region $TA_{m,n,h_1,h_2}^{(1)}$ is obtained by trimming the rectangle $AR_{2m,2n}^{(1)}$ by two zigzag cuts.

Theorem 25. Assume that $\lfloor \frac{h_1+1}{2} \rfloor + \lfloor \frac{h_2+1}{2} \rfloor = 2(m-n)$.

(a) The number of perfect matchings of a trimmed Aztec rectangle is given by

$$(5.1) \quad M\left(TA_{m,n,h_1,h_2}^{(1)}\right) = \begin{cases} \Psi_1(a,b,c)3^{\frac{h_1+h_2}{2}} & \text{if } h_1 \text{ and } h_2 \text{ are even;} \\ \Psi_1(a,b,c)3^{\frac{h_1}{2}} & \text{if } h_1 \text{ is even and } h_2 \text{ is odd;} \\ \Psi_1(a,b,c)3^{\frac{h_2}{2}} & \text{if } h_1 \text{ is odd and } h_2 \text{ is even;} \\ \Psi_1(a,b,c) & \text{if } h_1 \text{ and } h_2 \text{ are odd,} \end{cases}$$

where $\Psi_1(a,b,c)$ is defined as in the proof of Theorem 16, and where $a = n - \lfloor \frac{h_2+1}{2} \rfloor + 1$, $b = m - \lfloor \frac{h_2+1}{2} \rfloor + 1$ and $c = \lfloor \frac{h_1+1}{2} \rfloor$; and

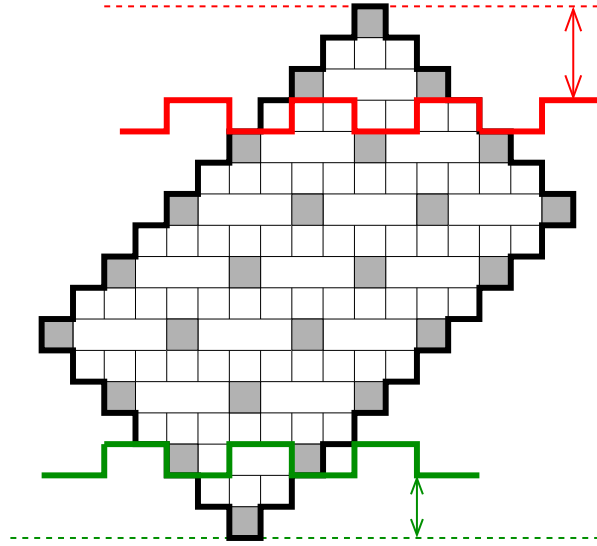


FIGURE 5.4. The region $TA_{m,n,h_1,h_2}^{(2)}$ is obtained by trimming the rectangle $AR_{2m,2n}^{(2)}$ by two zigzag cuts.

$$(5.2) \quad M\left(TA_{m,n,h_1,h_2}^{(2)}\right) = \begin{cases} \Psi_4(a', b', c') 3^{\frac{h_1+h_2+2}{2}} & \text{if } h_1 \text{ and } h_2 \text{ are odd;} \\ \Psi_4(a', b', c') 3^{\frac{h_1+1}{2}} & \text{if } h_1 \text{ is odd and } h_2 \text{ is even;} \\ \Psi_4(a', b', c') 3^{\frac{h_2+1}{2}} & \text{if } h_1 \text{ is even and } h_2 \text{ is odd;} \\ \Psi_4(a', b', c') & \text{if } h_1 \text{ and } h_2 \text{ are even,} \end{cases}$$

where $\Psi_4(a', b', c')$ is defined as in the proof of Theorem 16, and where $a' = n - \lfloor \frac{h_2+1}{2} \rfloor + 1$, $b' = m - \lfloor \frac{h_2+1}{2} \rfloor + 1$ and $c' = \lfloor \frac{h_1+1}{2} \rfloor$;

(b) Assume in addition that shaded squares are weighted $\frac{1}{2}$. Then the matching generating function of a trimmed Aztec rectangle is given by

$$(5.3) \quad M\left(TA_{m,n,h_1,h_2}^{(1)}\right) = \begin{cases} \phi(a, b, c) 2^{-\tau} 5^{\frac{h_1+h_2}{2}} & \text{if } h_1 \text{ and } h_2 \text{ are even;} \\ \phi(a, b, c) 2^{-\tau} 5^{\frac{h_1}{2}} & \text{if } h_1 \text{ is even and } h_2 \text{ is odd;} \\ \phi(a, b, c) 2^{-\tau} 5^{\frac{h_2}{2}} & \text{if } h_1 \text{ is odd and } h_2 \text{ is even;} \\ \phi(a, b, c) 2^{-\tau} & \text{if } h_1 \text{ and } h_2 \text{ are odd,} \end{cases}$$

where $\phi(a, b, c)$ is defined as in Theorem 2, $\tau = (2b - a - 2c) \lfloor \frac{h_1+1}{2} \rfloor + a \lfloor \frac{h_2+1}{2} \rfloor + (2b - a - c)(b - c) + c(c - 1)/2 + (2b - 2a - c)(2b - 2a - c - 1)/2$, and where a, b, c are defined as in part (a); and

$$(5.4) \quad M\left(TA_{m,n,h_1,h_2}^{(2)}\right) = \begin{cases} \psi(a', b', c') 2^{-\tau} 5^{\frac{h_1+h_2+2}{2}} & \text{if } h_1 \text{ and } h_2 \text{ are odd;} \\ \psi(a', b', c') 2^{-\tau} 5^{\frac{h_1+1}{2}} & \text{if } h_1 \text{ is odd and } h_2 \text{ is even;} \\ \psi(a', b', c') 2^{-\tau} 5^{\frac{h_2+1}{2}} & \text{if } h_1 \text{ is even and } h_2 \text{ is odd;} \\ \psi(a', b', c') 2^{-\tau} & \text{if } h_1 \text{ and } h_2 \text{ are even,} \end{cases}$$

where $\psi(a', b', c')$ is defined as in Theorem 2, $\tau = (2b' - a' - 2c') \lfloor \frac{h_1+1}{2} \rfloor + a' \lfloor \frac{h_2+1}{2} \rfloor + (2b' - a' - c')(b' - c') + c'(c' - 1)/2 + (2b' - 2a' - c')(2b' - 2a' - c' - 1)/2$, and where a', b', c' are defined as in part (a).

Proof. (a) Consider the rightmost subgraph G_1 restricted by dotted contour in TA_{m,n,h_1,h_2} . By the Graph Splitting Lemma 2.8(a)

$$(5.5) \quad M(TA_{m,n,h_1,h_2}) = M(TA_{m,n,h_1,h_2} - G_1) M(G_1).$$

Next, we consider the graph G' obtained from $TA_{m,n,h_1,h_2} - G_1$ by removing horizontal forced edges (the circled ones in Figure 5.5). Apply the Lemma 2.8(a) again to the second subgraph G_2 restricted by dotted contour

$$(5.6) \quad M(G') = M(G' - G_2) M(G_2).$$

Repeat $i := \lfloor \frac{h_1+1}{2} \rfloor$ times, we get graph \overline{G} and

$$(5.7) \quad M(TA_{m,n,h_1,h_2}) = M(\overline{G}) \prod_{j=1}^i M(G_j)$$

Apply the same process for the lower part of G . We get graph $\overline{\overline{G}}$ (the subgraph restricted by bold contour in figure 5.5) and

$$(5.8) \quad M(\overline{\overline{G}}) = M(\overline{\overline{G}}) \prod_{j=1}^k M(H_j)$$

where $k = \lfloor \frac{h_2+1}{2} \rfloor$, and H_j is the j -th (from the left) subgraph restricted by dotted contour in the lower part of G .

Thus, from (5.7) and (5.8)

$$(5.9) \quad M(TA_{m,n,h_1,h_2}) = M(\overline{\overline{G}}) \prod_{j=1}^i M(G_j) \prod_{j=1}^k M(H_j)$$

One can check easily that $M(G_j) = 1$ if h_1 is odd, and is 3 if h_1 is even, for any $j = 1, 2, \dots, i$. Similarly, $M(H_j) = 1$ if h_2 is odd, and is 3 if h_2 is even, for any $j = 1, 2, \dots, k$. Thus,

$$(5.10) \quad M(TA_{m,n,h_1,h_2}) = 3^t M(\overline{\overline{G}}),$$

for some nonnegative integer t .

On the other hand, $\overline{\overline{G}}$ is isomorphic to the graph $A_{a,b,c}^{(1)}$, where $a = n - \lfloor \frac{h_2+1}{2} \rfloor + 1$, $b = m - \lfloor \frac{h_2+1}{2} \rfloor + 1$ and $c = \lfloor \frac{h_1+1}{2} \rfloor$. From (5.10) and Theorem 16, the equality (5.1) follows.

Similarly, one gets equality (5.2).

(b) This part can be treated by the same way with the notice that (5.9) still holds, and $M(G_j)$ is $\frac{1}{2^{2b-a-2c}}$ if h_1 is odd, and is $\frac{5}{2^{2b-a-2c}}$ if h_1 is even, for any $j = 1, 2, \dots, i$.

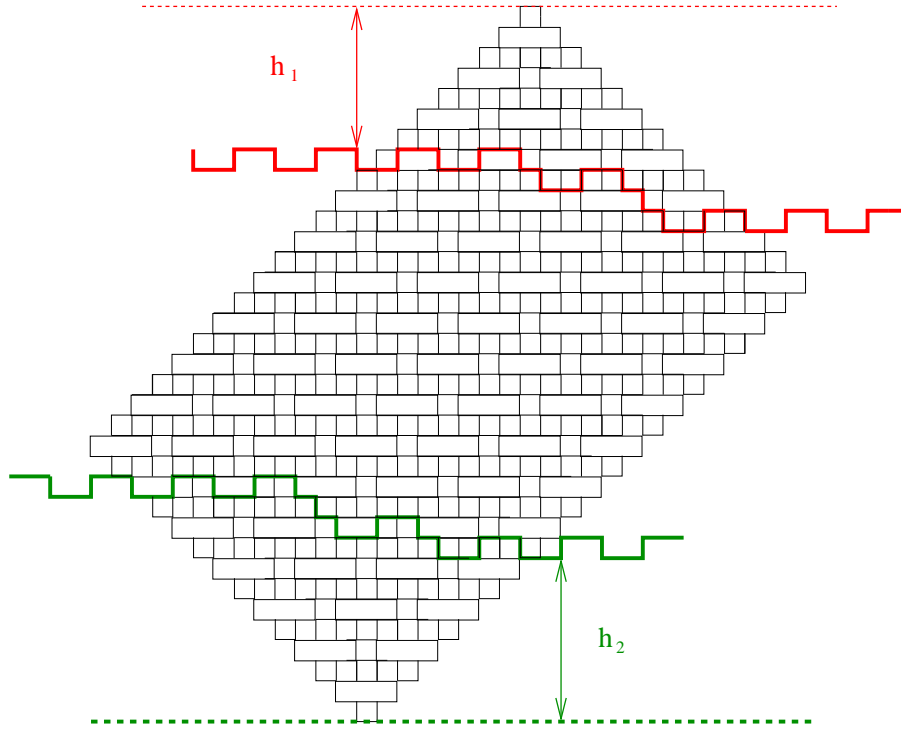


FIGURE 5.6.

We consider a generalization of Theorem 25 as follows. Instead of using horizontal trimming lines as in the Theorem 25, we consider two new stair-shaped trimming lines. The structure of each step in the new trimming lines is similar to the old ones, and each two consecutive steps (with different heights) are connected by a stair with unit steps (see Figure 5.6). Assume that h_1 is the distance between the top of the Aztec rectangle and the highest step of the upper trimming line, and h_2 is the distance between the bottom of the Aztec rectangle and the lowest step of the lower trimming line. Thus, by the Graph Splitting Lemma 2.8(a), we can “cut” multiple times small subgraphs with the same structure as G_i and H_j . We get finally the graph isomorphic to the graph $A_{a,b,c}^{(1)}$, with a, b, c are defined as in the proof of the Theorem 25. Therefore, we have the following result.

Theorem 26. Assume that $\lfloor \frac{h_1+1}{2} \rfloor + \lfloor \frac{h_2+1}{2} \rfloor = 2(m-n)$. Then

- (a) The number of perfect matchings of the Aztec rectangle trimmed by two stair-shaped lines has all of its prime factors less than or equal to 13.
- (b) We have the same property when the edges of shaded squares are weighted $\frac{1}{2}$.

6. MORE HEXAGONAL DUNGEONS

In this section we consider several variants of hexagonal dungeons and prove that their numbers of tilings are given by products of a power of 2 and a power of 3.

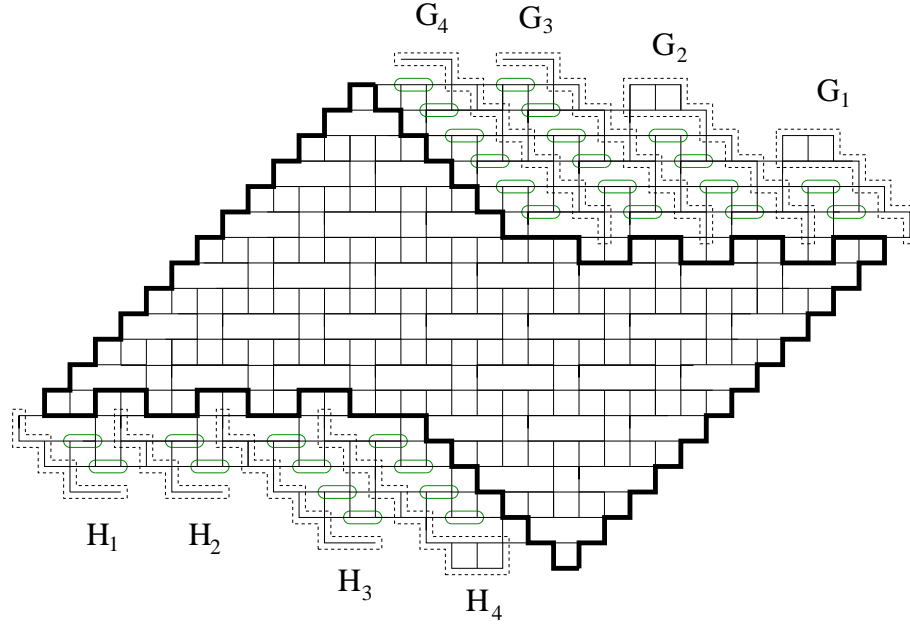


FIGURE 5.7.

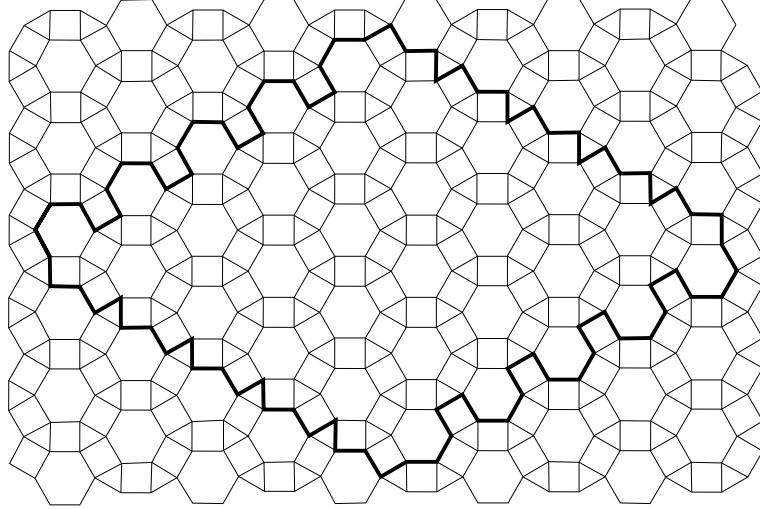


FIGURE 6.1. The Aztec dragon region of order 5.

In [8], Propp considered a family of regions called Aztec dragons (see the region restricted by the bold contour in Figure 6.1 for the Aztec dragon region of order 5), and their dual graphs are called *Aztec dragon graphs*. Blum [8] and Ciucu [1] proved that the number of tilings of the Aztec dragon of order n is $2^{n(n+1)}$. In [3], Cottrell and Young used domino shuffling technique to show that the number of perfect matchings of Aztec dragon graphs of *half-integer order* is also given by a power of 2. We consider next two families graphs that are a natural hybrid between Aztec

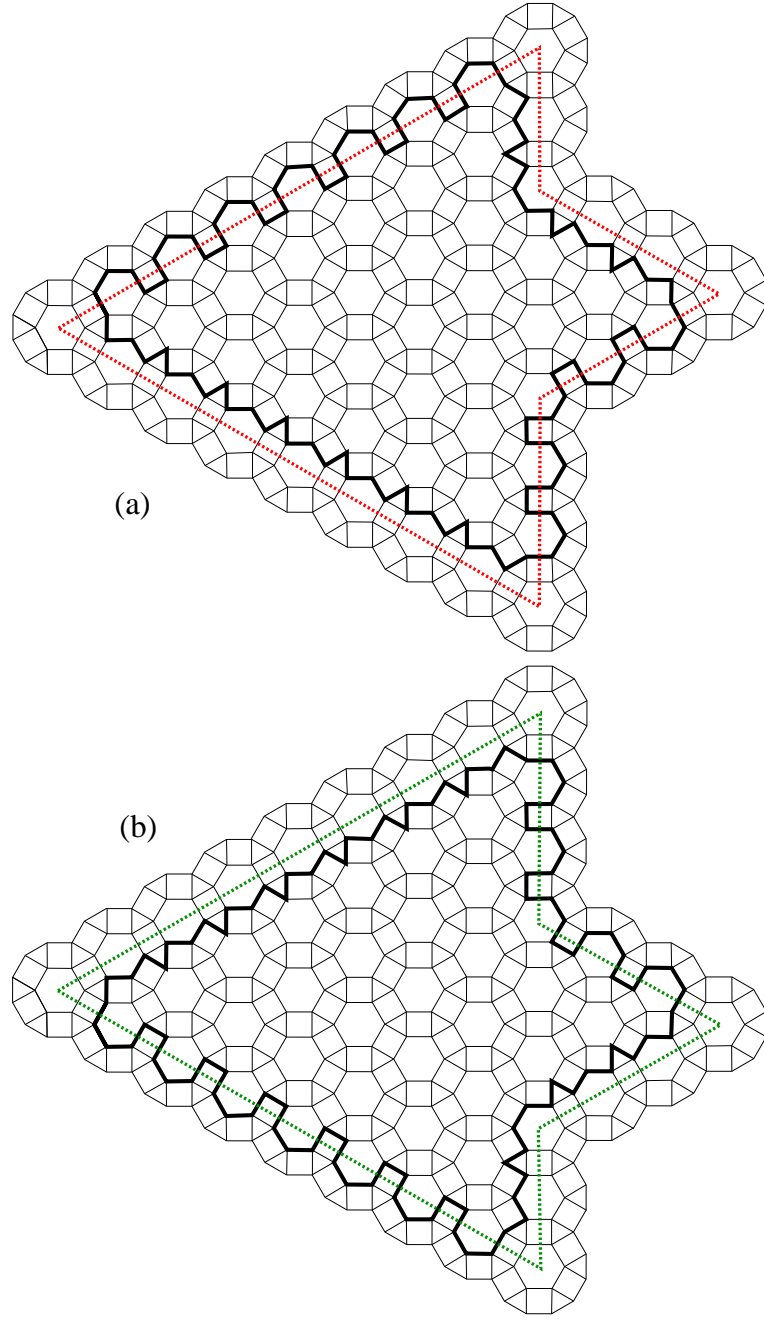


FIGURE 6.2. The regions $DR_{8,8,3}^{(1)}$ (a) and $DR_{8,8,2}^{(2)}$ (b).

dragon graphs and the dual graph of $D_{a,b,c}$, $E_{a,b,c}$ regions (mentioned in Theorem 2 of Section 2) as follows.

We notice that the lattice for Aztec dragon graphs is obtained from the hexagonal lattice by drawing in the intervals connecting the center of each unit hexagon to the middles of its edges.

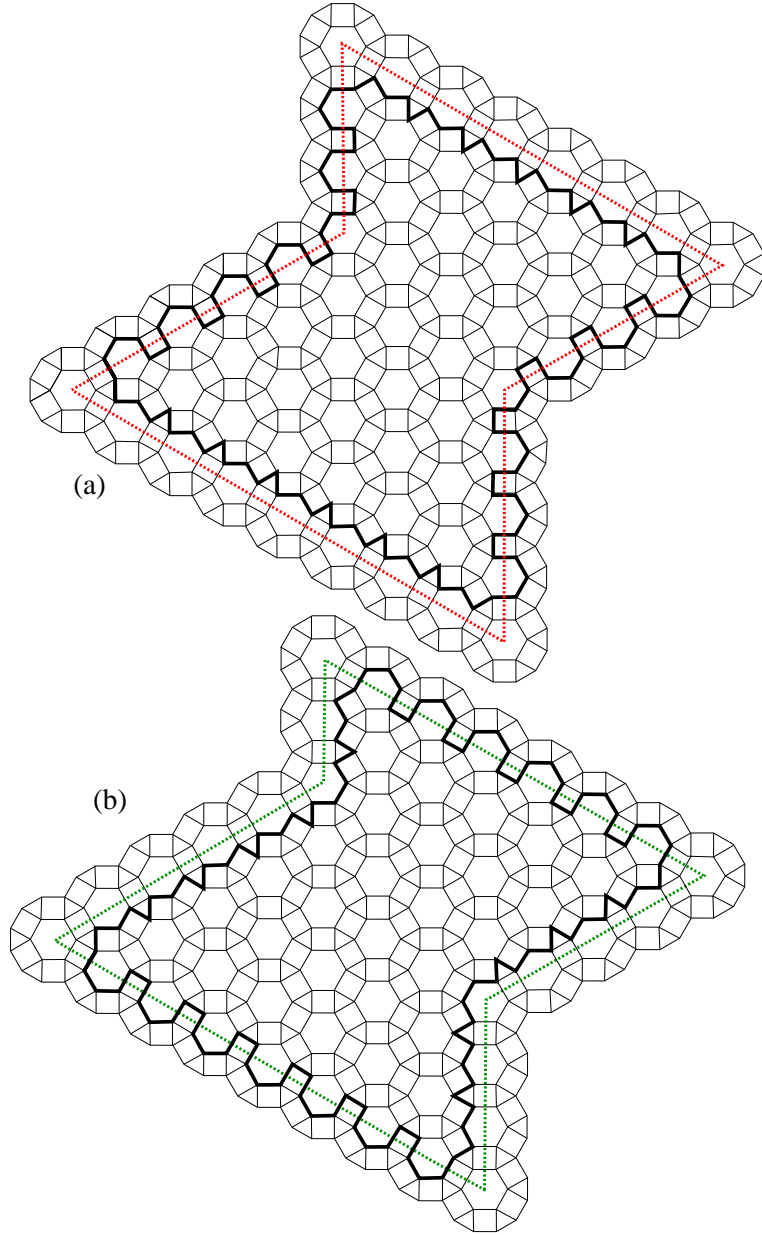


FIGURE 6.3. The regions $DR_{5,8,4}^{(1)}$ (a) and $DR_{5,8,3}^{(2)}$ (b).

Similar to the contour $\mathcal{C}(a, b, c)$ in the definition of $D_{a,b,c}$ and $E_{a,b,c}$, we consider two six-sided contours $\mathcal{C}^{(1)}(a, b, c)$ with sides $a, b, c, 2b - a - 2c + 1, 3b - 2a - 2c + 1, |2a - 2b + c - 1|$, and $\mathcal{C}^{(2)}(a, b, c)$ of side-lengths $a, b, c, 2b - a - 2c - 1, 3b - 2a - 2c - 1, |2a - 2b + c + 1|$ (in cyclic order) passing the centers of hexagonal fundamental regions in the lattice. We notice that the side-lengths¹ of the new contours need to satisfy some constraints as mentioned in Section 2 and in [2]: $b \geq 2$, $e = 3b - 2a - 2c \geq 0$,

¹The unit here is the smallest distance between the centers of two hexagonal fundamental regions.

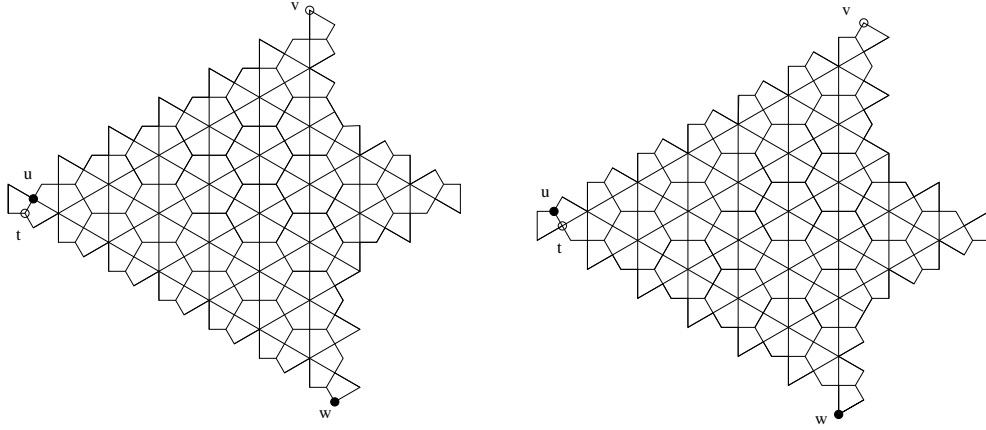


FIGURE 6.4. The dual graphs of $DR_{8,8,3}^{(1)}$ (left) and $DR_{8,8,2}^{(2)}$ (right) with the four vertices u, v, w, t .

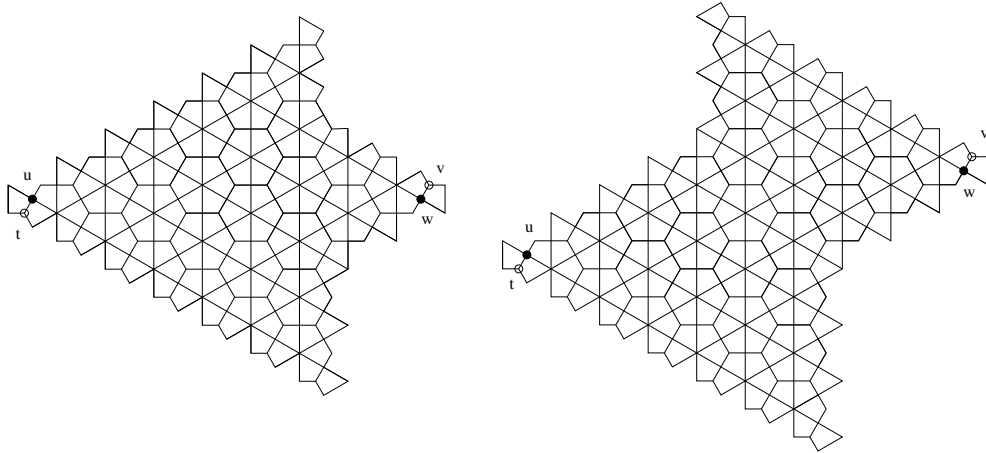


FIGURE 6.5. The dual graphs of $DR_{8,8,3}^{(1)}$ (left) and $DR_{5,8,4}^{(1)}$ (right) with the four vertices u, v, w, t .

and $f = |2a - 2b + c|$. The only difference is that we have $d = 2b - a - 2c + 1$ for the contour $\mathcal{C}^{(1)}(a, b, c)$, and $d = 2b - a - 2c - 1$ for the contour $\mathcal{C}^{(2)}(a, b, c)$ (as opposed to $d = 2b - a - 2c$ in the original contour $\mathcal{C}(a, b, c)$). Draw the jagged contour as the black bold contours in Figures 6.2 and 6.3, we get the regions $DR_{a,b,c}^{(1)}$ and $DR_{a,b,c}^{(2)}$, respectively.

We notice that the dual graph of $DR^{(1)}(a, b, c)$ in the case when $a \leq c + d$ was called *Aztec castle* in [7]. The number of tilings of the regions $DR^{(i)}(a, b, c)$'s is given by the following theorem.

Theorem 27. (a) Assume that a, b , and c are three nonnegative integers satisfying $b \geq 2$, $2b - a - 2c + 1 \geq 0$ and $3b - 2a - 2c + 1 \geq 0$. Then

$$(6.1) \quad \mathsf{M}\left(DR^{(1)}(a, b, c)\right) = 2^{(b-c+1)(2b-a-c)+(a-b)^2} 3^{\frac{(a-b+c)(a-b+c-1)}{2}}.$$

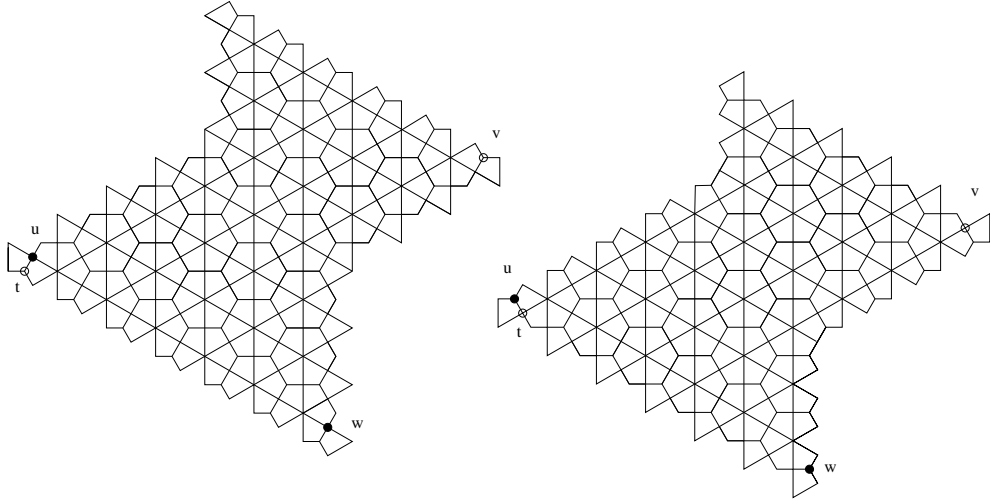


FIGURE 6.6. The dual graphs of $DR_{5,8,4}^{(1)}$ (left) and $DR_{5,8,3}^{(2)}$ (right) with the four vertices u, v, w, t .

(b) Moreover, if $2b - a - 2c - 1 \geq 0$ and $3b - 2a - 2c - 1 \geq 0$, then

$$(6.2) \quad M\left(DR^{(2)}(a, b, c)\right) = 2^{(b-c-1)(2b-a-c)+(a-b)^2} 3^{\frac{(a-b+c)(a-b+c+1)}{2}}.$$

Proof (sketch). Apply Kuo's graphical condensation to the dual graph of $DR_{a,b,c}^{(i)}$ with the four vertices u, v, w, t chosen as in Figure 6.4. It implies that the value $M\left(DR^{(i)}(a, b, c)\right)$ satisfies the same recurrence as in Lemma 4.1 in [2]. Similarly, they satisfy the recurrences in Lemmas 4.2(a) (by apply Kuo's condensation as in Figure 6.5) and 4.3(a) (by apply Kuo's condensation as in Figure 6.6).

However, we have small differences in the case when $c = 0$ in Lemma 4.2, and in the case when $d = 0$ in Lemma 4.3 in [2]. In particular, let a and b be nonnegative integers satisfying $a \geq 2$, $b \geq 4$, $2b - a + 1 \geq 2$, and $3b - 2a + 1 \geq 2$. Then

$$(6.3) \quad M\left(DR_{a,b,0}^{(1)}\right) M\left(DR_{a-2,b-2,0}^{(1)}\right) = M\left(DR_{a-1,b-1,0}^{(1)}\right)^2 + M\left(DR_{a,b,1}^{(1)}\right) M\left(DR_{3b-2a+1,2b-a+1,1}^{(2)}\right),$$

and if we assume $2b - a - 1 \geq 2$, and $3b - 2a - 1 \geq 2$, then

$$(6.4) \quad M\left(DR_{a,b,0}^{(2)}\right) M\left(DR_{a-2,b-2,0}^{(2)}\right) = M\left(DR_{a-1,b-1,0}^{(2)}\right)^2 + M\left(DR_{a,b,1}^{(2)}\right) M\left(DR_{3b-2a-1,2b-a-1,1}^{(1)}\right).$$

Moreover, assume that a, b, c are three nonnegative integers satisfying $a \geq 2$, $b \geq 5$, $c \geq 2$, $d := 2b - a - 2c = 0$, $e := 3b - 2a - 2c \geq 0$, and $a \leq c + d = c$. Then

$$(6.5) \quad M\left(DR_{a,b,c}^{(1)}\right) M\left(DR_{a-2,b-3,c-2}^{(1)}\right) = M\left(DR_{c,b-1,a-1}^{(1)}\right) M\left(DR_{a-1,b-2,c-2}^{(1)}\right) + M\left(DR_{a-2,b-2,c-1}^{(1)}\right) M\left(DR_{a,b-1,c-1}^{(1)}\right)$$

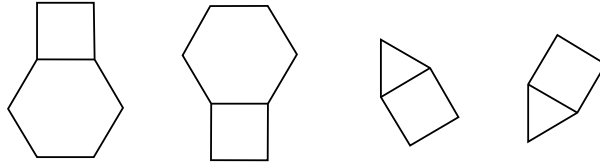


FIGURE 6.7. All types of tiles having weight 1 in the regions $\widetilde{DR}^{(i)}(a, b, c)$'s.

and

$$(6.6) \quad \begin{aligned} M\left(DR_{a,b,c}^{(2)}\right) M\left(DR_{a-2,b-3,c-2}^{(2)}\right) &= M\left(DR_{c,b-1,a-1}^{(2)}\right) M\left(DR_{a-1,b-2,c-2}^{(2)}\right) \\ &+ M\left(DR_{a-2,b-2,c-1}^{(2)}\right) M\left(DR_{a,b-1,c-1}^{(2)}\right). \end{aligned}$$

Let $dr(a, b, c)$ and $de(a, b, c)$ be the right hand sides in the (6.1) and (6.2), respectively. One can verify easily that the two functions satisfy the recurrences in Lemmas 5.1, 5.2(a), and 5.3(a) in [2]. Moreover, we get

$$(6.7) \quad \begin{aligned} dr(a, b, 0)dr(a-2, b-2, 0) &= dr(a-1, b-1, 0)^2 \\ &+ dr(a, b, 1)de(3b-2a+1, 2b-a+1, 1) \end{aligned}$$

and

$$(6.8) \quad \begin{aligned} de(a, b, 0)de(a-2, b-2, 0) &= de(a-1, b-1, 0)^2 \\ &+ de(a, b, 1)dr(3b-2a-1, 2b-a-1, 1). \end{aligned}$$

Moreover, we get

$$(6.9) \quad \begin{aligned} dr(a, b, c)dr(a-2, b-3, c-2) &= dr(c, b-1, a-1)dr(a-1, b-2, c-2) \\ &+ dr(a-2, b-2, c-1)dr(a, b-1, c-1) \end{aligned}$$

and

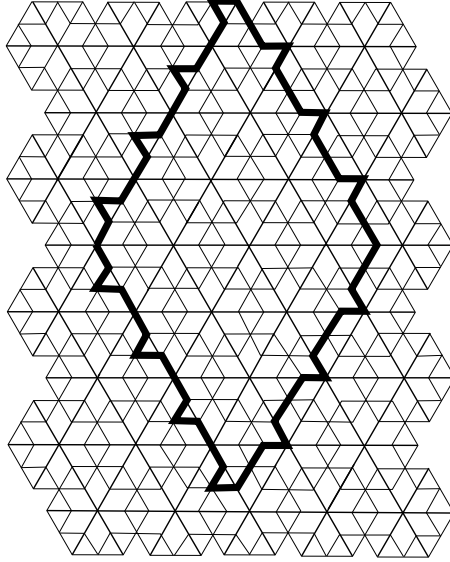
$$(6.10) \quad \begin{aligned} de(a, b, c)de(a-2, b-3, c-2) &= de(c, b-1, a-1)de(a-1, b-2, c-2) \\ &+ de(a-2, b-2, c-1)de(a, b-1, c-1). \end{aligned}$$

In summary, $M\left(DR_{a,b,c}^{(1)}\right)$, $M\left(DR_{a,b,c}^{(2)}\right)$ and $dr(a, b, c)$, $de(a, b, c)$ satisfy the same recurrences. Then the machinery in the proof of Blum's conjecture in [2] works here, and by induction we get the theorem. \square

Next, we state a weighted version of Theorem 27 as follows. We consider a weighted version $\widetilde{DR}^{(i)}(a, b, c)$ of the regions $DR^{(i)}(a, b, c)$ by assigning all tiles in Figure 6.7 a weight 1, and each of remaining tiles a weight $x > 0$. Then the tiling generating function of $\widetilde{DR}^{(i)}(a, b, c)$ is given by the following theorem.

Theorem 28. (a) Assume that a , b , and c are three nonnegative integers satisfying $b \geq 2$, $2b - a - 2c + 1 \geq 0$ and $3b - 2a - 2c + 1 \geq 0$. Then

$$(6.11) \quad M\left(\widetilde{DR}^{(1)}(a, b, c)\right) = 2^{\frac{(a-b)(a-b-1)}{2}} (x^2 + 1)^A (x^2 + 2)^B x^C,$$



where

$$A = (b - c + 1)(2b - a - c) + \frac{(b-a)(b-a-1)}{2},$$

$$B = \frac{(a-b+c)(a-b+c-1)}{2},$$

$$C = (a - b - 1)^2 + (a - b + c - 1)(a - b + c) - c + \min(2a - 2b + c - 1, 0).$$

(b) Moreover, if $2b - a - 2c - 1 \geq 0$ and $3b - 2a - 2c - 1 \geq 0$, then

$$(6.12) \quad M\left(\widetilde{DR}^{(2)}(a, b, c)\right) = 2^{\frac{(b-a)(b-a-1)}{2}} (x^2 + 1)^{A'} (x^2 + 2)^{B'} x^{C'},$$

where

$$A' = (b - c - 1)(2b - a - c) + \frac{(a-b)(a-b-1)}{2},$$

$$B' = \frac{(a-b+c)(a-b+c+1)}{2},$$

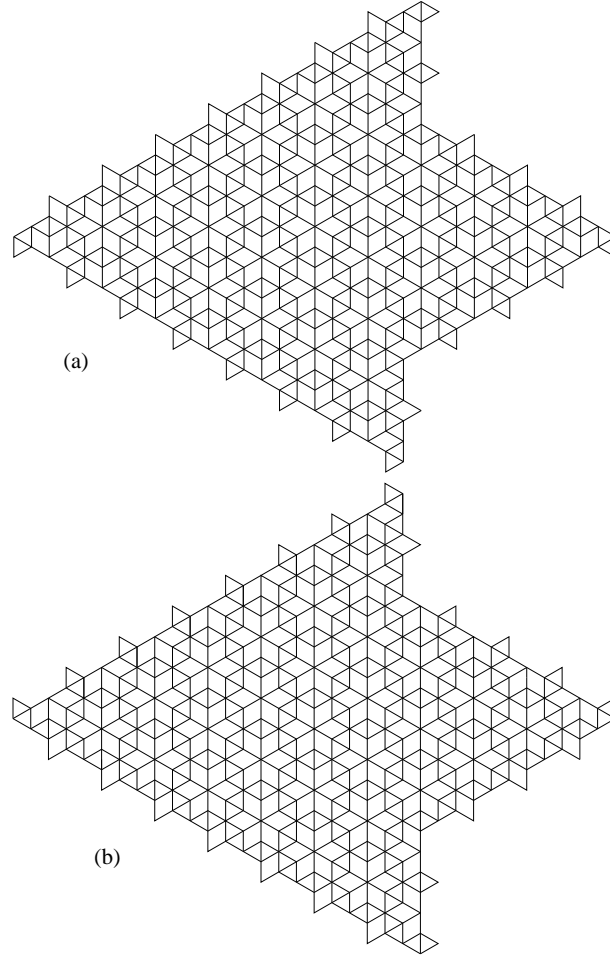
$$C' = (b - a - 1)^2 + (a - b + c + 1)(a - b + c) - \max(2a - 2b + c + 1, 0).$$

The proof of Theorem 28 is essentially the same as that of Theorem 27 and is omitted.

Next, we consider a variant of the triangular lattice as follows. Divide the triangular lattice to non-overlapped triangles of side-length 3 (the unit is the side length of unit triangles), and then remove all lattice segment opposite to the vertices of those side-3 triangles. In [6], author of the paper considered a variant of Aztec diamond on those lattice, denoted by R_n , and proved that its number of tilings is given by a power of 2 times a power of 2 (see Figure 6 for an example of the region R_3). In particular, we have the following theorem.

Theorem 29.

$$M(R_n) = 3^{n(n+1)} 2^{(n+1)^2}.$$

FIGURE 6.8. The regions $ND_{8,8,2}$ (a) and $NE_{8,8,2}$ (b).

As mentioned in [2], the region $D_{a,b,c}$ and $E_{a,b,c}$ can be viewed as a generalization of Aztec dungeon. In the same fashion, the following two families of regions can be viewed as a generalization of the region R_n . Similar to $D_{a,b,c}$ and $E_{a,b,c}$, the regions $ND_{a,b,c}$ and $NE_{a,b,c}$ are defined as in Figures 6.8 (for the case $a > c + d$) and 6.9 (for the case $a \leq c + d$)².

The number of tiling of the needle regions $ND_{a,b,c}$ and $NE_{a,b,c}$ is given by the product of a power of 2 and a power of 3 as in the below theorem.

Theorem 30. *Assume that a , b , and c are three nonnegative integers satisfying $b \geq 2$, $2b - a - 2c \geq 0$ and $3b - 2a - 2c \geq 0$. Then*

²The units here are three time the length of a fundamental regions, which are a unit triangle or a unit rhombus

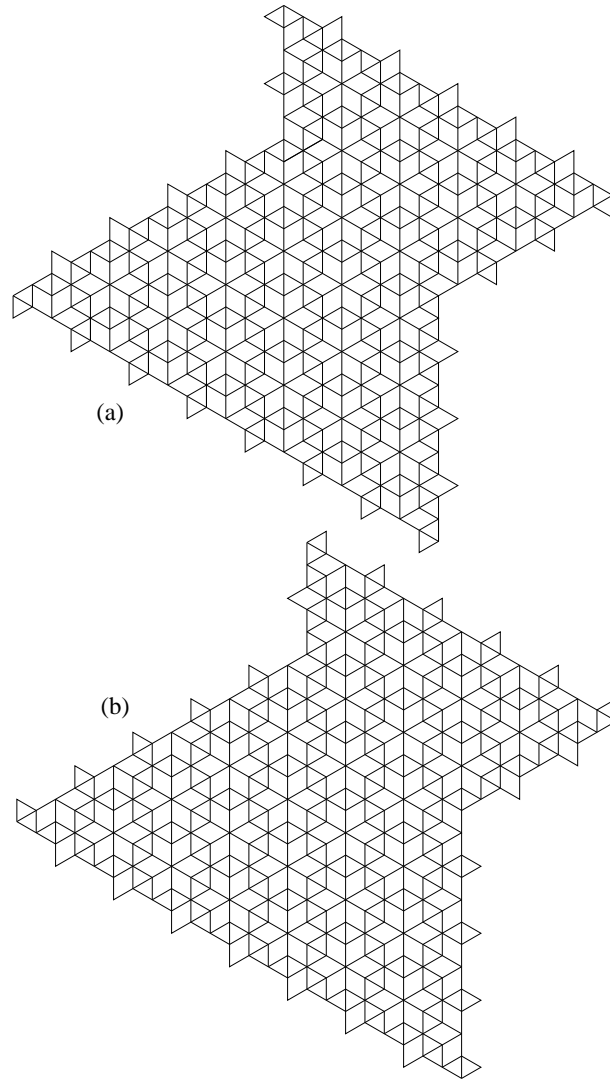


FIGURE 6.9. The regions $ND_{5,8,4}$ (a) and $NE_{5,8,4}$ (b).

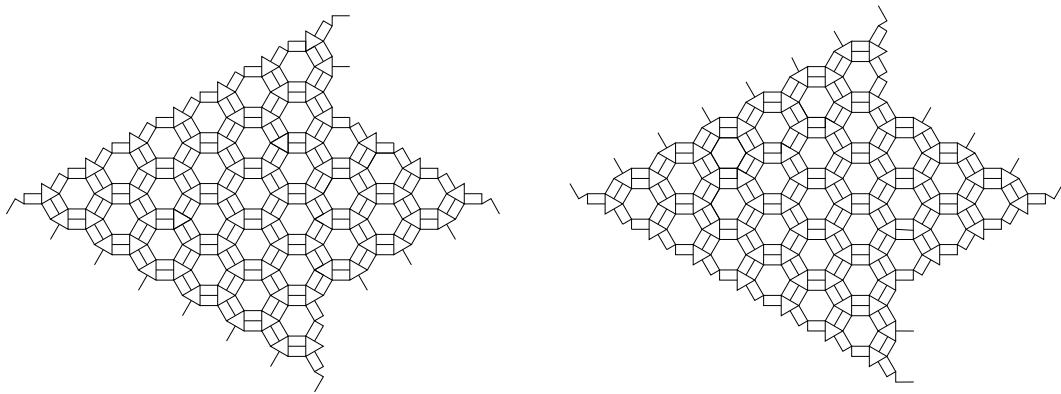


FIGURE 6.10. The dual graphs of the regions $ND_{8,8,2}$ (left) and $NE_{8,8,2}$ (right).

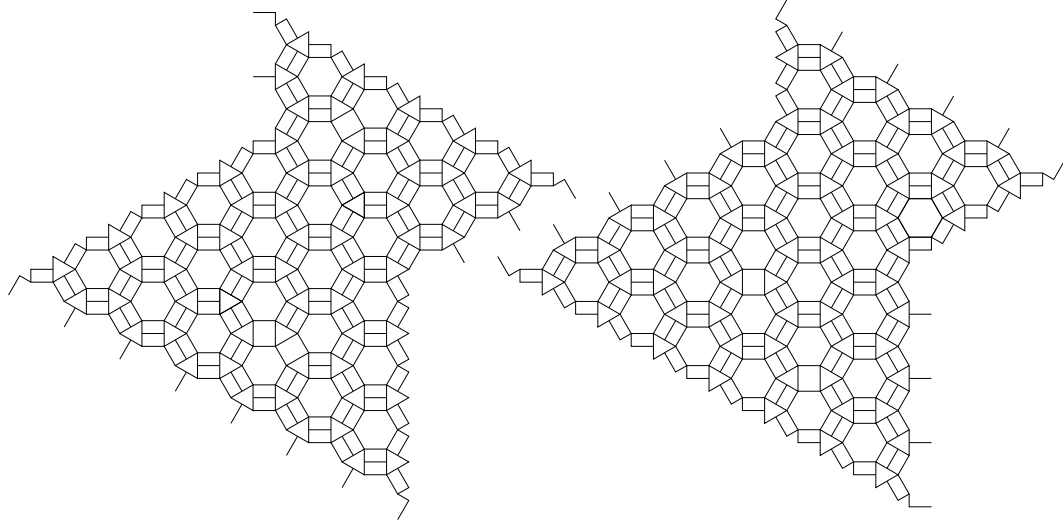


FIGURE 6.11. The dual graphs of the regions $ND_{5,8,4}$ (left) and $NE_{5,8,4}$ (right).

$$(6.13) \quad \begin{aligned} M(ND_{a,b,c}) &= 2^{a^2-3ab+3b^2-3bc+c^2+ac+a-b+\frac{1}{c}-\frac{1}{2}|2a-2b+c|} \\ &\times 3^{(5a-7b+5c+1)(a-b+c)/2+b(b-1)-ac} \end{aligned}$$

and

$$(6.14) \quad \begin{aligned} M(NE_{a,b,c}) &= 2^{a^2-3ab+3b^2-3bc+c^2+ac+a-b+\frac{1}{c}-\frac{1}{2}|2a-2b+c|} \\ &\times 3^{(5a-7b+5c+1)(a-b+c)/2+b(b-1)-ac+(b-a)+\min(2a-2b+c,0)}, \end{aligned}$$

By applying Kuo's condensation we get the following recurrences for $M(ND_{a,b,c})$ and $M(NE_{a,b,c})$.

Lemma 31. *Let a , b and c be nonnegative integers so that $b \geq 5$, $c \geq 2$, $d := 2b - a - 2c \geq 0$, and $3b - 2a - 2c \geq 0$. Assume in addition that $a \geq c + d + 1$. Then*

$$(6.15) \quad \begin{aligned} M(TRD_{a,b,c}) M(ND_{a-3,b-3,c-2}) &= 3 M(ND_{a-2,b-1,c}) M(ND_{a-1,b-2,c-2}) \\ &+ 9 M(ND_{a-1,b-1,c-1}) M(ND_{a-2,b-2,c-1}), \end{aligned}$$

and

$$(6.16) \quad \begin{aligned} M(NE_{a,b,c}) M(NE_{a-3,b-3,c-2}) &= 3 M(NE_{a-2,b-1,c}) M(NE_{a-1,b-2,c-2}) \\ &+ 9 M(NE_{a-1,b-1,c-1}) M(NE_{a-2,b-2,c-1}). \end{aligned}$$

Proof. We apply the Kuo's graphical condensation theorem to the dual graph G of $ND_{a,b,c}$ with four vertices u, v, w, t as in Figure 6.12(a).

By considering forced edges and Graph-splitting Lemma we have $M(G - \{x, y\}) = 3^{a+f-3} M(ND_{a-2,b-1,c})$ (see Figure 6.12(b), the bold edges are forced; and the subgraphs inside the contour are cut by Graph-splitting Lemma).

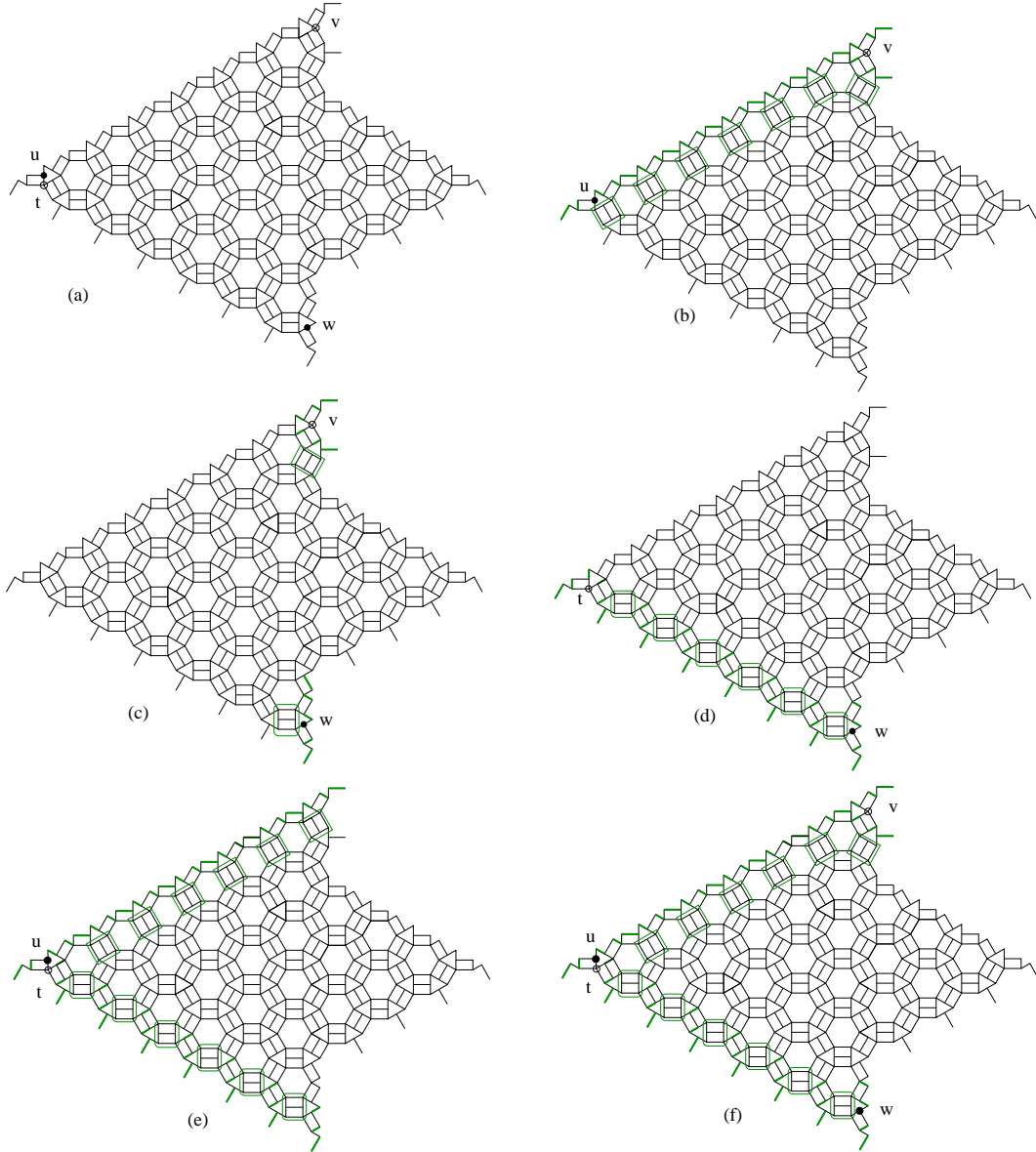


FIGURE 6.12. Illustrating the proof of Lemma 31.

Moreover, we have

$$M(G - \{y, z\}) = 3^{c+f-2} M(ND_{a-1,b-1,c-1}) \text{ (see Figure 6.12(c))},$$

$$M(G - \{z, t\}) = 3^{b+c-4} M(ND_{a-1,b-2,c-2}) \text{ (see Figure 6.12(d))},$$

$$M(G - \{t, x\}) = 3^{a+b-4} M(ND_{a-2,b-2,c-1}) \text{ (see Figure 6.12(e))},$$

$$M(G - \{x, y, z, t\}) = 3^{a+b+c+f-8} M(ND_{a-3,b-3,c-2}) \text{ (see Figure 6.12(f))}.$$

Then the equality (6.15) follows from Theorem 4.

By arguing similarly, we get (6.16). \square

Lemma 32. *Let a, b and c be nonnegative integers satisfying $a \geq 2$, $b \geq 4$, $d := 2b - a - 2c \geq 2$, and $e := 3b - 2a - 2c \geq 2$.*

(a). *If $c \geq 1$ and $f > 0$, then*

$$(6.17) \quad \begin{aligned} M(ND_{a,b,c}) M(ND_{a-2,b-2,c}) &= 9 M(ND_{a-1,b-1,c})^2 \\ &\quad + M(ND_{a,b,c+1}) M(ND_{a-2,b-2,c-1}) \end{aligned}$$

and

$$(6.18) \quad \begin{aligned} M(NE_{a,b,c}) M(NE_{a-2,b-2,c}) &= 9 M(NE_{a-1,b-1,c})^2 \\ &\quad + M(NE_{a,b,c+1}) M(NE_{a-2,b-2,c-1}). \end{aligned}$$

(b). *If $c = 0$ and $f > 0$, then*

$$(6.19) \quad \begin{aligned} M(ND_{a,b,0}) M(ND_{a-2,b-2,0}) &= 9 M(ND_{a-1,b-1,0})^2 \\ &\quad + 3 M(ND_{a,b,1}) M(ND_{e,d,1}) \end{aligned}$$

and

$$(6.20) \quad \begin{aligned} M(NE_{a,b,0}) M(NE_{a-2,b-2,0}) &= 9 M(NE_{a-1,b-1,0})^2 \\ &\quad + M(NE_{a,b,1}) M(NE_{e,d,1}), \end{aligned}$$

where, as usual, $d = 2a - b - 2c$ and $e = 3a - 2b - 2c$.

(c). *If $c = f = 0$, then $a = b = d = e$,*

$$(6.21) \quad \begin{aligned} M(ND_{a,a,0}) M(ND_{a-2,a-2,0}) &= 9 M(ND_{a-1,a-1,0})^2 \\ &\quad + 3 M(ND_{a,a,1})^2, \end{aligned}$$

and

$$(6.22) \quad \begin{aligned} M(NE_{a,a,0}) M(NE_{a-2,a-2,0}) &= 9 M(NE_{a-1,a-1,0})^2 \\ &\quad + 3 M(NE_{a,a,1})^2. \end{aligned}$$

Lemma 33. *Assume that a, b, c are three nonnegative integers satisfying $a \geq 2$, $b \geq 5$, $c \geq 2$, $d := 2b - a - 2c \geq 0$, and $e := 3b - 2a - 2c \geq 0$. Assume in addition that $a \leq c + d$.*

(a). *If $d \geq 1$, then*

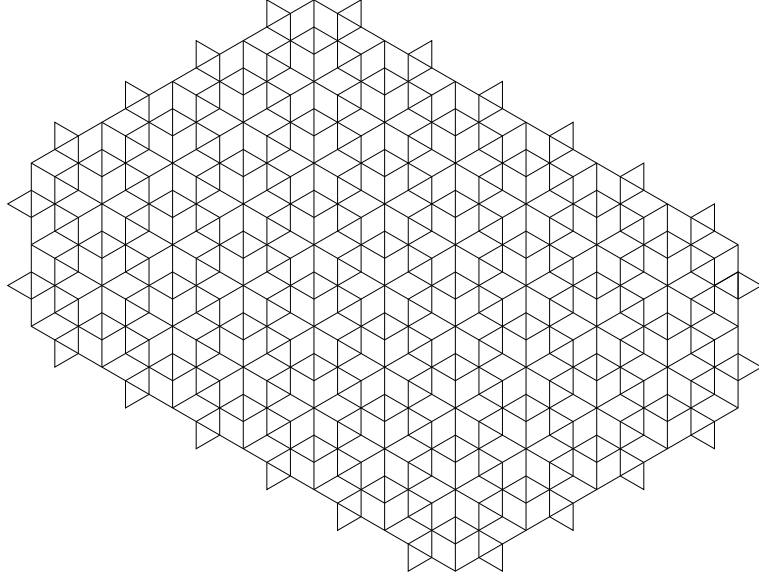
$$(6.23) \quad \begin{aligned} M(ND_{a,b,c}) M(ND_{a-2,b-3,c-2}) &= 3 M(ND_{a-1,b-1,c}) M(ND_{a-1,b-2,c-2}) \\ &\quad + 3 M(ND_{a-2,b-2,c-1}) M(ND_{a,b-1,c-1}) \end{aligned}$$

and

$$(6.24) \quad \begin{aligned} M(NE_{a,b,c}) M(NE_{a-2,b-3,c-2}) &= 3 M(NE_{a-1,b-1,c}) M(NE_{a-1,b-2,c-2}) \\ &\quad + 3 M(NE_{a-2,b-2,c-1}) M(NE_{a,b-1,c-1}). \end{aligned}$$

(b). *If $d = 0$ and $f > 0$, then*

$$(6.25) \quad \begin{aligned} M(ND_{a,b,c}) M(ND_{a-2,b-3,c-2}) &= 3 M(ND_{c,b-1,a-1}) M(ND_{a-1,b-2,c-2}) \\ &\quad + 3 M(ND_{a-2,b-2,c-1}) M(ND_{a,b-1,c-1}) \end{aligned}$$

FIGURE 6.13. The needle hexagon $NH_{2,4,6}$.

and

$$(6.26) \quad \begin{aligned} M(NE_{a,b,c}) M(NE_{a-2,b-3,c-2}) &= 9 M(NE_{c,b-1,a-1}) M(NE_{a-1,b-2,c-2}) \\ &\quad + 3 M(NE_{a-2,b-2,c-1}) M(NE_{a,b-1,c-1}). \end{aligned}$$

(c). If $d = f = 0$, then $a = c = 2q$ and $b = 3q$,

$$(6.27) \quad \begin{aligned} M(ND_{2q,3q,2q}) M(ND_{2q-2,3q-3,2q-2}) &= 3 M(ND_{2q,3q-1,2q-1}) M(ND_{2q-1,3q-2,2q-2}) \\ &\quad + 3 M(ND_{2q-2,3q-2,2q-1}) M(ND_{2q,3q-1,2q-1}) \end{aligned}$$

and

$$(6.28) \quad \begin{aligned} M(NE_{2q,3q,2q}) M(NE_{2q-2,3q-3,2q-2}) &= 9 M(NE_{2q,3q-1,2q-1}) M(NE_{2q-1,3q-2,2q-2}) \\ &\quad + 9 M(NE_{2q-2,3q-2,2q-1}) M(NE_{2q,3q-1,2q-1}). \end{aligned}$$

We can proof the Theorem 30 by the same way as in Theorems 2 and 5. First, we need to verify the right hand sides of equalities (6.13) and (6.14) in the theorem satisfy the same recurrences in the lemmas above. This work is straightforward and will be omitted. One realized that we have more recurrences here than in Theorems 2 and 5, so we need several small adjustments in our proof.

We conclude this section by a consequence of Theorem 30. We consider a "needle hexagon" of sides $a, 2a, b$, with $b \geq 2a$, as in Figure 6.13. Denote by $NH_{a,2a,b}$ the needle hexagon.

The following corollary gives an explicit formula for the number of tilings of a needle hexagon.

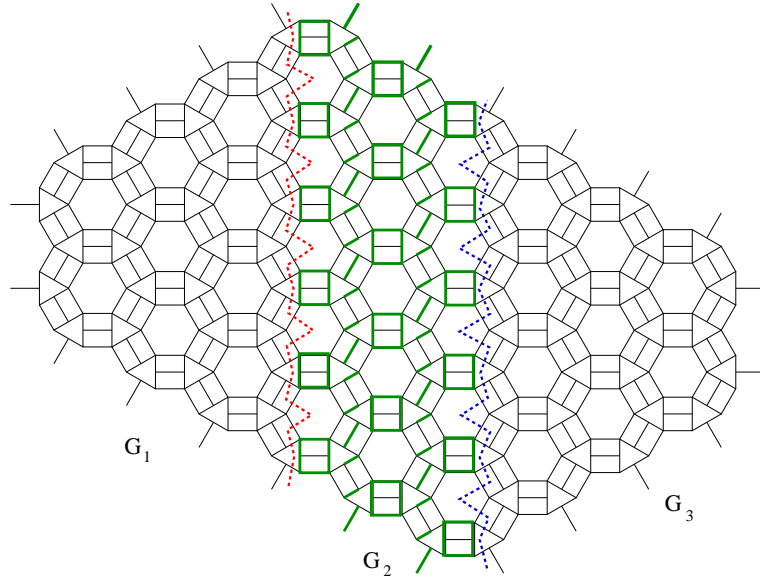


FIGURE 6.14. Illustrating the proof of Corollary 34.

Corollary 34. Assume that a and b are two positive integers so that $b \geq 2a$. Then

$$(6.29) \quad M(NH_{a,2a,b}) = 2^{6a^2+2a} 3^{3ab+3a^2}.$$

Proof. We consider two cuts on the dual graph of the needle hexagon $NH_{a,2a,b}$ (see Figure 6.14). Denote by G_1, G_2, G_3 the three graphs obtaining from the graph splitting process. We have G_1 and G_2 are isomorphic to $NE_{2a,3a,2a}$. By considering forced edges and Graph-splitting Lemma, we get $M(G_2) = 3^{(b-2a+1)3a}$ (the bold edges in Figure 6.14 are the forced ones; the subgraphs restricted in bold rectangular contour are cut by graph-splitting process for G_2). Thus, we get

$$(6.30) \quad M(NH_{a,2a,b}) = M(G_1) M(G_2) M(G_3)$$

$$(6.31) \quad = M(NE_{2a,3a,2a})^2 3^{(b-2a+1)3a}.$$

Then the corollary follows from Theorem 30. \square

REFERENCES

- [1] M. Ciucu, *Perfect matchings and perfect powers*, J. Algebraic Combin. **17** (2003), 335–375.
- [2] M. Ciucu and T. Lai, *Proof of Blum’s Conjecture on Hexagonal Dungeons*, to appear in J. Combin. Theory Ser. A, 2014.
- [3] C. Cottrell and B. Young, *Domino shuffling for the Del Pezzo 3 lattice*, arXiv:1011.0045. <http://arxiv.org/abs/1011.0045>
- [4] N. Elkies, G. Kuperberg, M. Larsen, and J. Propp, *Alternating-sign matrices and domino tilings (Part I)*, J. Algebraic Combin. **1** (1992), 111–132.
- [5] E. H. Kuo, *Applications of Graphical Condensation for Enumerating Matchings and Tilings*, Theor. Comput. Sci. **319** (2004), 29–57.
- [6] T. Lai, *New aspects of regions whose tilings are enumerated by perfect powers*, Electronic Journal of Combinatorics Volume 20, Issue 4 (2013), P31.

- [7] M. Leoni, S. Neel, and P. Turner *Aztec Castles and the $dP3$ Quiver*, arXiv:1308.3926. [textt-
http://arxiv.org/abs/1308.3926](http://arxiv.org/abs/1308.3926)
- [8] J. Propp, *Enumeration of matchings: Problems and progress*, New Perspectives in Geometric Combinatorics, Cambridge University Press, 1999, 255–291.
- [9] J. Propp, *Generalized Domino-Shuffling*, Theor. Comput. Sci. **303** (2003), 267–301.
- [10] W. Yan and F. Zhang, *Graphical Condensation for Enumerating of Perfect Matchings*, J. Combin. Theory Ser. A **110** (2005), 113–125.